Universidade de São Paulo
Instituto de Física

Não Markovianidade em modelos colisionais Gaussianos

Rolando Ramirez Camasca

Orientador: Prof. Dr. Gabriel Teixeira Landi

Dissertação de mestrado apresentada ao Instituto de Física da Universidade de São Paulo, como requisito parcial para a obtenção do título de Mestre em Ciências.

Banca Examinadora:
Prof. Dr. Gabriel Teixeira Landi - Instituto de Física da Universidade de São Paulo
Prof. Dr. -
Prof. Dr. -

São Paulo
2020

University of São Paulo
Physics Institute

Non-Markovianity in Gaussian Collisional Models

Rolando Ramirez Camasca

Supervisor: Prof. Dr. Gabriel Teixeira Landi

Dissertation submitted to the Physics Institute of the University of São Paulo in partial fulfillment of the requirements for the degree of Master of Science.

Examining Committee:
Prof. Dr. Gabriel Teixeira Landi - Physics Institute of the University of São Paulo
Prof. Dr. -
Prof. Dr. -

São Paulo
2020

Ernest Hemingway once wrote: "The world is a fine place and worth fighting for." I agree with the second part.

— Se7en (1995)

To my grandfather...

Abstract

Memory effects in the dynamics of open systems have been the subject of significant interest in the last decades. The methods involved in quantifying this effect, however, are often difficult to compute and may lack analytical insight. With this in mind, we study collisional models where non-Markovianity is introduced by means of additional interactions between neighboring environmental units. We show that the dynamics can be cast in terms of a Markovian Embedding of the covariance matrix, which yields closed form expressions for the memory kernel that governs the dynamics, a quantity that can seldom be computed analytically. The same is also possible for a divisibility monotone, based on the complete positivity of intermediate maps. By focusing on continuous-variables Gaussian dynamics, we are able to analytically study models of arbitrary size. We analyze in detail two types of interactions, a beam-splitter implementing a partial SWAP and a two-mode squeezing, which entangles the ancillas and, at the same time, feeds excitations into the system. By analyzing the memory kernel and divisibility for these two representative scenarios, our results help to shed light on the intricate mechanisms behind memory effects in the quantum domain.

Keywords: Open Quantum Systems; Collisional Model; Non-Markovianity; Memory Kernel; Map Divisibility.

Resumo

Os efeitos da memória na dinâmica dos sistemas abertos têm sido objeto de grande interesse nas últimas décadas. Os métodos envolvidos na quantificação desse efeito, no entanto, muitas vezes são difíceis de calcular e podem carecer de uma visão analítica. Com isso em mente, estudamos modelos colisionais em que a não markovianidade é introduzida por meio de interações adicionais entre unidades ambientais vizinhas. Mostramos que a dinâmica pode ser moldada em termos de um Embedding Markoviano da matriz de covariância, que produz expressões de forma fechada para o kernel de memória que governa a dinâmica, uma quantidade que raramente pode ser calculada analiticamente. O mesmo também é possível para uma divisibilidade monótona, baseada na positividade completa dos mapas intermediários. Ao focarmos na dinâmica gaussiana de variáveis contínuas, podemos estudar analiticamente modelos de tamanho arbitrário. Analisamos em detalhes dois tipos de interações, um beam splitter implementando um SWAP parcial e uma compressão de dois modos, que emaranha as ancillas e, ao mesmo tempo, alimenta excitações no sistema. Ao analisar o kernel de memória e a divisibilidade para esses dois cenários representativos, nossos resultados ajudam a lançar luz sobre os intrincados mecanismos por trás dos efeitos da memória no domínio quântico.

Keywords: Sistemas quânticos abertos; Modelos colisionais; Não-Markovianidade; Kernels de memoria; CP-Divisibilidade.

Contents

List of Figures

Chapter 1

Introduction

The theory of open quantum systems is the backbone of modern research in quantum mechanics and its applications. Some examples include the decay of unstable states in nuclei, transport of electrons through quantum dots, molecular networks, nanophotonic structures, among others. This is because, in real life phenomena, the systems are never isolated, but are constantly interacting with its surrounding environment. In some cases, when the effects of the environment are negligible, the closed system description is accurate, described by the well-known Liouvillian equation. Nevertheless, more often than not, it is not possible. Obtaining the most general microscopic description of the open system dynamics is a very difficult problem, one that is yet to be solved.

One instance we can get a microscopic derivation is when we assume that the system-environment interaction is weak but also that the bath correlation functions decay quickly. This is known as the Born-Markov approximation [1–3]. Typically, when the system interacts with the environment, information about the former is translated to the latter. When the environment is very large and complex, this information may never return. In this case the dynamics is called Markovian. This is characterized by the Lindblad equation given by [4]:

$$\frac{d}{dt}\rho_S = -\frac{i}{\hbar}[H, \rho_S] + \sum_k g_k \Big(L_k \rho_S L_k^\dagger - \frac{1}{2}\Big\{ L_k^\dagger L_k, \rho_S \Big\}\Big), \tag{1.1}$$

where ρ_S is the system's density matrix, H is the Hamiltonian, and L_k are arbitrary operators. In general, however, there may be a partial backflow of information which charac-

terizes the non-Markovian evolution [5]. The dynamics of the open quantum systems in the non-Markovian regime can generally be written as [6, 7]:

$$\frac{d\rho_S}{dt} = -i[H_S, \rho_S] + \int_0^t \mathcal{K}_{t-t'}[\rho_S(t')]\, dt', \tag{1.2}$$

where $\mathcal{K}_{t-t'}$, called the memory kernel (MK), is a linear superoperator condensing all the information on how the evolution of ρ_S at time t depends on its past values. We see that the Markovian case (1.1) is recovered when $\mathcal{K}_{t-t'} \propto \delta(t-t')$. The MK has been intensively studied in recent years, as it provides clear insights onto the inner workings of non-Markovianity [8–13]. From the point of view of causality, this backflow quantifies the ability of the dynamics to communicate past information to the future [14]. Non-Markovianity therefore touches at the core of information processing where the notion of information flow is fundamental.

Considerable attention was given in recent years on how to characterize and quantify non-Markovianity in the quantum domain [15, 16]. Due to the richness involved, however, there is no single approach capable of capturing its full essence. The most important notion is that of map divisibility: non-Markovianity requires that the underlying dynamical map should not be divisible [17, 18]. The notion of information flow, on the other hand, relies on information-theoretic quantifiers and is thus not uniquely defined. The most widely used measures involve the trace distance [17–20] between different initial states or entanglement [21] between the system and an ancilla. Several other quantifiers have also been explored [22–30]. However, analyzing non-Markovianity for general environments is in general an extremely difficult task. First, the calculations quickly become impractical when the size of the bath is large. And second, realistic baths often have many additional features which tend to mask the effects one is interested in. This motivates the search for controllable models, where the degree of non-Markovianity can be finely tuned.

One way to accomplish this, which has seen an enormous surge in popularity in recent years, are through the so-called collisional models [31–42]. Usually, a common configuration to study non-Markovianity is to consider the system S coupled to N environmental units E_n all at the same time (e.g. the Caldeira-Legett model [43]). In the collisional models setup instead only a small part of the environment is interacting with the sys-

tem at each instant of time. Afterwards, this part leaves and returns to the bath where it will collide with the other bath units and thermalize, forgetting all information about the system. We model this by replacing the open dynamics of a system by a series of sequential interactions between the system S and small environmental units $E_1, E_2, E_3 \ldots$ (henceforth referred to as ancillas). All ancillas are prepared in the same state and each interaction only lasts for a fixed time, after which they never interact again. This therefore leads to a stroboscopic dynamics for the system.

Although seemingly artificial, collisional models actually faithfully describe some experimentally relevant situations, for instance when a system is coupled to a 1D waveguide [44–47]. The dispersion relation of 1D waveguides allows one to discretize the field operator into time bins, so that the interaction at each time interval only involves one bin operator. The picture that emerges is then exactly that of a collisional model. Moreover, this model is in general non-Markovian by construction, which depends on the input state of the electromagnetic field, as well as on the nature of the interaction. The specific conditions determining whether the ensuing dynamics will be Markovian or not are discussed in detail in a recent review on the subject [48].

The advantage of collisional models is that non-Markovianity can be introduced in a fully controllable manner. There are two main ways to do so. The first is to consider that the ancillas already start correlated [49–53]. The other one is to assume information is transmitted between them during the process [54–62]. In this dissertation, we shall focus on the second case. That is, we consider a scenario where neighboring ancillas $E_n E_{n+1}$ interact with each other in between the interactions SE_n and SE_{n+1}. (see Fig. 1.1(a)). This additional interaction *signals* information from the past to the future, so that when the SE_{n+1} interaction arrives, the ancilla E_{n+1} will already contain some information about the system.

In particular, we focus on continuous-variable collisional models, undergoing Gaussian-preserving dynamics [63–71]. The advantages that come with the Gaussian toolbox allows us to construct a complete framework for the study of non-Markovianity, which: (i) encompass a broad range of scenarios; (ii) can be easily use to compute the mutual information; (iii) allows for the explicit construction and computation of the memory kernel and (iv) provides access to a CP-divisibility monotone, which can be directly compared

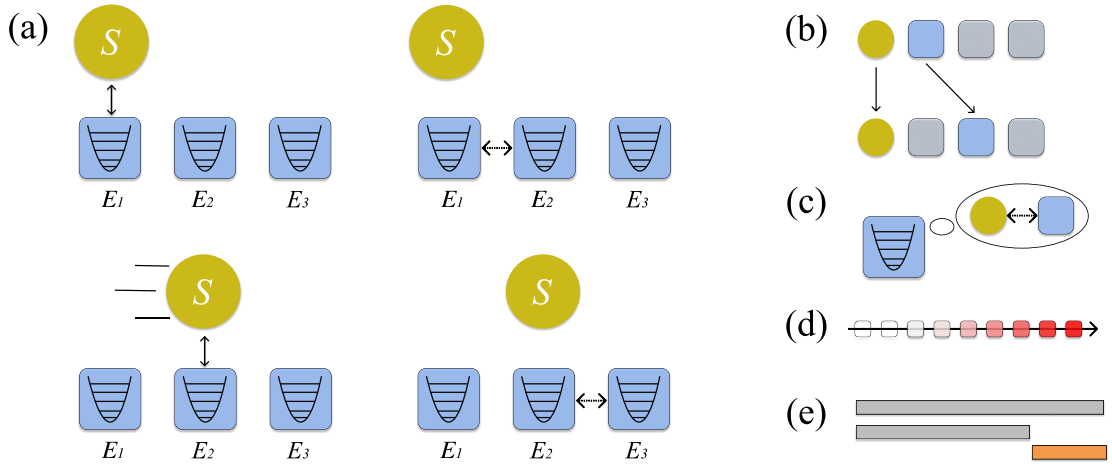

Figure 1.1: Non-Markovian collisional models. (a) First few steps of the dynamics. The system-ancilla interactions SE_n are interspersed by ancilla-ancilla interactions E_nE_{n+1}, which propagate information forward, making the dynamics non-Markovian in a fully controllable way. (b) Basic structure of the Markovian embedding dynamics, which is a map from the Hilbert space of SE_n to that of SE_{n+1}. (c) Mutual information. Previous interactions SE_n and E_nE_{n+1} correlate the system S and the ancilla E_{n+1} even before explicitly interacting. (d) The memory kernel quantifies how different instants of the past affect the evolution at present times. (e) CP-divisibility. The maps in gray, from time 0 to t_n or t_m are, by construction, CPTP. But the intermediate map from t_n to $t_m > t_n$ may not necessarily be.

with the memory kernel. The framework is also amenable to analytical calculations and extremely efficient from a numerical perspective. Thus, despite being restricted to Gaussian interactions, it offers multiple advantages over more general maps. We also provide a complete numerical library for efficiently simulating Gaussian collisional models in Python [72]. All plots were generated with this code.

The dissertation is divided as follows. We begin in Chapter 2 by introducing important concepts of open quantum systems and review the different methods to describe the open system's dynamics. Particularly, we consider a qubit interacting with a bosonic environment to exemplify the approximations needed to obtain a microscopic derivation. Next, we study the continuous variable formalism in Chapter 3. Specifically, we examine Gaussian states and maps as they will become cornerstone for this work. The following chapters are the most important of the dissertation. They represent the original contribution from the authors to the field of non-Markovianity in collisional models. The general framework is developed in Chapter 4. We show that the full non-Markovian dynamics

can be cast as a Makorvian embedding, involving a Markovian map at a higher dimension (Fig. 1.1(b)). We then specialize this to the case of Gaussian models, where the embedding is written as a set of matrix-difference equations with clear physical interpretation. Throughout this chapter our exposition will be example-oriented, with a focus on two specific types of interactions. The framework, however, is general and we will specify, in each part, how to properly make this generalization. Following, in Chapter 5, we review non-Markovianity in the quantum domain as well as the quantifiers we will use for our collisional model. Armed with all these results, in Chapter 6 we provide a full characterization of the memory effects using the mutual information (Fig. 1.1(c)), the memory kernel (Fig. 1.1(d)) and the map divisibility (Fig. 1.1(e)). Finally, in Chapter 7 we draw our conclusions and our perspectives on future works which can be done using this robust framework.

Chapter 2

Open Quantum Systems

2.1 States and Dynamics

Quantum mechanics is the fundamental theory that describes the behavior of nature at the micro scale [73–78]. However, it is often assumed that the quantum system is isolated, overlooking the effects of the interaction with its surroundings. Such effects can lead to dramatic changes in the system's dynamics such as the dissipation of the quantum correlations, making them necessary for an accurate depiction of real phenomena. The field that studies this kind of phenomenon is called open quantum systems [1–3].

The description of open quantum systems starts by defining what the object of study is: the states. In quantum mechanics, we were interested in kets $|\psi_i\rangle$ which live in a Hilbert space $\mathcal{H}$. Analogously, open quantum systems is interested in the density matrix $\rho = \sum c_i \, |\psi_i\rangle\langle\psi_i|$ which lives in $\mathcal{L}(\mathcal{H})$, the state space of linear operators from $\mathcal{H}$ to $\mathcal{H}$. This density matrix ρ satisfies the following properties:

$$\begin{aligned} \text{Hermicity:} \quad & \rho = \rho^\dagger, \\ \text{Positivity:} \quad & \rho \geq 0, \\ \text{Normalization:} \quad & \mathrm{Tr}(\rho) = 1. \end{aligned}$$

Besides these properties, we also want to know how a state ρ evolves in time. For that purpose, we look at the evolution of isolated systems which evolve through Schörindger's

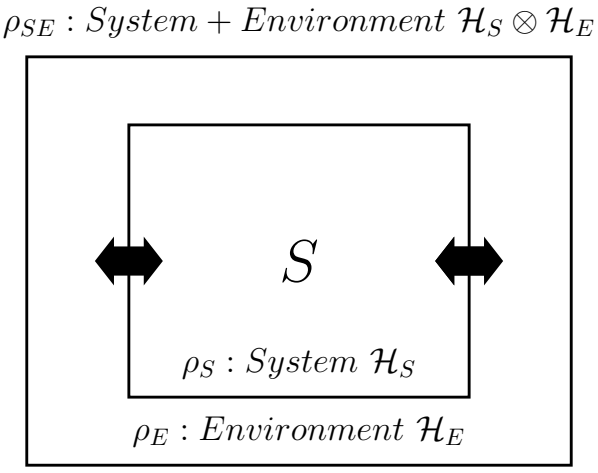

Figure 2.1: Schematics of an open quantum system. The system S is interacting with the environment while the whole bipartite system ρ_{SE} is consider as closed.

equation:

$$\partial_t |\psi(t)\rangle = -\frac{i}{\hbar} H(t) |\psi(t)\rangle . \tag{2.1}$$

The analogue evolution in the density matrix formalism is known as von Neumann's equation:

$$\frac{d\rho(t)}{dt} = -\frac{i}{\hbar}[H(t), \rho(t)]. \tag{2.2}$$

This result holds only for closed systems. The next step is to obtain a description of the open system's dynamics. One way to achieve this is to consider a bipartite system ρ_{SE} which contemplates both the system S and an environment E, as a closed system evolving under von Neumann's equation, as depicted in Fig. 2.1. Tracing out the environment E will then lead to an effective description of the system's density matrix ρ_S dynamics. Unfortunately, this is a complicated task, often relying on multiple approximation schemes to obtain analytical results. We study this procedure in detail in the next sections.

2.2 Memory Kernel

We follow the seminal works of Nakajima and Zwanzig throughout this subsection [6, 7]. We consider the complete density matrix ρ_{SE} of a system S plus an environment E initially uncorrelated $\rho_{SE}(t_0) = \rho_S(t_0) \otimes \rho_E(t_0)$ evolving under a Hamiltonian $H_{SE} =$

$H_S + H_E + V$:

$$\frac{d\rho_{SE}(t)}{dt} = -\frac{i}{\hbar}[H_{SE}, \rho_{SE}(t)]. \tag{2.3}$$

It is convenient to formulate (2.3) in the interaction picture $\rho^I_{SE} = e^{iH_0t}\,\rho_{SE}\,e^{-iH_0t}$ with respect to $H_0 = H_S + H_E$:

$$\frac{d\rho^I_{SE}(t)}{dt} = -\frac{i}{\hbar}\big[V_I(t), \rho^I_{SE}(t)\big] := \mathcal{L}_t\rho^I_{SE}(t), \qquad V_I = e^{iH_0t}Ve^{-iH_0t}, \tag{2.4}$$

where we defined the superoperator $\mathcal{L}_t$. From here on, we will loose the superscript I in ρ^I_{SE} for notational convenience.

Our goal is to obtain the master equation for the system $\rho_S(t) = \mathrm{Tr}_E(\rho_{SE}(t))$. To that end, we define a pair of orthogonal projection operators $\mathcal{P}$ and $\mathcal{Q}$

$$\mathcal{P}\rho_{SE} = \mathrm{Tr}_E(\rho_{SE}) \otimes \rho^*_E, \qquad \mathcal{Q}\rho_{SE} = \rho_{SE} - \mathrm{Tr}_E(\rho_{SE}) \otimes \rho^*_E, \tag{2.5}$$

where ρ^*_E is an arbitrary environmental density matrix, not necessarily related to the state of the environment. Being projection operators, they satisfy $\mathcal{P}\mathcal{Q} = \mathcal{Q}\mathcal{P} = 0$ and $\mathcal{P}+\mathcal{Q} = \mathcal{I}$ which follow from the definition. Applying $\mathcal{P}$ to Eq. (2.4) we obtain

$$\frac{d}{dt}\mathcal{P}\rho_{SE}(t) = \mathcal{P}\mathcal{L}_t\rho_{SE}(t). \tag{2.6}$$

We can then introduce the identity $\mathcal{I} = \mathcal{P} + \mathcal{Q}$ to get a differential equation for $\mathcal{P}\rho_{SE}(t)$

$$\frac{d}{dt}\mathcal{P}\rho_{SE}(t) = \mathcal{P}\mathcal{L}_t\big(\mathcal{P} + \mathcal{Q}\big)\rho_{SE}(t) = \mathcal{P}\mathcal{L}_t\mathcal{P}\rho_{SE}(t) + \mathcal{P}\mathcal{L}_t\mathcal{Q}\rho_{SE}(t). \tag{2.7}$$

Similarly, we can obtain a differential equation for $\mathcal{Q}\rho_{SE}(t)$ applying $\mathcal{Q}$ to Eq. (2.3)

$$\frac{d}{dt}\mathcal{Q}\rho_{SE}(t) = \mathcal{Q}\mathcal{L}_t\mathcal{Q}\rho_{SE}(t) + \mathcal{Q}\mathcal{L}_t\mathcal{P}\rho_{SE}(t). \tag{2.8}$$

We now have two coupled differential equations. We solve Eq. (2.8) for $\mathcal{Q}\rho_{SE}(t)$,

$$\mathcal{Q}\rho_{SE}(t) = G(t, t_0)\mathcal{Q}\rho_{SE}(t_0) + \int_{t_0}^{t} dt'\, G(t, t')\mathcal{Q}\mathcal{L}_{t'}\mathcal{P}\rho_{SE}(t'), \tag{2.9}$$

where $G(t,t')$ is the Green's function $G(t,t_0) = \mathcal{T}\exp\big(\int_{t_0}^{t} dt'\,\mathcal{Q}\mathcal{L}_{t'}\big)$. Inserting (2.9) in (2.7) leads to the Nakajima-Zwanzig master equation

$$\frac{d}{dt}\mathcal{P}\rho_{SE}(t) = \mathcal{P}\mathcal{L}_t\big(\mathcal{P}\rho_{SE}(t)+G(t,t_0)\mathcal{Q}\rho_{SE}(t_0)+\int_{t_0}^{t} dt'\,G(t,t')\mathcal{Q}\mathcal{L}_{t'}\mathcal{P}\rho_{SE}(t')\big). \quad (2.10)$$

This is a reduced equation for $\mathcal{P}\rho_{SE}(t)$ after integrating out the environment. Most importantly, this equation is exact. We can further reduce this expression by fixing the arbitrary ρ_E^* to be the environment's initial state $\rho_E(t_0)$. This selection implies that $\mathcal{Q}\rho_{SE}(t_0) = 0$, leading to

$$\frac{d}{dt}\rho_S(t)\otimes\rho_E(t_0) = \mathcal{P}\mathcal{L}_t\mathcal{P}\rho_{SE}(t)+\int_{t_0}^{t} dt'\ \mathrm{Tr}_E\left(\mathcal{L}_t G(t,t')\mathcal{Q}\mathcal{L}_{t'}\big(\rho_S(t')\otimes\rho_E(t_0)\big)\right)\otimes\rho_E(t_0). \quad (2.11)$$

Finally, if $[\rho_E(t_0), H_E] = 0$ we can redefine the interaction such that $\mathcal{P}\mathcal{L}_t\mathcal{P}\rho_{SE}(t) = 0$, thus arriving to:

$$\frac{d}{dt}\rho_S(t) = \int_{t_0}^{t} dt'\,K_{t,t'}\rho_S(t'), \qquad \mathcal{K}_{t,t'} = \mathrm{Tr}_E\left(\mathcal{L}_t G(t,t')\mathcal{Q}\mathcal{L}'_t(\ldots\otimes\rho_E(t_0))\right), \quad (2.12)$$

where $\mathcal{K}_{t,t'}$ is the memory kernel, a linear superoperator condensing all the information on how the evolution of $\rho_S(t)$ depends on its past values.

2.3 Microscopic derivation:

Eq. (2.12) still involves a superoperator, which is quite generally difficult to compute analytically. Approximations are then needed to obtain a more manageable equation, one which will be more useful under certain conditions. We start by re-scaling the interaction term V_I to αV_I by a dimensionless small parameter α. The assumption that α is small is usually called the Born approximation. Expanding the memory kernel to second order, we get

$$\mathcal{K}_{t,t'} = \alpha^2\,\mathrm{Tr}_E\left(\mathcal{L}_t\mathcal{Q}\mathcal{L}_{t'}\mathcal{P}\right) + \mathcal{O}\big(\alpha^3\big), \quad (2.13)$$

which leads to an equation of motion of second order for $\rho_S(t)$

$$\frac{d}{dt}\rho_S(t) = \alpha^2 \int_{t_0}^{t} dt' \ \mathrm{Tr}_E \left(\mathcal{L}_t \mathcal{L}_{t'} \rho_S(t') \otimes \rho_E(t_0)\right). \tag{2.14}$$

Putting the explicit expressions for the superoperator $\mathcal{L}_t$ we get

$$\frac{d}{dt}\rho_S(t) = -\int_{t_0}^{t} dt' \ \mathrm{Tr}_E \left[V_I(t), [V_I(t'), \rho_S(t') \otimes \rho_E(t_0)]\right]. \tag{2.15}$$

Next, we proceed with the Markovian approximation. We assume that the environment's correlations decays much faster than the system's so that the state of the system at time t only depends on the present state $\rho_S(t)$. To that end, we make the previous equation time local by replacing $\rho_S(t')$ by $\rho_S(t)$:

$$\frac{d}{dt}\rho_S(t) = -\int_{t_0}^{t} dt' \ \mathrm{Tr}_E \left[V_I(t), [V_I(t'), \rho_S(t) \otimes \rho_E(t_0)]\right]. \tag{2.16}$$

This is called the Redfield equation. Still this equation is not yet Markovian since the time evolution depends upon the initial time t_0. We can make the substitution t' by $t - t'$ in Eq. (2.16) and integrate up to infinity. This is possible as we are assuming that the time scale over which the state of the system varies is large compared to the time scale of the decay of the environment's correlations. Without loss of generally, we can set $t_0 = 0$ and obtain

$$\frac{d}{dt}\rho_S(t) = -\int_{0}^{\infty} dt' \ \mathrm{Tr}_E \left[V_I(t), [V_I(t-t'), \rho_S(t) \otimes \rho_E(0)]\right]. \tag{2.17}$$

The result is an integro-equation for $\rho_S(t)$ which we can calculate by plugging in the interaction potential in the interaction picture. Even so, we will often need to add more approximations to obtain a differential equation for the $\rho_S(t)$.

2.4 Qubit interacting with bosonic environment

One interesting model which simulates the effects an environment can have on the system is a two-level system interacting with a bosonic bath. For example, this describes an atom

interacting with the many modes of a radiation field. The Hamiltonian of this model is:

$$H = \frac{1}{2}\omega_0\sigma_z + \sum_k \omega_k b_k^\dagger b_k + \sum_k g_k(\sigma_+ b_k + \sigma_- b_k^\dagger), \tag{2.18}$$

where we are modeling the environment as infinite harmonic oscillators, all with different frequencies ω_k. The interaction between our qubit system and the environment is of the form of a typical exchange: creates an excitation on the system/bath by destroying one on the bath/system with strength g_k.

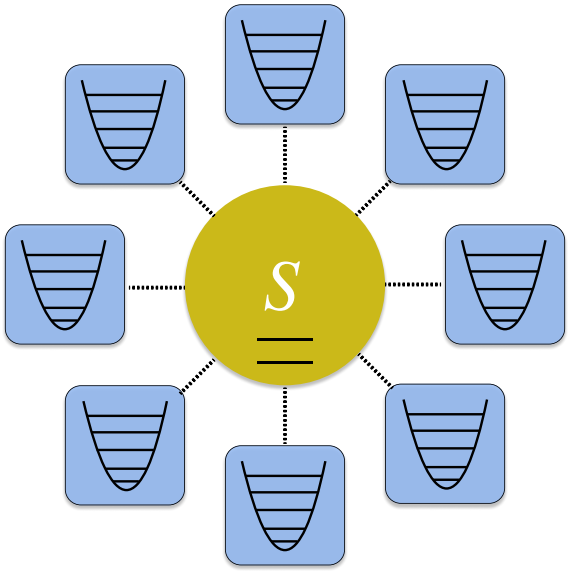

Figure 2.2: Qubit system S interchanging excitations with infinite bosonic environments. The environmental units are modeled as harmonic oscillators with frequency ω_k interacting only with the system proportional to the coupling strength g_k.

We move to the interaction picture to get $V_I(t)$:

$$V_I(t) = e^{iH_0 t} V e^{-iH_0 t} = \sum_k g_k\left(e^{i\Delta_k t}\sigma_+ b_k + e^{-i\Delta_k t}\sigma_- b_k^\dagger\right), \tag{2.19}$$

where $\Delta_k = \omega_0 - \omega_k$, and compute the commutator term inside the trace of Eq. (2.17).

$$\frac{d}{dt}\rho_S(t) = -\int_0^\infty dt'\ \mathrm{Tr}_E\left(V_I(t)\rho_S(t)\rho_E V_I(t-t') - \rho_S(t)\rho_E V_I(t-t')V(t)\right) + h.c. \tag{2.20}$$

where $h.c.$ stands for hermitian conjugate. We focus on the first term inside the integral

$\mathrm{Tr}_E\, V_I(t)\rho_S(t)\rho_E V_I(t-t')$:

$$\sum_{k,q} g_k g_q \Big(e^{i(\Delta_k+\Delta_q)t - i\Delta_q t'} \sigma_+ \rho_S \sigma_+ \langle b_q b_k \rangle + e^{i(\Delta_k-\Delta_q)t + i\Delta_q t'} \sigma_+ \rho_S \sigma_- \langle b_q^\dagger b_k \rangle$$
$$e^{-i(\Delta_k-\Delta_q)t - i\Delta_q t'} \sigma_- \rho_S \sigma_+ \langle b_q b_k^\dagger \rangle + e^{-i(\Delta_k+\Delta_q)t + i\Delta_q t'} \sigma_- \rho_S \sigma_- \langle b_q^\dagger b_k^\dagger \rangle \Big).$$

To compute the correlations, we need to know the state of the environment. We assume that the bath is in a thermal state, meaning that:

$$\langle b_q b_k \rangle = \langle b_q^\dagger b_k^\dagger \rangle = 0, \qquad \langle b_q^\dagger b_k \rangle = \langle b_k b_q^\dagger \rangle - \delta_{kq} = \delta_{kq} n_{\omega_k}, \tag{2.21}$$

where n_{ω_k} is the bosonic occupation distribution $1/(e^{\beta\omega_k} - 1)$. This leads to:

$$\mathrm{Tr}_E\, V_I(t)\rho_S\rho_E V_I(t-t') = \sum_k g_k^2 \big(e^{i\Delta_k t'} n_{\omega_k} \sigma_+ \rho_S \sigma_- + e^{-i\Delta_k t'} (n_{\omega_k}+1) \sigma_- \rho_S \sigma_+ \big). \tag{2.22}$$

It is useful to define a quantity called the spectral density of the bath:

$$J(\omega) = 2\pi \sum_k g_k^2 \delta(\omega - \omega_k), \tag{2.23}$$

such that the first term in Eq. (2.20) now looks like:

$$\int_0^\infty dt' \int_0^\infty \frac{d\omega}{2\pi} J(\omega) \big(e^{i(\omega_0-\omega)t'} n_\omega \sigma_+ \rho_S \sigma_- + e^{-i(\omega_0-\omega)t'} (n_\omega + 1) \sigma_- \rho_S \sigma_+ \big). \tag{2.24}$$

To compute the integral we use the known identity:

$$\int_0^\infty \frac{dt'}{2\pi} e^{i(\omega_0-\omega)t'} = \frac{1}{2}\delta(\omega_0 - \omega) - \frac{i}{2} P\left(\frac{1}{\omega_0 - \omega} \right), \tag{2.25}$$

where P is the Cauchy principal value. This term only accounts to a rescaling of the frequency ω_0 to $\omega_0 + \Delta$ in the unitary dynamics. This net effect is called the Lamb shift. On the other hand, the first term will lead to new terms in the evolution of ρ_S which are of dissipative nature. Focusing on this term we then get:

$$\int_0^\infty \frac{d\omega}{2} J(\omega) \delta(\omega_0 - \omega) \big(n_\omega \sigma_+ \rho_S \sigma_- + (n_\omega + 1) \sigma_- \rho_S \sigma_+ \big) = \frac{J(\omega_0)}{2} \big(n_{\omega_0} \sigma_+ \rho_S \sigma_- + (n_{\omega_0} + 1) \sigma_- \rho_S \sigma_+ \big).$$

A similar precedure can be done to the other terms in Eq. (2.20), resulting in equal terms up to some permutations of the operators. Plugging them back, we get:

$$\frac{d}{dt}\rho_S(t) = \gamma\bar{n}\big(\sigma_+\rho_S\sigma_- - \frac{1}{2}\{\sigma_-\sigma_+, \rho_S\}\big) + \gamma(\bar{n}+1)\big(\sigma_-\rho_S\sigma_+ - \frac{1}{2}\{\sigma_+\sigma_-, \rho_S\}\big). \quad (2.26)$$

Going back to the Schrödinger picture simply reintroduces the unitary contribution and we thus finally arrive at

$$\frac{d}{dt}\rho_S(t) = -\frac{i}{\hbar}\left[\frac{\omega_0+\Delta}{2}\sigma_z, \rho_S(t)\right] + \mathcal{D}(\rho_S(t)), \quad (2.27)$$

where the first term is the familiar unitary term and $\mathcal{D}(\rho_S(t))$ is the dissipative contribution found in Eq. (2.26). By comparison with the closed system's evolution, the effects of tracing out the environment results in new additional terms. Still, several approximations and assumptions were needed to arrive to this equation, most of which do not hold in real experiments.

2.5 Lindblad Equation

Suppose the evolution of the system is time local,

$$\frac{d}{dt}\rho_S(t) = \mathcal{R}_t\rho_S(t), \quad (2.28)$$

for some superoperator $\mathcal{R}_t$. We then ask: What is the general structure of $\mathcal{R}_t$ required to ensure that starting with a density matrix $\rho(0)$, the evolved state $\rho(t)$ is always a genuine density matrix for all later times t? Let us start with a simpler question. Suppose the solution is given by a linear map of the form:

$$\rho_S(t) = \mathcal{V}_t(\rho_S(0)), \quad (2.29)$$

for some superoperator $\mathcal{V}_t$. The question now becomes: What conditions shall $\mathcal{V}_t$ fulfill in order for $\rho_S(t)$ be a density matrix? The answer is that the map should be a quantum operation, one that is completely positive trace preserving (CPTP) [79]. This can be

represented by the operator-sum representation

$$\mathcal{V}_t(\rho_S(0)) = \sum_k M_k \rho_S(0) M_k^\dagger, \qquad \sum_k M_k^\dagger M_k = 1, \tag{2.30}$$

where the set of M_k are called the Kraus operators [80].

Returning now to the original question, if (2.29) is to be the solution of (2.28) then $\mathcal{V}_t$ must satisfy the semi-group property

$$\mathcal{V}_{t_2}\mathcal{V}_{t_1} = \mathcal{V}_{t_2+t_1}. \tag{2.31}$$

The semi-group property, together with the restriction that $\mathcal{V}_t$ must be a quantum operation, completely determines the basic structure of $\mathcal{R}_t$. The generator of any quantum operation satisfying the semigroup property must have the form [4]

$$\frac{d}{dt}\rho_S = -\frac{i}{\hbar}[H, \rho_S] + \sum_k g_k \Big(L_k \rho_S L_k^\dagger - \frac{1}{2}\Big\{ L_k^\dagger L_k, \rho_S \Big\}\Big), \tag{2.32}$$

where H is an Hermitian operator, L_k are arbitrary operators and $g_k \geq 0$. This is called Lindblad's theorem and master equations having this structure are called Lindblad equations. We can see that our microscopic derivation of the system's density evolution Eq. (2.27) already has this structure.

We proceed to formally proof Lindblad's theorem. The semigroup property ensures that the evolution of the density matrix for an infinitesimal Δt is

$$\rho_S(t + \Delta t) = \sum_k M_k(\Delta t) \rho_S(t) M_k^\dagger(\Delta t), \tag{2.33}$$

and expanding $\rho_S(t + \Delta t)$ to first order in Δt, we find

$$\rho_S(t + \Delta t) = \rho_S(t) + \Delta t \frac{d}{dt}\rho_S(t) + \mathcal{O}\big(\Delta t^2\big). \tag{2.34}$$

This fixes the correct scaling of the M_k on Δt. We choose the $k = 0$ term to be proportional to the identity which will guarantee that in the limit of $\Delta t \to 0$ we get the correct result. Similarly, the other terms are proportional to $\sqrt{\Delta t}$ to ensure that products

$M_k(\ldots)M_k^\dagger$ are of order Δt. That is, we take

$$M_0 = I + G\Delta t, \qquad M_k = \sqrt{\Delta t}L_k, \qquad k \neq 0, \tag{2.35}$$

where G and L_k are arbitrary operators. Normalization of the Kraus operators leads to

$$\sum_k M_k^\dagger M_k = \big(I + G^\dagger\Delta t\big)\big(I + G\Delta t\big) + \Delta t\sum_{k\neq 0} L_k^\dagger L_k, \tag{2.36}$$

$$= I + (G + G^\dagger)\Delta t + \Delta t\sum_{k\neq 0} L_k^\dagger L_k + \mathcal{O}\big(\Delta t^2\big). \tag{2.37}$$

We can parametrize $G = K - iH$ where K and H are both Hermitian. It follows from the normalization condition

$$K = -\frac{1}{2}\sum_{k\neq 0} L_k^\dagger L_k. \tag{2.38}$$

We now substitute our results into Eq. (2.33) to finally get:

$$\rho_S(t+\Delta t) = \big(I + G\Delta t\big)\rho_S\big(I + G^\dagger\Delta t\big) + \Delta t\sum_{k\neq 0} L_k\rho_S L_k^\dagger, \tag{2.39}$$

$$= \rho_S(t) + \Delta t\big(G\rho_S + \rho_S G^\dagger\big) + \Delta t\sum_{k\neq 0} L_k\rho_S L_k^\dagger, \tag{2.40}$$

$$= \rho_S(t) - \frac{i}{\hbar}\Delta t[H,\rho_S] + \sum_{k\neq 0}\Big(L_k\rho_S L_k^\dagger - \frac{1}{2}\Big\{L_k^\dagger L_k, \rho_S\Big\}\Big). \tag{2.41}$$

Rearranging and taking the limit $\Delta t \to 0$ we get:

$$\frac{\rho_S(t+\Delta t) - \rho_S(t)}{\Delta t} = \frac{d}{dt}\rho_S = -\frac{i}{\hbar}[H,\rho_S] + \sum_{k\neq 0}\Big(L_k\rho_S L_k^\dagger - \frac{1}{2}\Big\{L_k^\dagger L_k, \rho_S\Big\}\Big), \tag{2.42}$$

which is exactly Eq. (2.32).

Chapter 3

Continuous Variable Formalism

3.1 Coherent States

A useful set of physical states are the coherent states. This basis allows the description of several experiments, most prominently in quantum optics where the electromagnetic field is described by quantized harmonic oscillators [2, 81]; it allows for the description of quantum many-body phenomena by means of the coherent path integral [82–86]; and, specially in quantum information, they represent a cornerstone in all facets of information processing [63, 79, 87, 88].

The coherent states $|\alpha\rangle$ are defined as the eigenstates of the anhilation operator a:

$$a\,|\alpha\rangle = \alpha\,|\alpha\rangle\,, \qquad |\alpha\rangle = e^{\alpha a^\dagger - \alpha^* a}\,|0\rangle\,, \tag{3.1}$$

where we will henceforth refer to $|0\rangle$ as the vacuum state. Although not crucial, it will be useful to state some properties of the coherent states [2, 73, 82]:

- Taking the hermitian conjugate of Eq. (3.1), we get the bra $\langle\alpha|$ which is a left eigenstate of the creation operator $a^\dagger$,

$$\langle\alpha|\,a^\dagger = \langle\alpha|\,\alpha^*, \tag{3.2}$$

  where α^* is the complex conjugate of α.

- The action of the creation operator a on the coherent state yields

$$a^\dagger |\alpha\rangle = \partial_\alpha |\alpha\rangle . \tag{3.3}$$

- The overlap between two coherent states is given by

$$\langle \mu|\alpha\rangle = e^{\mu^*\alpha - \frac{1}{2}|\mu|^2 - \frac{1}{2}|\alpha|^2}. \tag{3.4}$$

  In particular, the norm of a coherent state is $|\langle\alpha|\alpha\rangle|^2 = 1$.

- Most importantly, the coherent states form an overcomplete set of states:

$$\int \frac{d^2\alpha}{\pi} |\alpha\rangle\langle\alpha| = 1, \tag{3.5}$$

  where $d^2\alpha = d\,\mathrm{Re}\,\alpha\, d\,\mathrm{Im}\,\alpha$.

- The trace of a density matrix ρ in the coherent basis is given by

$$\mathrm{Tr}(\rho) = \int \frac{d^2\alpha}{\pi} \langle\alpha|\,\rho\,|\alpha\rangle . \tag{3.6}$$

- The expectation value of any operator $\mathcal{O}$ in the coherent basis is

$$\langle\mathcal{O}\rangle = \mathrm{Tr}(\rho\mathcal{O}) = \int \frac{d^2\alpha}{\pi} \langle\alpha|\rho\mathcal{O}|\alpha\rangle . \tag{3.7}$$

The coherent basis is particularly useful when representing the density matrix in quantum phase space, the quantum analogue of classical phase space. Among the different representations, we choose the Husimi-Q function [89]. This is defined as the expectation value of the density matrix ρ in the coherent basis $|\alpha\rangle$

$$Q(\alpha,\alpha^*) = \frac{1}{\pi}\langle\alpha|\rho|\alpha\rangle . \tag{3.8}$$

As an example, let us take ρ to be the thermal Gibbs state

$$\rho = \frac{e^{-\beta\omega a^\dagger a}}{\mathrm{Tr}\left(e^{-\beta\omega a^\dagger a}\right)}. \tag{3.9}$$

Its Husimi function will be

$$Q(\alpha,\alpha^*) = \frac{1-e^{-\beta\omega}}{\pi}\sum_{n=0}^{\infty} e^{-\beta\omega n}\,\langle\alpha|n\rangle\,\langle n|\alpha\rangle = \frac{1}{\pi(\bar{n}+1)}e^{-\frac{|\alpha|^2}{\bar{n}+1}}, \tag{3.10}$$

where $\bar{n} = (e^{\beta\omega}-1)^{-1}$ is the bosonic occupation number. We plot in Fig. 3.1 the Gibbs state with $\tilde{n} = 20$.

We can also use the Husimi function to calculate the expectation value of anti-normally ordered operators. That is operators of the form

$$\left\langle a^k (a^\dagger)^l \right\rangle = \int d^2\alpha\ \alpha^k (\alpha^*)^l Q(\alpha,\alpha^*), \tag{3.11}$$

which reduces to an integral in the complex plane of α.

3.2 Gaussian States and Maps

The Gibbs state is an example of a Gaussian state. These are characterized by their representation in quantum phase space where its Husimi-Q function is a Gaussian function of the coherent variables

$$Q(\alpha,\alpha^*) = \frac{1}{\pi\sqrt{|\Theta|}}\exp\Big(-\frac{1}{2}\vec{\alpha}^\dagger\Theta^{-1}\vec{\alpha}\Big), \quad \vec{\alpha} = (\alpha,\alpha^*), \tag{3.12}$$

where Θ is called the covariance matrix and $|\Theta|$ is the determinant of such matrix.

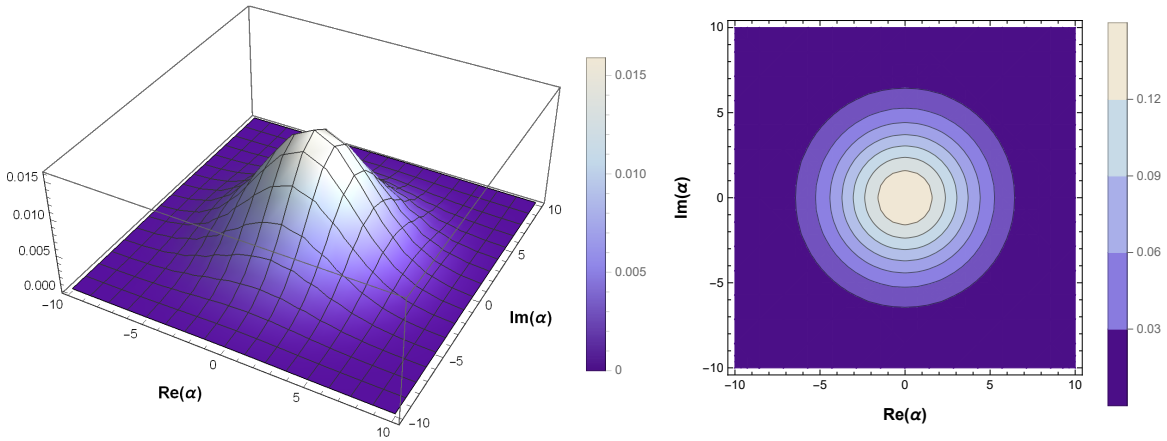

Figure 3.1: Husimi-Q function of the thermal Gibbs state with occupation number $\bar{n} = 20$.

Related to Gaussian states is the concept of Gaussian maps [67–69, 71, 90]. Gaussian maps are transformations that preserves Gaussianity. That is, that take Gaussian states into Gaussian states. Dynamically, this is achieved by imposing certain restrictions in the Lindblad equation (2.32):

- The Hamiltonian H must be at most quadratic in a and $a^\dagger$. Thus, the most general Gaussian preserving Hamiltonian has the form

$$H = \omega a^\dagger a + \gamma a^\dagger a^\dagger + \gamma^* a a + f a^\dagger + f^* a. \tag{3.13}$$

- The Lindblad generators L_k must be linear on a and $a^\dagger$. As an example the thermal bath generator

$$\mathcal{D}(\rho) = \gamma\bar{n}\big(a^\dagger \rho a - \frac{1}{2}\{aa^\dagger, \rho\}\big) + \gamma(\bar{n}+1)\big(a\rho a^\dagger - \frac{1}{2}\{a^\dagger a, \rho\}\big), \tag{3.14}$$

  is a Gaussian preserving map.

Gaussian states and Gaussian maps are an important tool since they simplify dramatically a potentially unsolvable problem. While, in general, continuous variable systems require an infinite dimensional Hilbert space, Gaussian states are fully determined by the first and second moments. Moreover, using Gaussian maps allows the dynamics to be described by a finite set of parameters. The reason is that for a Gaussian map, the equations for the first and second moments are closed, therefore reducing the complexity of the problem which otherwise would be intractable.

Even though we could, in principle, tackle the one-mode problem numerically, the approach becomes obsolete as we start considering multi-mode states. Gaussianity becomes esential to obtain analytical solutions.

3.3 Multi-mode States

We consider N bosonic modes with algebra given by

$$\big[a_i, a_j^\dagger\big] = \delta_{ij}, \quad \big[a_i, a_j\big] = 0, \tag{3.15}$$

and quadratures by

$$q_i = \frac{1}{\sqrt{2}}(a_i + a_i^\dagger), \quad p_i = \frac{i}{\sqrt{2}}(a_i^\dagger - a_i). \tag{3.16}$$

We would like to merge all these relations into a single condition. For this reason, we define two $2N$ dimensional vectors

$$\vec{X} = \left(a_1, a_1^\dagger, a_2, a_2^\dagger, \dots a_N, a_N^\dagger\right), \quad \vec{Y} = \left(q_1, p_1, q_2, p_2, \dots q_N, p_N\right). \tag{3.17}$$

These two vectors are equivalent representations of the N bosonic modes. It will be convenient to write down the basic results for both of them. The connection between these two vectors is given by

$$\vec{Y} = \Lambda \vec{X}, \quad \Lambda = \bigoplus_{i=1}^{N} \begin{pmatrix} \frac{1}{\sqrt{2}} & \frac{1}{\sqrt{2}} \\ -\frac{i}{\sqrt{2}} & \frac{i}{\sqrt{2}} \end{pmatrix}, \tag{3.18}$$

where Λ is a unitary transformation analogue to (3.16). Additionally, the multi-mode commutation relations (3.15) are now condensed in the vector commutators

$$\left[\vec{X}, \vec{X}^{\mathrm{T}}\right] = \bigoplus_{i=1}^{N} \begin{pmatrix} 1 & 0 \\ 0 & -1 \end{pmatrix}, \quad \left[\vec{Y}, \vec{Y}^{\mathrm{T}}\right] = \bigoplus_{i=1}^{N} \begin{pmatrix} 0 & 1 \\ -1 & 0 \end{pmatrix}, \tag{3.19}$$

where the vector commutator is defined as $\left[\vec{A}, \vec{B}^{\mathrm{T}}\right] = \vec{A} \otimes \vec{B}^{\mathrm{T}} - (\vec{B}^{\mathrm{T}} \otimes \vec{A})^{\mathrm{T}}$. Equations (3.17)-(3.19) establishes the algebra of the group of operators.

As mentioned in the previous section, we are interested in the first and second moments. We define the first moments $\vec{x}$ and $\vec{y}$ related to $\vec{X}$ and $\vec{Y}$ as simply $x_i = \langle X_i \rangle$ and $y_i = \langle Y_i \rangle$. More interesting, we define the covariance matrices (CM) as

$$\Theta = \frac{1}{2}\langle \{X_i, X_j^\dagger\} \rangle - \langle X_i \rangle \langle X_j^\dagger \rangle, \quad \sigma = \frac{1}{2}\langle \{Y_i, Y_j\} \rangle - \langle Y_i \rangle \langle Y_j \rangle, \tag{3.20}$$

where by construction Θ is Hermitian, and σ is real and symmetric. For example, for two

modes the covariance matrices would look like:

$$\sigma = \begin{pmatrix} \langle q_1^2 \rangle & \frac{1}{2}\langle\{q_1, p_1\}\rangle & \langle q_1 q_2 \rangle & \langle q_1 p_2 \rangle \\ \frac{1}{2}\langle\{q_1, p_1\}\rangle & \langle p_1^2 \rangle & \langle p_1 q_2 \rangle & \langle p_1 p_2 \rangle \\ \langle q_2 q_1 \rangle & \langle q_2 p_1 \rangle & \langle q_2^2 \rangle & \frac{1}{2}\langle\{q_2, p_2\}\rangle \\ \langle p_2 q_1 \rangle & \langle p_2 p_1 \rangle & \frac{1}{2}\langle\{q_2, p_2\}\rangle & \langle p_2^2 \rangle \end{pmatrix}, \tag{3.21}$$

and

$$\Theta = \begin{pmatrix} \langle a_1^\dagger a_1 \rangle + \frac{1}{2} & \langle a_1 a_1 \rangle & \langle a_1 a_2^\dagger \rangle & \langle a_1 a_2 \rangle \\ \langle a_1^\dagger a_1^\dagger \rangle & \langle a_1^\dagger a_1 \rangle + \frac{1}{2} & \langle a_1^\dagger a_2^\dagger \rangle & \langle a_1^\dagger a_2 \rangle \\ \langle a_1^\dagger a_2 \rangle & \langle a_1 a_2 \rangle & \langle a_2^\dagger a_2 \rangle + \frac{1}{2} & \langle a_2 a_2 \rangle \\ \langle a_1^\dagger a_2^\dagger \rangle & \langle a_1 a_2^\dagger \rangle & \langle a_2^\dagger a_2^\dagger \rangle & \langle a_2^\dagger a_2 \rangle + \frac{1}{2} \end{pmatrix}, \tag{3.22}$$

where is implicitly assumed that $\langle a_i \rangle = 0$. Notice that the covariance matrix is structured in 2×2 blocks where the diagonal blocks are the CMs of modes 1 and 2, while the off-diagonal blocks represent their correlations. These two matrices are also related via the unitary transformation (3.18), namely

$$\sigma = \Lambda \, \Theta \, \Lambda^\dagger. \tag{3.23}$$

3.4 Gaussian Dynamics

We now focus on the dynamical evolution of Gaussian states subject to the Lindblad equation:

$$\frac{d}{dt}\rho = -i[H, \rho] + \mathcal{D}(\rho), \tag{3.24}$$

where H is a Gaussian Hamiltonian and $\mathcal{D}$ is a Gaussian preserving dissipator. Given the master equation, we can obtain the evolution of any observable by taking the expectation value of such operator:

$$\frac{d}{dt}\langle \mathcal{O} \rangle = i\langle [H, \mathcal{O}] \rangle + \mathrm{Tr}(\mathcal{O}\mathcal{D}(\rho)). \tag{3.25}$$

Using the cyclic property of the trace, we can write

$$\mathrm{Tr}\left(\mathcal{O}\left(L\rho L^\dagger - \frac{1}{2}\{L^\dagger L, \rho\}\right)\right) = \langle L^\dagger \mathcal{O} L - \frac{1}{2}\{L^\dagger L, \mathcal{O}\}\rangle := \langle \tilde{\mathcal{D}}(\mathcal{O})\rangle. \tag{3.26}$$

Hence, we can rewrite Eq. (3.25) as:

$$\frac{d}{dt}\langle \mathcal{O}\rangle = i\langle [H, \mathcal{O}]\rangle + \langle \tilde{\mathcal{D}}(\mathcal{O})\rangle. \tag{3.27}$$

So far we haven't use the fact that the evolution is described by Gaussian maps. Imposing Gaussianity results in the equations for the first and second moments to close. That means that the expected values of operators like $\langle a_i\rangle$ or $\langle a_i^\dagger a_j\rangle - \langle a_i^\dagger\rangle\langle a_j\rangle$ will only depend on the elements of the vector $\vec{x}$ and the covariance matrix Θ. In contrast, in the non-Gaussian scenario the equations for these moments will depend also on the higher moments, leading to an infinite hierarchy of coupled equations. Thus, the Gaussian dynamics will be encapsulated in the evolution of the vector of averages and the covariance matrix.

Taking the evolution of the vector of averages $\vec{x}$ and $\vec{y}$ into Eq. (3.27) we get

$$\frac{d}{dt}\vec{x} = W\vec{x} - \vec{f}, \quad \frac{d}{dt}\vec{y} = M\vec{y} - \vec{g}, \tag{3.28}$$

where W and M depend on the choice of Hamiltonian H while $\vec{f}$ and $\vec{g}$ on the choice of dissipator $\mathcal{D}$. Similarly, we get for the covariance matrices:

$$\frac{d}{dt}\Theta = W\Theta + \Theta W^\dagger + F, \quad \frac{d}{dt}\sigma = M\sigma + \sigma M^{\mathrm{T}} + G, \tag{3.29}$$

where the matrices F and G depend only on the dissipator $\mathcal{D}$ whereas the matrices W and M are the same as Eq. (3.28).

Let us illustrate the procedure with two simple examples that we will further explore in Chapter 4. Suppose we have two bosonic modes a_1 and a_2 interacting via a beam-splitter Hamiltonian

$$H_{BS} = ig(a_1^\dagger a_2 - a_2^\dagger a_1). \tag{3.30}$$

This will create/destroy a particle in one mode and destroy/create a particle in the other

mode, conserving always the total number of particles $N = a_1^\dagger a_1 + a_2^\dagger a_2$. We use Eq. (3.27) to get the first moments evolution

$$\frac{d\langle a_1\rangle}{dt} = \langle i\big[H_{BS}, a_1\big]\rangle = g\langle a_2\rangle, \tag{3.31}$$

$$\frac{d\langle a_1^\dagger\rangle}{dt} = \langle i\big[H_{BS}, a_1^\dagger\big]\rangle = g\langle a_2^\dagger\rangle, \tag{3.32}$$

$$\frac{d\langle a_2\rangle}{dt} = \langle i\big[H_{BS}, a_2\big]\rangle = -g\langle a_1\rangle, \tag{3.33}$$

$$\frac{d\langle a_2^\dagger\rangle}{dt} = \langle i\big[H_{BS}, a_2^\dagger\big]\rangle = -g\langle a_1^\dagger\rangle. \tag{3.34}$$

The matrix W associated to this beam-splitter Hamiltonian is given by

$$W_{BS} = \begin{pmatrix} 0 & 0 & g & 0 \\ 0 & 0 & 0 & g \\ -g & 0 & 0 & 0 \\ 0 & -g & 0 & 0 \end{pmatrix}. \tag{3.35}$$

The solution for the first moments vector $\vec{x}(t)$ is thus

$$\vec{x}(t) = V_{BS}(t)\,\vec{x}_0, \tag{3.36}$$

where the V_{BS} matrix introduced is

$$V_{BS}(t) := e^{W_{BS}t} = \begin{pmatrix} \cos(gt) & 0 & \sin(gt) & 0 \\ 0 & \cos(gt) & 0 & \sin(gt) \\ -\sin(gt) & 0 & \cos(gt) & 0 \\ 0 & -\sin(gt) & 0 & \cos(gt) \end{pmatrix}. \tag{3.37}$$

It will be useful to re-state this matrix in terms of 2×2 blocks

$$V_{BS}(t) = \begin{pmatrix} \cos(gt)\mathbb{I} & \sin(gt)\mathbb{I} \\ -\sin(gt)\mathbb{I} & \cos(gt)\mathbb{I} \end{pmatrix}, \tag{3.38}$$

where $\mathbb{I}$ is the 2×2 identity matrix.

We can also obtain the $\vec{y}(t)$ solution by the interdependence relation (3.18),

$$\vec{y}(t) = S_{BS}(t)\,\vec{y}_0, \quad S_{BS}(t) = \Lambda^\dagger\, V_{BS}(t)\,\Lambda = \begin{pmatrix} \cos(gt)\mathbb{I} & \sin(gt)\mathbb{I} \\ -\sin(gt)\mathbb{I} & \cos(gt)\mathbb{I} \end{pmatrix}. \tag{3.39}$$

Likewise, the solution for the covariance matrices are:

$$\Theta(t) = V_{BS}(t)\,\Theta_0\,V_{BS}^\dagger(t), \quad \sigma(t) = S_{BS}(t)\,\sigma_0\,S_{BS}^{\mathrm{T}}(t). \tag{3.40}$$

Particularly, we will be interested in obtaining the solution of one of the modes (the system) by tracing out the other modes (environment). This is achieved by looking at the system's block term in Eq. (3.40). As an example, let us take the first mode as the system and the second mode as the environment. Tracing out the second mode, we get:

$$\sigma_1(t) = \cos^2(gt)\,\sigma_1(0) + \sin^2(gt)\,\sigma_2(0). \tag{3.41}$$

This equation can be also expressed as:

$$\sigma_1(t) = X\sigma_1(0)X^{\mathrm{T}} + Y, \tag{3.42}$$

where $X = \cos(gt)\,\mathbb{I}$, and $Y = \sin^2(gt)\,\sigma_2(0)$. This is the Gaussian analogue of Eq. (2.30) and it is known as a Gaussian CPTP map.

Another Gaussian Hamiltonian we will be interested in is the two-mode squeezing

$$H_{SQ} = i\mu(a_1^\dagger a_2^\dagger - a_2 a_1). \tag{3.43}$$

In opposition to the beam-splitter, this Hamiltonian does not conserve the total number of particles N: it creates/destroys a particle in both modes with strength μ.

The equations of motion for the first moments are:

$$\frac{d\langle a_1\rangle}{dt} = \langle i\big[H_{SQ}, a_1\big]\rangle = \mu\langle a_2^\dagger\rangle, \tag{3.44}$$

$$\frac{d\langle a_1^\dagger\rangle}{dt} = \langle i\big[H_{SQ}, a_1^\dagger\big]\rangle = \mu\langle a_2\rangle, \tag{3.45}$$

$$\frac{d\langle a_2\rangle}{dt} = \langle i\big[H_{SQ}, a_2\big]\rangle = \mu\langle a_1^\dagger\rangle, \tag{3.46}$$

$$\frac{d\langle a_2^\dagger\rangle}{dt} = \langle i\big[H_{SQ}, a_2^\dagger\big]\rangle = \mu\langle a_1\rangle. \tag{3.47}$$

The matrix W associated with this Hamiltonian is

$$W_{SQ} = \begin{pmatrix} 0 & 0 & 0 & \mu \\ 0 & 0 & \mu & 0 \\ 0 & \mu & 0 & 0 \\ \mu & 0 & 0 & 0 \end{pmatrix}. \tag{3.48}$$

Similar solutions (3.36)-(3.40) are obtained for the two-mode squeezing provided we change V_{BS} with the corresponding V_{SQ} matrix

$$V_{SQ}(t) := e^{W_{SQ}t} = \begin{pmatrix} \cosh(\mu t)\mathbb{I} & \sinh(\mu t)\sigma_x \\ \sinh(\mu t)\sigma_x & \cosh(\mu t)\mathbb{I} \end{pmatrix}, \tag{3.49}$$

and change S_{BS} with S_{SQ}

$$S_{SQ}(t) = \Lambda^\dagger\, V_{SQ}(t)\, \Lambda = \begin{pmatrix} \cosh(\mu t)\mathbb{I} & \sinh(\mu t)\sigma_z \\ \sinh(\mu t)\sigma_z & \cosh(\mu t)\mathbb{I} \end{pmatrix}, \tag{3.50}$$

where σ_x and σ_z are the familiar 2×2 Pauli Matrices.

Finally, we can get the CPTP Gaussian map (3.42) for the two-mode squeezing:

$$\sigma_1(t) = \cosh^2(\mu t)\, \sigma_1(0) + \sinh^2(\mu t)\, \sigma_z\, \sigma_2(0)\, \sigma_z, \tag{3.51}$$

where $X = \cosh(\mu t)\, \mathbb{I}$, and $Y = \sinh^2(\mu t)\, \sigma_z\, \sigma_2(0)\, \sigma_z$.

Chapter 4

Collisional Models

This chapter contains one of the main original results developed in this dissertation. It presents the theoretical model to be studied in these last chapters. The exposition here follows closely Sec. II of the submitted arXiv preprint [91].

4.1 Motivation

As we have seen previously, obtaining a microscopic description of the open quantum system's dynamics is a really complicated task, often relying on approximation schemes to get analytical results. We particularly analyzed the case of a qubit interacting with a bosonic environment and realized how many approximations were made to obtain the system's evolution. This motivates the search for alternative models, where analytic equations can be obtained without resourcing to such severe approximations. One way to accomplish this, which has seen an enormous surge in popularity in recent years, are through the so-called collisional models [31–42, 91]. The basic idea is to replace the open dynamics of a system by a series of sequential interactions between the system S and small environmental units E_1, E_2, E_3 ... (also referred to as ancillas). All interactions lasts for a fixed time after which they never interact again. This therefore leads to a stroboscopic dynamics for the system.

The collisional model we are interested in this work is the one depicted in Fig. 4.1. That is, we consider a scenario where neighboring ancillas E_nE_{n+1} interact with each other in between the interactions SE_n and SE_{n+1}. This additional interaction *signals*

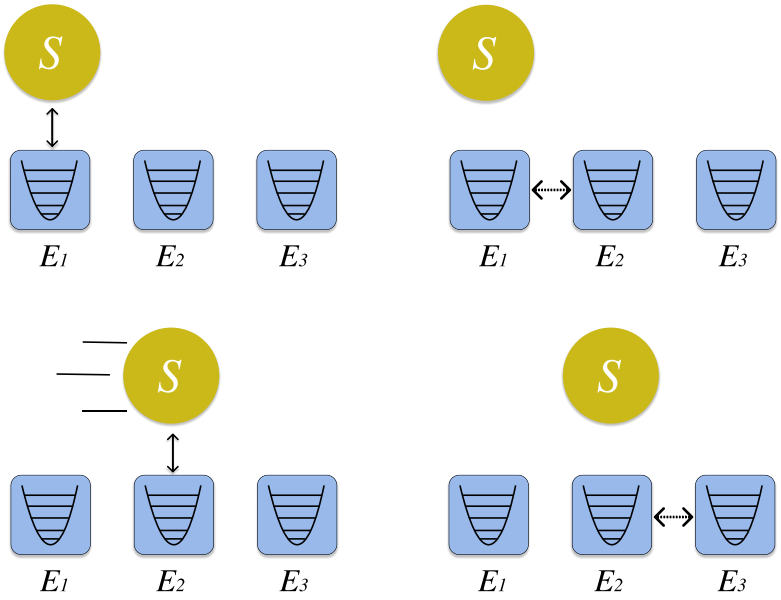

Figure 4.1: First few steps of the collisional model dynamics. The system-ancilla interactions SE_n are interspersed by ancilla-ancilla interactions E_nE_{n+1}, which propagate information forward, making the dynamics non-Markovian in a fully controballe way.

information from the past to the future, so that when the SE_{n+1} interaction arrives, the ancilla E_{n+1} will already contain some information about the system.

4.2 Formal Framework

Here we consider the collisional model scenario presented in Fig. 4.1. A system S is put to interact sequentially with an arbitrary number of environment ancillas E_1, E_2, E_3 ... The ancillas are independent and identically prepared, each with the initial density matrix ρ_E. The interaction between S and E_n is described by a unitary U_n. After this, S and E_n never interact again. After the collision SE_n but before the SE_{n+1}, we put ancillas E_n and E_{n+1} to interact with each other by means of another unitary $V_{n,n+1}$. Since E_n already interacted with S, it contains some information about each other, obtained from E_n. Past information about S can thus *backflow* at SE_{n+1}.

Let $\rho^0 = \rho_S \otimes \rho_{E_1} \otimes \rho_{E_2} \otimes$ ... denote the initial state of the composite system SE_1E_2 ... We count time in integer steps, such that at time n the collisions SE_n and E_nE_{n+1} already took place. That is, at time n the system has already interacted with its corresponding

ancilla E_n *and* this ancilla has already passed down its information to the next one. The map taking the composite system SE_1E_2 ... from $n-1$ to n reads

$$\rho^n = V_{n,n+1} U_n \, \rho^{n-1} \, U_n^\dagger V_{n,n+1}^\dagger. \tag{4.1}$$

To avoid confusion we henceforth use superscripts to denote time so that ρ^n refers to the global state of SE_1E_2 ... at time n. The map (4.1) involves only SE_nE_{n+1}. All ancillas E_m with $m \geq n+2$ did not yet participate in the process and therefore remain in a product state with everything else. In addition, the ancillas with $m < n$ will never participate again and hence can be traced out (discarded). The process (4.1) can thus be equivalently written as

$$\rho^n_{SE_nE_{n+1}} = V_{n,n+1} U_n \big(\rho^{n-1}_{SE_n} \otimes \rho_{E_{n+1}}\big) U_n^\dagger V_{n,n+1}^\dagger, \tag{4.2}$$

where $\rho^{n-1}_{SE_n}$ is the state of SE_n at time $n-1$ and $\rho_{E_{n+1}} = \rho_E$ refers to the initial state of E_{n+1}. This also holds for the first step, provided one recalls that $\rho^0_{SE_1} = \rho^0_S \otimes \rho_{E_1}$. After the interaction (4.2), one may trace out E_n, leading to

$$\rho^n_{SE_{n+1}} = \mathrm{Tr}_{E_n}\Big(V_{n,n+1} U_n \big(\rho^{n-1}_{SE_n} \otimes \rho_{E_{n+1}}\big) U_n^\dagger V_{n,n+1}^\dagger\Big) := \Phi(\rho^{n-1}_{SE_n}). \tag{4.3}$$

This can now be fed again to Eq. (4.2) to evolve to the next step. This equation also defines the quantum channel $\Phi(.)$, which is a map from the Hilbert space of SE_n to that of SE_{n+1}. Moreover, since we are assuming that the unitaries U_n and $V_{n,n+1}$ are the same for all collisions, the map Φ itself is actually independent of n; the only n dependence is in the input $\rho^{n-1}_{SE_n}$.

Crucially, we see that the map $\Phi(.)$ is both time-local and completely positive since it is written as a Stinespring dilation [92]. Hence, it represents an entirely Markovian evolution. Eq. (4.3) is known as a Markovian embedding of the dynamics [59]: it expresses a non-Markovian evolution as a Markovian one at the expense of working with maps that act between different Hilbert spaces and also have a higher dimension.

It is convenient to define the more compact notation $\varrho^n = \rho^n_{SE_{n+1}}$ for the joint state of SE_{n+1} at time n. The entire dynamics can then be captured by the stroboscopic,

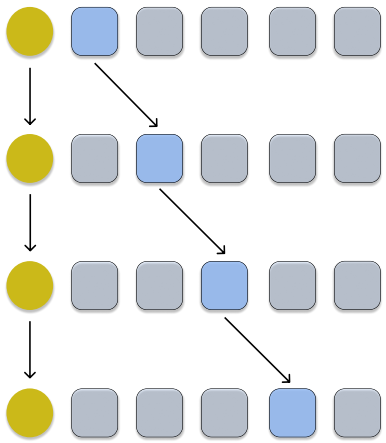

Figure 4.2: Basic structure of the Markovian embedding dynamics (4.20), which is a map from the Hilbert space of SE_n to that of SE_{n+1}

Markovian, CPTP evolution:

$$\varrho^{n+1} = \Phi(\varrho^n), \tag{4.4}$$

and the corresponding sequence of states ϱ^0, ϱ^1, ϱ^2, ... that it generates. At each step, the reduced state of the system is always available as $\rho_S^n = \mathrm{Tr}_{E_{n+1}}\, \varrho^n$. The Markovian embedding (4.4) will be central to this work.

Since initially the system is uncorrelated from all ancillas, it is possible to define a CPTP map taking $\rho_S^0 \to \rho_S^n$:

$$\rho_S^n = \mathcal{E}_n(\rho_S^0) = \mathrm{Tr}_{E_{n+1}}\, \Phi^n(\rho_S^0 \otimes \rho_{E_1}). \tag{4.5}$$

Even though this map is CPTP, the map taking $\rho_S^m \to \rho_S^n$ will not generally be CPTP due to the non-Markovian dynamics.

4.3 Gaussian Collisional Model

We are interested in obtaining analytical results. To accomplish this, we therefore specialize now to the case of continuous-variable systems undergoing Gaussian-preserving dynamics reviewed in Chapter 3. Our exposition, in what follows, will be example oriented. However, the final results will be quite general [Eqs. (4.19), (4.20) and (4.22)].

We assume the system S is described by bosonic annhilation operator a and corresponding quadrature $Q = (a + a^\dagger)/\sqrt{2}$ and $P = i(a^\dagger - a)/\sqrt{2}$. Similarly, the ancillas are described by bosonic annhilation operators b_1, b_2, ... with corresponding quadratures q_n, p_n. The generalization to multimode system is straightforward. We take the system-ancilla interaction U_n in Eq. (4.2) to be a simple beam-splitter-type unitary

$$U_n = e^{\lambda_s(a^\dagger b_n - b_n^\dagger a)}, \tag{4.6}$$

described by a parameter λ_s. One can view (4.6) as an interaction with a Hamiltonian $ig(a^\dagger b_n - b_n^\dagger a)$ that lasts for a time τ such that $g\tau = \lambda_s$. Since we are only interested in the stroboscopic dynamics, we can omit the internal details for simplicity. As for the E_nE_{n+1} collision unitary $V_{n,n+1}$, we shall explore two possibilities. The first is again a beam-splitter map

$$V_{n,n+1} = e^{\lambda_e(b_n^\dagger b_{n+1} - b_{n+1}^\dagger b_n)}, \tag{4.7}$$

with interaction strength λ_e. We shall henceforth refer to this as the BS dynamics. In addition, we shall also look at a two-mode squeezing interaction (TMS),

$$\tilde{V}_{n,n+1} = e^{\nu_e(b_n^\dagger b_{n+1}^\dagger - b_{n+1} b_n)}, \tag{4.8}$$

with strength ν_e and view (4.8) as coming from a Hamiltonian $ig(b_n^\dagger b_{n+1}^\dagger - b_{n+1}b_n)$ for a time τ such that $g\tau = \nu_e$. The reason behind this choice is related to the fact that two-mode squeezing interactions generate stronger forms of correlations (e.g. entanglement) between the ancillas.

The unitaries (4.6)-(4.8) are Gaussian preserving. If we assume that the initial state is Gaussian, the dynamics will then be completely characterized by the first and second moments. We assume for simplicity that the first moments are initially zero so that they will remain so throughout. The covariance matrix of the initial state is block-diagonal, of the form

$$\sigma^0 = \text{diag}(\theta^0, \epsilon, \epsilon, ...), \tag{4.9}$$

where each block is 2×2: θ^0 is the arbitrary initial CM of the system and ϵ is the initial CM of the ancillas (which are all the same, since we are assuming the ancillas are iid).

The global dynamics of $SE_1E_2\ldots$ is unitary. As a consequence, the map (4.1) is translated into a symplectic evolution for the CM:

$$\sigma^n = S_{n,n+1}S_n\ \sigma^{n-1}S_n^{\mathrm{T}}S_{n,n+1}^{\mathrm{T}}, \tag{4.10}$$

where S_n and $S_{n,n+1}$ are the symplectic matrices associated with the unitaries U_n and $V_{n,n+1}$. The symplectic matrix associated to the beam-splitter interaction (4.6) is remarkably simple because all entries are proportional to the 2×2 identity (3.39) [this is partially because of the choice of phase in the exponent of (4.6)]. For instance, the interaction S_2 between the S and E_2 reads

$$S_2 = \begin{pmatrix} x & 0 & y & 0 & \ldots \\ 0 & 1 & 0 & 0 & \ldots \\ -y & 0 & x & 0 & \ldots \\ 0 & 0 & 0 & 1 & \ldots \\ \vdots & \vdots & \vdots & \vdots & \ddots \end{pmatrix}, \tag{4.11}$$

where each entry is a 2×2 matrix, with $x=\cos(\lambda_s)$ and $y=\sin(\lambda_s)$. The same structure also holds for the BS unitary $V_{n,n+1}$ between E_nE_{n+1} [Eq. (4.7)], except that now the position of the non-zero entries changes. For instance,

$$S_{1,2} = \begin{pmatrix} 1 & 0 & 0 & 0 & \ldots \\ 0 & z & w & 0 & \ldots \\ 0 & -w & z & 0 & \ldots \\ 0 & 0 & 0 & 1 & \ldots \\ \vdots & \vdots & \vdots & \vdots & \ddots \end{pmatrix}, \tag{4.12}$$

where $z=\cos(\lambda_e)$ and $w=\sin(\lambda_e)$. The TMS interaction (4.8) is slightly more complicated since some entries are proportional to the identity, while others are proportional to

the Pauli matrix σ_z as seen in (3.50). For instance,

$$\tilde{S}_{1,2} = \begin{pmatrix} 1 & 0 & 0 & 0 & \dots \\ 0 & \tilde{z} & \tilde{w}\sigma_z & 0 & \dots \\ 0 & \tilde{w}\sigma_z & \tilde{z} & 0 & \dots \\ 0 & 0 & 0 & 1 & \dots \\ \vdots & \vdots & \vdots & \vdots & \ddots \end{pmatrix}, \tag{4.13}$$

with $\tilde{z} = \cosh(\nu_e)$ and $\tilde{w} = \sinh(\nu_e)$.

The BS dynamics is completely characterized by the pair (λ_s, λ_e), while the TMS dynamics is characterized by (λ_s, ν_e). On top of that, one also has the choice of ancilla initial state ϵ. More general Gaussian maps will continue to have a similar structure. The symplectic S_n will have the form

$$S_2 = \begin{pmatrix} A & 0 & B & 0 & \dots \\ 0 & 1 & 0 & 0 & \dots \\ C & 0 & D & 0 & \dots \\ 0 & 0 & 0 & 1 & \dots \\ \vdots & \vdots & \vdots & \vdots & \ddots \end{pmatrix}, \tag{4.14}$$

for block matrices A, B, C, D. The matrices S_n for other values of n are obtained by simply placing A, B, C, D at the correct positions. Note also that the condition that S must be symplectic imposes constraints on A, B, C, D which, however, are not particularly illuminating. Similarly, the $E_n E_{n+1}$ interaction reads

$$\tilde{S}_{1,2} = \begin{pmatrix} 1 & 0 & 0 & 0 & \dots \\ 0 & E & F & 0 & \dots \\ 0 & G & J & 0 & \dots \\ 0 & 0 & 0 & 1 & \dots \\ \vdots & \vdots & \vdots & \vdots & \ddots \end{pmatrix}, \tag{4.15}$$

for block matrices E, F, G, J. Note that these two expressions also naturally contemplate the case where either the system or each ancilla are, individually, composed of multiple

modes (which would simply affect the size of the matrices $A, \ldots, J$).

4.4 Markovian Embedding

The biggest advantage of Gaussian collisional models, as we will now show, is that the full evolution can be converted into a simple system of matrix difference equations for only a handful of entries of the full CM σ^n. As already discussed below Eq. (4.2), the step from σ^{n-1} to σ^n involves only S, E_n and E_{n+1}. At time $n-1$ the ancilla E_{n+1} is still uncorrelated from the rest, whereas S and E_n are already correlated because of the previous step. Thus, the tripartite CM of SE_nE_{n+1}, at time $n-1$, will have the block structure

$$\sigma^{n-1}_{SE_nE_{n+1}} = \begin{pmatrix} \theta^{n-1} & \xi_n^{n-1} & 0 \\ \xi_n^{n-1,\mathrm{T}} & \epsilon_n^{n-1} & 0 \\ 0 & 0 & \epsilon \end{pmatrix}, \tag{4.16}$$

where ϵ_n^{n-1} is the state of ancilla E_n at time $n-1$, which is no longer the original value ϵ because it already interacted with E_{n-1} in the previous step. Moreover, ξ_n^{n-1} are the correlations between SE_n that were developed in the previous step. We then apply the map (4.10) to Eq. (4.16), using the matrices in Eqs. (4.11)-(4.13)

$$\sigma^{n}_{SE_nE_{n+1}} = S_{n,n+1}S_n \left(\sigma^{n-1}_{SE_nE_{n+1}}\right) S_n^{\mathrm{T}} S_{n,n+1}^{\mathrm{T}}. \tag{4.17}$$

This will lead to a matrix σ^n with many non-zero entries. However, as far as the dynamics of S is concerned, only three entries are needed: the state of the system θ^n, the state ϵ^n_{n+1} of ancilla E_{n+1} and the correlations ξ^n_{n+1} between S and E_{n+1}.

To gain intuition, let us first analyze the BS case, which is simple since all blocks in Eq. (4.12) are proportional to the identity. Using Eqs. (4.11) and (4.12) in (4.17), one

finds the following system of matrix difference equations:

$$\begin{aligned}
\theta^n &= x^2\theta^{n-1} + y^2\epsilon_n^{n-1} + xy(\xi_n^{n-1} + \xi_n^{n-1,\mathrm{T}}),\\
\epsilon_{n+1}^n &= z^2\epsilon + w^2\Big[x^2\epsilon_n^{n-1} + y^2\theta^{n-1} - xy(\xi_n^{n-1} + \xi_n^{n-1,\mathrm{T}})\Big],\\
\xi_{n+1}^n &= w\Big[xy(\theta^{n-1} - \epsilon_n^{n-1}) + y^2\xi_n^{n-1,\mathrm{T}} - x^2\xi_n^{n-1}\Big].
\end{aligned} \tag{4.18}$$

This provides a neat illustration of the map $\Phi(\,\cdot\,)$ in Eq. (4.3): the quantities on the left-hand and right-hand side refer to different ancillas: for instance, ϵ_{n+1}^n is the state of ancilla E_{n+1} at time n, whereas ϵ_n^{n-1} is the state of E_n at time $n-1$. Of course, one could also compute ϵ_n^n, but this is not necessary for describing the dynamics of S.

The system of matrix difference equations (4.18) contains the minimum amount of information required to fully account for the dynamics of S. These equations can also be recast in a more compact form in terms of the Markovian embedding (4.4). We define the reduced CM of SE_{n+1} at time n as

$$\gamma_{n+1}^n \equiv \gamma^n = \begin{pmatrix} \theta^n & \xi_{n+1}^n \\ \xi_{n+1}^{n,\mathrm{T}} & \epsilon_{n+1}^n \end{pmatrix}, \tag{4.19}$$

where the notation γ^n will be used to simplify the expressions. Eq. (4.18) can then be written compactly as

$$\gamma^{n+1} = X\gamma^n X^{\mathrm{T}} + Y, \tag{4.20}$$

where the time index was shifted by 1. Here X and Y are 4×4 matrices with block form

$$X = \begin{pmatrix} x & y \\ yw & -wx \end{pmatrix}, \qquad Y = \begin{pmatrix} 0 & 0 \\ 0 & z^2\epsilon \end{pmatrix}, \tag{4.21}$$

where, again, each block is proportional to the identity.

Eq. (4.20) beautifully illustrates the notion of Markovian embedding. It has the structure of a typical Gaussian CPTP map (3.40), being Markovian (time-local) by construction. However, this Markovian dynamics takes place at the larger space of the system plus one ancilla (which one, in specific, changes at each collision). Thus, we have embedded

the non-Markovian dynamics into a Markovian dynamics at a larger space. Notice how the size of the space is directly related to the fact that we chose E_n to only interact with its nearest neighbor E_{n+1}. That is, we fixed the memory length to be 1, which defines the size of the minimal space required for the embedding [59].

The matrices (4.21) refer to the beam-splitter unitary (4.7). The generalization to the arbitrary Gaussian interactions (4.14) and (4.15) is similar, albeit more cumbersome. The result is

$$X = \begin{pmatrix} A & B \\ GC & GD \end{pmatrix}, \qquad Y = \begin{pmatrix} 0 & 0 \\ 0 & J\epsilon J^{\mathrm{T}} \end{pmatrix}. \tag{4.22}$$

For instance, in the case of the TMS interaction, Eq. (4.13), one has $G = \tilde{w}\sigma_z$ and $J = \tilde{z}$, in addition to $A = D = x$, $B = y$ and $C = -y$ (which come from S_n in (4.11)). One then finds that

$$X = \begin{pmatrix} x & y \\ -y\tilde{w}\sigma_z & \tilde{w}x\sigma_z \end{pmatrix}, \qquad Y = \begin{pmatrix} 0 & 0 \\ 0 & \tilde{z}^2\epsilon \end{pmatrix}. \tag{4.23}$$

The blocks in X are therefore no longer proportional to the identity, but some are proportional to σ_z.

To summarize, the general non-Markovian dynamics will be described by the embedding (4.20), with γ^n defined in (4.19), and with X and Y given by (4.22). This framework therefore provides a quite general platform, enabling one to study a broad range of situations.

4.5 Example Dynamics

Eqs (4.20)-(4.23) are the first main results of this work. They provide a compact and efficient way of describing the non-Markovian dynamics of a bosonic mode in terms of a simple matrix difference equation for the augmented CM γ^n. The reduced state of the system is always readily accessible from the first 2×2 block [Eq. (4.19)]. Before proceeding to quantify the non-Markovianity of the process, we first illustrate the typical behavior of the BS and TMS maps, by plotting the average system occupation $\langle a^\dagger a \rangle$ as a function of time for different values of the E_nE_{n+1} interaction strength λ_e (for the BS case) or ν_e (for the TMS case). We choose the system to start in a thermal state with

occupation number $\langle a^\dagger a\rangle^0 = 20$, while the ancillas start in the vacuum, $\epsilon = \mathbb{I}_2/2$. The results are summarized in Fig. 4.3 for the BS evolution and in Fig. 4.4 for the TMS evolution.

The BS dynamics is sensitive to the relative signs between λ_s and λ_e (and, consequently, of $y = \sin(\lambda_s)$ and $w = \sin(\lambda_e)$). This is an interference effect, which occurs due to the fact we are combining two beam-splitters [Eqs. (4.6) and (4.7)]. A similar effect was also observed in Refs [61, 62]. We emphasize this in Fig. 4.3 by comparing $\lambda_e > 0$ and $\lambda_e < 0$, with $\lambda_s > 0$. In both cases we see that for small λ_e the system's excitations [Fig. 4.3(a,b)] tend to decay monotonically, which is what one would expect of a Markovian BS interaction with a vacuum bath. For larger λ_e, on the other hand, the occupations present oscillations. Since the interaction conserves the number of quanta, these revivals in excitations must necessarily be due to a backflow caused by the non-Markovian behavior. That is, some of the excitations that leave the system towards E_n are transferred from E_n to E_{n+1} and then make it back into the system in the SE_{n+1} interaction. The nature of these oscillations, however, is different whether $\lambda_e > 0$ or $\lambda_e < 0$, being fast in the former and slow in the latter. Irrespective of the value of λ_e, however, after an infinite time the system will always thermalize to the ancilla's state, which in this case means $\langle a^\dagger a\rangle^\infty = 0$ [the only exception is at $\lambda_e = \pm\pi/2$, which is somewhat pathological]. Despite its resemblance with the system's behavior, the ancilla's excitations [Fig. 4.3(c,d)] will have some unique features. First, the excitations spike at the first steps and then tend to decay monotonically. There are no lost particles yet and the ancilla gets the maximum amount from the system. And second, the number of excitations oscillates in the opposite manner to the system's oscillations. This is due to the conservation of total number of quanta: the amount that the system loses, the ancilla gains it. Finally, we can also look at the correlations build between the system and the n^{th} ancilla [Fig. 4.3(e,f)]. The modulus of the correlations will be influenced by the number of total excitations. This is related to the fact that, in order to correlate the system with the ancilla, there needs to be intermediary ancilla's excitations acting as messengers for the parties.

Results for the TMS interaction are shown in Fig. 4.4. In this case the relative signs are immaterial, but the dynamics becomes more sensitive on the magnitude of ν_e, since $\tilde{z}$ and $\tilde{w}$ are hyperbolic functions. The TMS interaction entangles E_nE_{n+1}, even if both

are initially in the vacuum. As a consequence, it also spontaneously create excitations, so that the number of quanta is not preserved. At each $E_n E_{n+1}$ collision the net number of excitations therefore increases. Part of these excitations are lost when the ancillas are discarded and part flow to the system. As a consequence, depending on the rate at which excitations are created, the dynamics can be either stable or unstable. This occurs at the critical point $\nu_e^{\text{crit}} = \sinh^{-1}(1) \simeq 0.8813$, which is when $\tilde{w} = 1$, thus marking the situation where the total number of excitations grow unboundedly [c.f. Eq. (4.23)]. When $\nu_e < \nu_e^{\text{crit}}$ the dynamics will be stable and both, the system and the ancilla, will converge to an uncorrelated steady-state value $\langle a^\dagger a \rangle = \sinh^2 \nu_e (1 - \sinh^2 \nu_e)^{-1}$ independently of λ_s [Fig. 4.4(a,c,e)]. Conversely, for $\nu_e \geqslant \nu_e^{\text{crit}}$, the dynamics becomes unstable. Therefore, the number of excitations and correlations diverge [Fig. 4.4(b,d,f)]. These asymptotic values can be understood from arguments of stability theory, as shown in Appendix A.

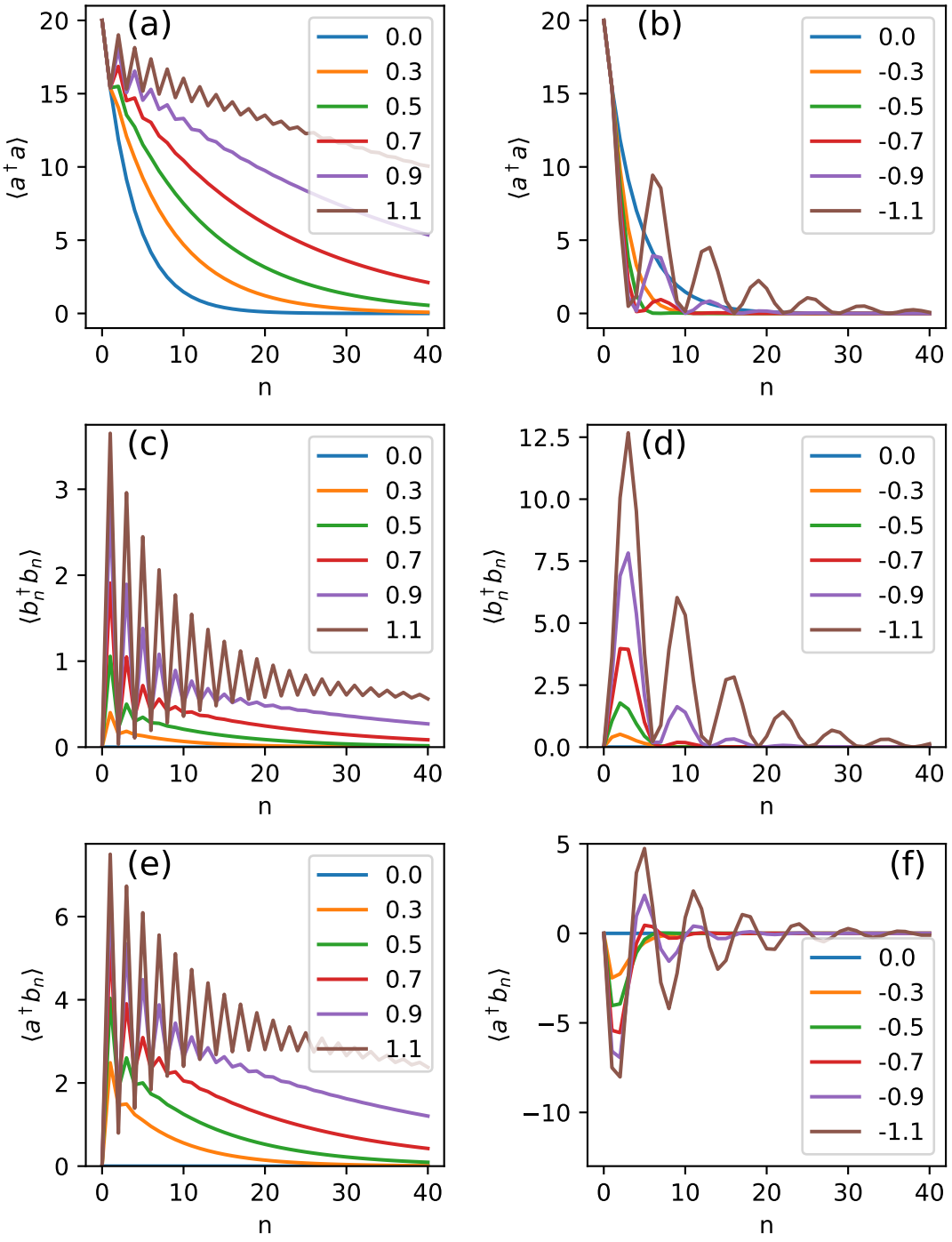

Figure 4.3: Second moments as a function of time, computed from Eq. (4.20) for the BS dynamics (4.21) with $\lambda_s = 0.5$ and different values of λ_e (with $\lambda_e > 0$ on the left column and $\lambda_e < 0$ on the right column). The ancillas are assumed to start in the vacuum, and the system in a thermal state with $\langle a^\dagger a \rangle^0 = 20$. (a,b) Number of excitations in the system $\langle a^\dagger a \rangle$. (c,d) Number of excitation in the n^{th} ancilla $\langle b_n^\dagger b_n \rangle$. (e,f) Correlation function between the system and the n^{th} ancilla $\langle a^\dagger b_n \rangle$.

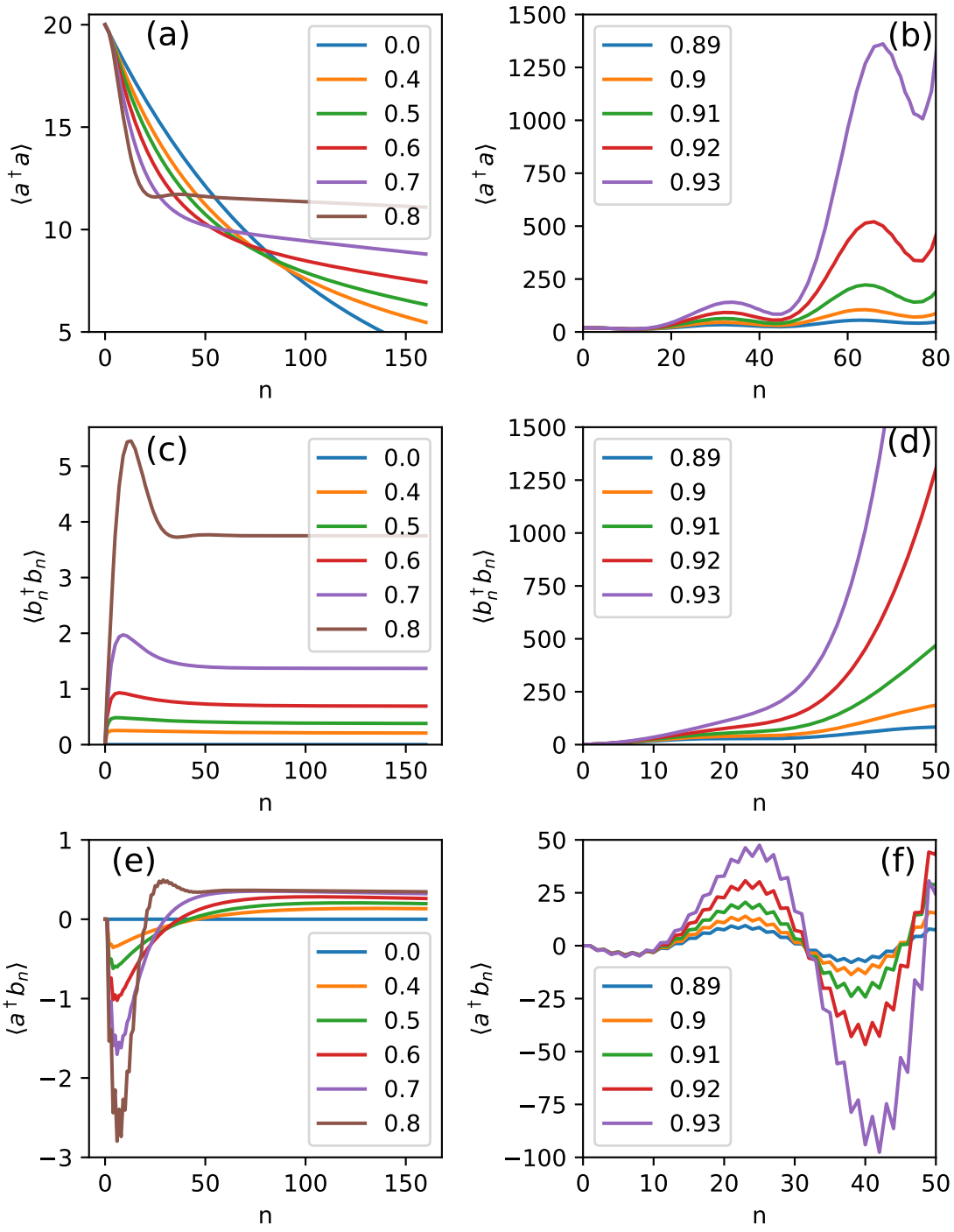

Figure 4.4: Second moments as a function of time, computed from Eq. (4.20) for the TMS dynamics (4.23) with $\lambda_s = 0.1$ and different values of ν_e (with $\nu_e < \nu_e^{\text{crit}}$ on the left column and $\nu_e \geq \nu_e^{\text{crit}}$ on the right column, where $\nu_e^{\text{crit}} = \sinh^{-1}(1)$). The ancillas are assumed to start in the vacuum, and the system in a thermal state with $\langle a^\dagger a \rangle^0 = 20$. (a,b) Number of excitations in the system $\langle a^\dagger a \rangle$. (c,d) Number of excitations in the n^{th} ancilla $\langle b_n^\dagger b_n \rangle$. (e,f) Correlation function between the system and the n^{th} ancilla $\langle a^\dagger b_n \rangle$.

Chapter 5

Non-Markovianity

5.1 Quantum non-Markovianity

In Chapter 2, we reviewed the dynamics of open quantum systems, in which we describe the system's evolution by a Lindblad master equation (2.32). We found out in Sec. 2.3 that a microscopic derivation was possible provided we resort to some approximation schemes, for example the Born-Markov approximation. However, these approximations cannot be employed to many processes in open quantum systems and thus, the system's dynamics cannot be described by a divisible dynamical map. Typically, this is because the environment's correlation time scale is not small compared to the system's decoherence time, rendering the Markov approximation impossible. Examples are the cases of strongly correlated systems, low temperatures, finite reservoirs, or large initial correlations for which some experimental demonstrations can be found in [93–97]. These processes are called non-Markovian.

Non-Markovianity first arose in the theory of classical stochastic processes [98–101]. Its classical definition is based on classical probability theory where we say that a process is non-Markovian if the conditional probability of the future states of the process depends on the sequence of events that preceded it. Quantum theory, however, cannot be formulated as a statistical theory on classical probability space [1, 102]. Therefore, the concept of quantum non-Markovianity cannot be based on the classical notions only.

On the one hand, there's the notion of information flow between the system and the surrounding environment. In the quantum realm, information leaks are much more effi-

cient, so that when a system interacts with an environment, information about the former is inevitably transferred to the latter. When the environment is very large and complex, this information may never return. In general, however, there may be a partial backflow of information, which characterizes a non-Markovian evolution. From the point of view of causality, this backflow quantifies the ability of the dynamics to communicate past information to the future. On the other hand, there's the notion of map divisibility. For instance, considering the case of collisional models studied in Chapter 4, the map from $\rho_S^0 \to \rho_S^n$ in Eq. (4.5) is always CPTP by construction. One may also define more general maps $\mathcal{E}_{m\to n}$ taking the density matrix ρ_S^m to ρ_S^n $(m < n)$. Assuming that the inverse $\mathcal{E}_n^{-1}$ exists, they are defined as $\mathcal{E}_n \circ \mathcal{E}_m^{-1}$. Albeit mathematically well defined, these maps are in general not CP. Markovian maps, conversely, are CP by construction. This defines the notion of CP-divisibility, which provides a widely used criteria for characterization of non-Markovianity: a map is CP-divisible when the intermediate maps $\mathcal{E}_{m\to n}$ are CP.

Considerable attention was given in recent years on how to characterize and quantify non-Markovianity in the quantum domain (for recent reviews, see [15, 16]). Due to the richness involved, however, there is no single approach capable of capturing its full essence. Several quantifiers have been studied: dynamical divisibility [22, 103–105], trace distance [17, 19, 20], mutual information [23], relative entropy [24, 25], memory kernel [8–10], among others [26–30]. In this work, we will be particularly interested on the ones best suited for the collisional model setup described in Chapter 4. We will explore them in detail in the following sections.

5.2 Mutual Information

The first approach to quantum non-Markovianity to be discussed is based on the idea that memory effects in the open quantum system's dynamics are linked to the exchange of information between the system and its environment. While in a Markovian process the open system continuously loses information to the environment, a non-Markovian process is characterized by a flow of information from the environment back into the system. In this way, quantum non-Markovianity is associated with a notion of quantum memory, namely, information which has been transferred to the environment, in the form

of system-environment correlations or changes in the environmental states, and is later recovered by the system.

Non-Markovianity and backflow of information must be related to correlations that develop between system and bath. However, when a system interacts with multiple modes of the bath at the same time, there are many different correlations one may consider, between the system and all possible parts of the bath. And it is not clear which of these correlations are relevant for the non-Markovian evolution. For instance, the correlation with a part of the bath the system will never interact again is irrelevant, as far as non-Markovianity is concerned. But in the standard scenario, it is in general not possible to identify which are the relevant correlations.

In a collisional model picture, on the other hand, this is unambiguous: the relevant correlations are those between S and ancilla E_{n+1} at time n (see Fig. 4.1). These are the correlations that ancilla E_n transferred to E_{n+1} after its interaction. Hence, they represent the only possible source of information backflow at each collision. Conveniently, this is also exactly what the Markovian embedding (4.4) offers. A useful measure of correlations, for instance, is the quantum mutual information (MI), defined as

$$\mathcal{I}^n(SE_{n+1}) = S(\rho_S^n) + S(\rho_{E_{n+1}}^n) - S(\varrho^n), \tag{5.1}$$

where $S(\rho) = -\operatorname{tr}(\rho \ln \rho)$ is the von Neumann entropy. The states ρ_S^n and $\rho_{E_{n+1}}^n$ are both computed from ϱ^n by taking the appropriate partial trace. Thus, by monitoring ϱ^n as a function of time, one has direct access to the relevant measure of correlation. Of course, $\mathcal{I}^n(SE_{n+1})$ is not the only relevant measure of correlation. Different choices, from two-point functions, to quantifiers of entanglement and quantum discord, may also be of interest. The relevant point is that any such measure will, necessarily, be contained in ϱ^n.

5.3 Memory Kernel

A much older notion of non-Markovianity is that of a memory kernel, as present already in the seminal works of Nakajima and Zwanzig [6, 7]. The basic idea is that the open

dynamics of a system's density matrix ρ_S can, quite generally, be written as

$$\frac{d\rho_S}{dt} = -i[H_S, \rho_S] + \int_0^t \mathcal{K}_{t-t'}[\rho(t')]\, dt', \tag{5.2}$$

where $\mathcal{K}_{t-t'}$, called the memory kernel (MK), is a linear superoperator condensing all the information on how the evolution of ρ at time t depends on its past values. The MK has been studied intensively in recent years [8–13], as it provides clear insights onto the inner workings of non-Markovianity. It can also be given an operational interpretation, in terms of the so-called transfer tensors [106], rendering it accessible to experiments [107]. However, being a superoperator, it is generally difficult to compute it analytically. We also mention in passing that, the broader notion of process tensor, which includes also all possible input and output operations performed in the system [108–110].

In the original formulation of Nakajima and Zwanzig [6, 7], the memory kernel (MK) was represented as a single-parameter continuous superoperator $\mathcal{K}_t$ that quantifies the memory that is retained about the system's configuration a time t in the past [c.f. Eq. (5.2)]. The collisional model analog of that will be a superoperator $\mathcal{K}_n$, labeled by the discrete time index n. Thus, the stroboscopic analog of Eq. (5.2) should be of the form

$$\rho_S^n = \sum_{m=0}^{n-1} \mathcal{K}_{n-m}(\rho_S^m). \tag{5.3}$$

For instance, $\rho_S^3 = \mathcal{K}_1(\rho_S^2) + \mathcal{K}_2(\rho_S^1) + \mathcal{K}_3(\rho_S^0)$. The term $\mathcal{K}_1(\rho_S^{n-1})$ describes the short-term memory from the very last step, while $\mathcal{K}_n(\rho_S^0)$ describes the long-term memory all the way from the initial state. An explicit formula for the MK can be constructed using a reasoning similar to that used for transfer tensors in Ref. [106]: Starting with the reduced map $\mathcal{E}_n$ in Eq. (4.5), we define the MK recursively from

$$\mathcal{K}_n = \mathcal{E}_n - \sum_{m=1}^{n-1} \mathcal{K}_{n-m}\mathcal{E}_m. \tag{5.4}$$

That this is indeed the correct formula can now be verified by substituting it back in Eq. (5.3). For instance, $\mathcal{K}_1 = \mathcal{E}_1$, $\mathcal{K}_2 = \mathcal{E}_2 - \mathcal{K}_1\mathcal{E}_1$, $\mathcal{K}_3 = \mathcal{E}_3 - \mathcal{K}_2\mathcal{E}_1 - \mathcal{K}_1\mathcal{E}_2$, and so on. Eq. (5.4) provides an algorithmic method for computing the MK. However, this requires

heavy numerics, even in simple cases. For instance, $\mathcal{K}_3 = \mathcal{E}_3 - \mathcal{E}_2\mathcal{E}_1 - \mathcal{E}_1\mathcal{E}_2 + \mathcal{E}_1\mathcal{E}_1\mathcal{E}_1$, and the complexity of the formulas only grow from there. One of the main results in this work will be to show that, for the case of Gaussian collisions, it is possible to write down a closed and compact formula for $\mathcal{K}_n$ (Sec. 6.2), which provides valuable insight into the inner workings of the memory kernel.

5.4 CP-Divisibility

Lastly, let us return to the idea of the divisibility of the map. Given that the inverse map $\mathcal{E}^{-1}$ exists for all times $t > 0$, we can define the family of intermediate maps $\mathcal{E}_{m\to n}$ from state ρ_S^m to state ρ_S^n $(m < n)$

$$\mathcal{E}_{m\to n} = \mathcal{E}_n \circ \mathcal{E}_m^{-1}. \tag{5.5}$$

The existence of the inverse is what allows the notion of divisibility. Even though $\mathcal{E}_n$ and $\mathcal{E}_m$ are completely-positive by construction, the intermediate map $\mathcal{E}_{m\to n}$ will not necessarily be. This is because the inverse map $\mathcal{E}_m^{-1}$ of the completely-positive map $\mathcal{E}_m$ need not to be positive.

Now, if these maps (5.5) are CP for all m, the evolution is Markovian. For non-Markovianity to occur there must exist a m value to not be completely positive. Hence, by measuring how much the intermediate map $\mathcal{E}_{m\to n}$ departs from the CP map, we are measuring the degree of non-Markovianity of the time evolution. Testing CP divisibility, however, is not always easy. For instance, it may it require analyzing the distance between different pairs of initial conditions ρ_S^0 [16]. According to the data processing inequality, these distances are always contractive for CP maps. Violations of contractivity are thus identified as violations of divisibility. This, however, requires a maximization over all possible initial conditions. In Sec. 6.3 we discuss the Gaussian version of this concept and show that the maximization is replaced by an alternative condition, that provides a clean and easily applicable formula for quantifying CP-divisibility.

Chapter 6

Memory effects in Gaussian Collisional Models

This chapter continues with the remaining original results obtained in this dissertation. The exposition here follows closely Sec. III and IV of the submitted arXiv preprint [91].

6.1 Gaussian Mutual Information

The Gaussian framework developed in Sec. 4.3 makes the mutual information (5.1) readily accessible from the CM γ^n in Eq. (4.19). Correlations are related to the off-diagonal blocks ξ^n_{n+1} (the MI would be zero if γ^n was block-diagonal). The three entropies in Eq. (5.1) can be readily computed in terms of the symplectic eigenvalues of γ^n [63]. Illustrative results are shown in Fig. 6.1, for the same collection of parameters as Fig. 4.3 and Fig. 4.4. As a sanity check, the MI is identically zero when $\lambda_e = \nu_e = 0$. It also tends to be larger for short times, tending to zero as n grows. The only exception is the unstable dynamics in Fig. 6.1(d), where the MI grows unboundedly. The oscillatory patterns in $\langle a^\dagger a\rangle$ are also present in the MI. The mutual information will also be highly dependent on the total number of excitations, as intermediary ancilla excitations are needed for information backflow (See also Sec. 4.5).

To better understand the role of the MI in the non-Markovian dynamics we present in Fig. 6.2 a comparison between the occupation number $\langle a^\dagger a\rangle$ of Fig. 4.3(a) and the MI of Fig. 6.1 for the BS dynamics. We focus on early times (small n) and also compare $\langle a^\dagger a\rangle$

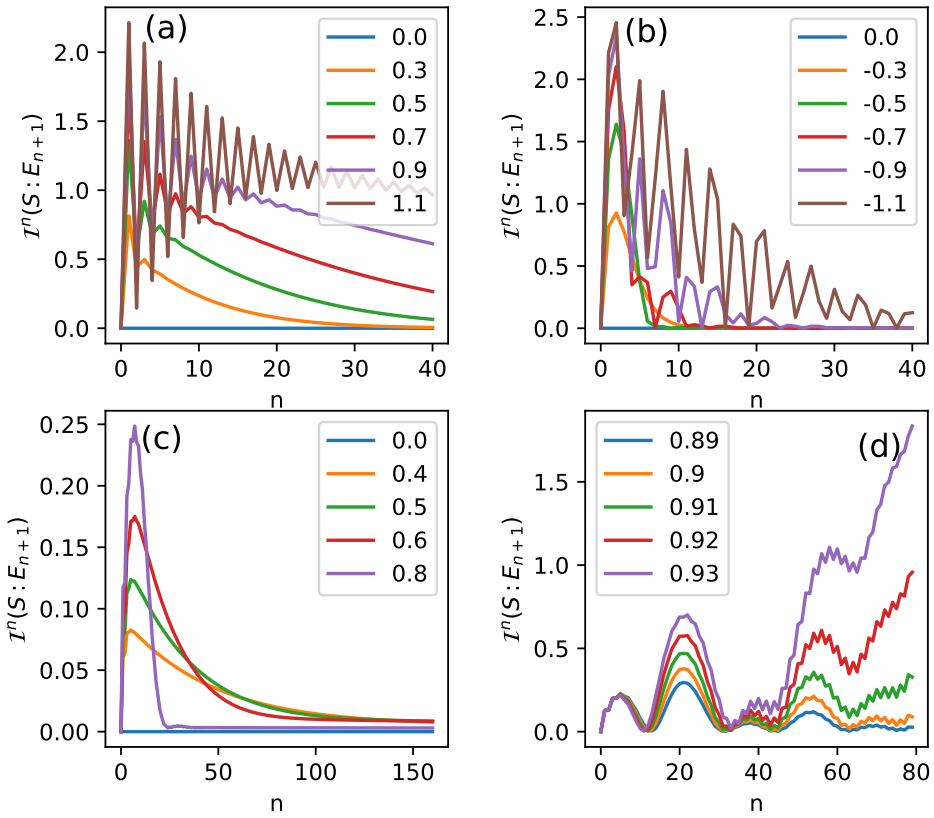

Figure 6.1: Quantum Mutual Information (5.1) for the BS (a,b) with $\lambda_s = 0.5$ ($\lambda_e > 0$ in (a) and $\lambda_e < 0$ in (b)), and TMS (c,d) dynamics with $\lambda_s = 0.1$ ($\nu_e < \nu_e^{\text{crit}}$ in (a) and $\nu_e \geq \nu_e^{\text{crit}}$ in (b)). Other parameters are the same as Fig. 4.3 and Fig. 4.4.

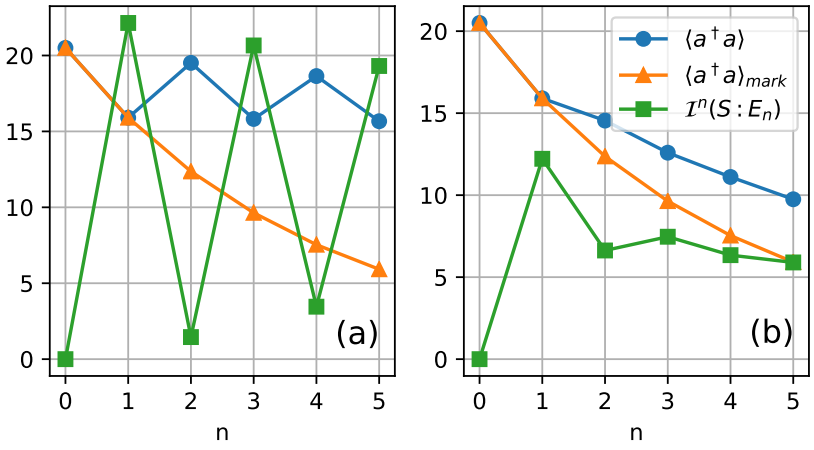

Figure 6.2: Comparison between Markovian and non-Markovian dynamics and role of the Mutual Information. In blue circles we show the early dynamics of $\langle a^\dagger a\rangle$ vs. n for the BS dynamics with (a) $\lambda_e = 1.1$ and (b) $\lambda_e = 0.3$, with fixed $\lambda_s = 0.5$ [c.f. Fig. 4.3(a)]. The corresponding Markovian case ($\lambda_e = 0$) is shown in orange triangles. These curves are to be compared with the MI (5.1), shown by green squares in the two cases [Fig. 6.1(a)]. The heights of each curve were adjusted for better visibility.

with the corresponding Markovian dynamics ($\lambda_e = 0$). The difference between the non-Markovian (blue circles) and Markovian (orange triangles) dynamics reflects the extent to which the backflow of information affects the evolution. This, as can be seen in the figure, is directly correlated with the MI (green squares) *of the previous step*. That is, a large MI in a given step implies a large difference between the blue and orange curves in the following one. This is particularly clear in Fig. 6.2(a) and serves to illustrate how the correlations built between SE_{n+1}, at step n, affect the future interaction between S and E_{n+1} at the next step.

6.2 Memory Kernel

The Memory Kernel (MK) discussed in Eqs. (5.2) and (5.3), and Sec. 5.3, is perhaps the most physically transparent way of analyzing non-Markovianity. Starting from any global map between system and bath, one can always write down a differential equation for the reduced density matrix ρ_S of the system. This equation, however, will in general be time-non-local; i.e., it will be an integro-differential equation of the form (5.2), where $\mathcal{K}_{t-t'}[\rho_S(t')]$ describes how $d\rho_S(t)/dt$ depends on $\rho_S(t')$ in previous times $t' < t$. The MK therefore contains all the information about the dynamics, with non-Markovianity being related to its overall dependence on $t - t'$: the slower the decay of $\mathcal{K}_{t-t'}$ with $t - t'$, the longer the memory and hence the more non-Markovian is the dynamics. The Markovian case is recovered when $\mathcal{K}_{t-t'} \propto \delta(t - t')$.

The memory kernel $\mathcal{K}_{t-t'}$ is a superoperator acting on the full Hilbert space of the system. Computing it is thus, in general, a very difficult task. Within our framework, however, one may equivalently formulate a memory kernel acting only in the system's CM θ^n. This can be accomplished starting from Eq. (4.20) and writing down a difference equation for θ^n only. As we will demonstrate below, this equation will have the form (contrast with (2.12) and (5.3)):

$$\theta^{n+1} = x^2\theta^n + \sum_{r=0}^{n-1} \mathcal{K}_{n-r-1}(\theta^r) + G_n, \tag{6.1}$$

where G_n is a contribution that depends only on the initial state of the ancillas [1] and $\mathcal{K}_n$ is the memory kernel. The way we define the MK is such that $\mathcal{K}_0$ measures how the step from θ^n to θ^{n+1} is affected by θ^{n-1} and $\mathcal{K}_{n-1}$ measures how it is affected by θ^0. $\mathcal{K}_n$ is still a superoperator, but one which acts on the space of 2×2 CMs. One can write it more explicitly in terms of a Kraus operator-sum representation [88, 111]

$$\mathcal{K}_n(\theta) = \sum_{ij} \kappa_{ij}^n M_i \theta M_j^{\mathrm{T}}, \tag{6.2}$$

where κ_{ij}^n are coefficients that depend on time and $\{M_i\}$ are a complete set of 2×2 matrices; a convenient choice is the set of Pauli matrices $\{\mathbb{I}_2, \sigma_z, \sigma_+, \sigma_-\}$. A general recipe to compute the coefficients κ_{ij}^n in Eq. (6.2) is given below in Eq. (6.21). Crucially, as we show, it depends *only* on the matrix X of the Markovian embedding (4.20).

The memory itself is contained in the dependence of κ_{ij}^n on n. The dependence on i, j determines how different elements of θ^r affect θ^n. For instance, as we will show below, in the case of the BS map [Eq. (4.21)], the only non-zero coefficient will be the one proportional to $\mathbb{I}_2\theta\mathbb{I}_2 = \theta$, which we refer to as κ_{11}^n; that is, the memory kernel is actually a c-number, $\mathcal{K}_n(\theta) = \kappa_{11}^n\theta$. This implies that the MK is the same for all entries of θ^n and each entry $(\theta^n)_{ij}$ is only affected by the corresponding entry $(\theta^r)_{ij}$ at past times. Conversely, in the TMS map there will be four non-zero coefficients, corresponding to combinations of $M_1 = \mathbb{I}_2$ and $M_2 = \sigma_z$; we refer to them as κ_{11}^n, $\kappa_{1,z}^n$, $\kappa_{z,1}^n$ and $\kappa_{z,z}^n$. This means that the memory kernel of $(\theta^n)_{11}$ will be different from that of $(\theta^n)_{2,2}$ and so on (each entry will have its own memory kernel). Finally, a memory kernel containing a dependence on $\sigma_\pm$ would imply that $(\theta^n)_{11}$ would depend on the past values of other entries, such as $(\theta^r)_{12}$ and $(\theta^r)_{22}$.

6.2.1 General derivation of the Memory Kernel

We now carry out the derivation of the memory kernel for the Gaussian collisional model. We consider here a more general scenario, which relies only on the structure of the Markovian embedding in Eq. (4.20). We also assume that the system and ancillas are each

[1] In principle one could also interpret G_n as being part of the memory kernel. However, we have opted not to do so, since G_n refers only to the states of the ancillas, while the actual dependence on the state of the system, which is what one expects from a memory kernel to model, is fully contained in $\mathcal{K}_n$.

composed of an arbitrary number of modes N_S and N_E [Eqs. (4.21) and (4.23) are recovered for $N_S = N_E = 1$]. More specifically, we take the matrices X and Y to have the following block structure,

$$X = \begin{pmatrix} X_{11} & X_{12} \\ X_{21} & X_{22} \end{pmatrix}, \qquad Y = \begin{pmatrix} 0 & 0 \\ 0 & Y_{22} \end{pmatrix}, \tag{6.3}$$

where e.g., X_{11} and X_{22} are of size $2N_S$ and $2N_E$ respectively. This therefore contemplates both multimode system and ancillas, as well as collisions with longer memory. For instance, if E_n collides with E_{n+1} and E_{n+2}, then we would have $N_S = 1$ and $N_E = 2$.

Our derivation follows the general approach of Nakajima and Zwanzig [6, 7], but adapted to the present context. We begin by noting the following property [112]: the solution of a generic difference equation of the form

$$\psi(n+1) = \alpha\psi(n) + g(n), \tag{6.4}$$

is given by

$$\psi(n) = \alpha^n \psi(0) + \sum_{r=0}^{n-1} \alpha^{n-r-1} g(r). \tag{6.5}$$

This solution holds for arbitrary objects ψ, provided α is a linear operator. It therefore holds when ψ is a vector and α is a matrix, or when ψ is a matrix and α is a superoperator. Thus, for instance, the solution of Eq. (4.20) is

$$\gamma^n = X^n \gamma^0 (X^{\mathrm{T}})^n + \sum_{r=0}^{n-1} X^{n-r-1} Y (X^{\mathrm{T}})^{n-r-1}. \tag{6.6}$$

Here the notation γ^n, to denote the time index, becomes a bit ambiguous since X^n is the matrix X to the power n. But there is no room for confusion, since X^n will be the only quantity where the superscript does not refer to the time.

We now introduce the vectorization operation [113], which transforms a matrix A into

a vector $\vec{A} = \text{vec}(A)$ by stacking its columns. For instance,

$$\text{vec}\begin{pmatrix} a & b \\ c & d \end{pmatrix} = \begin{pmatrix} a \\ c \\ b \\ d \end{pmatrix}. \tag{6.7}$$

One may verify that, for any three matrices A, B, C,

$$\text{vec}(ABC) = (C^{\text{T}} \otimes A)\text{vec}(B). \tag{6.8}$$

With this, the matrix difference equation (4.20) is converted into a vector difference equation

$$\vec{\gamma}^{\,n+1} = (X \otimes X)\vec{\gamma}^{\,n} + \vec{Y}. \tag{6.9}$$

We also introduce projection matrices onto the subspaces of system and ancilla,

$$P_S = \begin{pmatrix} \mathbb{I}_{2N_S} & 0 \\ 0 & 0 \end{pmatrix}, \qquad P_E = \begin{pmatrix} 0 & 0 \\ 0 & \mathbb{I}_{2N_E} \end{pmatrix}, \tag{6.10}$$

which are of size $2N_S + 2N_E$. In the larger space relevant for vectorization there are four possible projections, $P_S(\ldots)P_S$, $P_S(\ldots)P_E$ and so on. These operations chop the covariance matrix γ^n in 4 blocks, as in Eq. (4.19). Our interest is in $P_S(\gamma^n)P_S$, as it contains the system CM θ^n. We therefore also introduce

$$P = P_S \otimes P_S, \tag{6.11}$$

together with its complement $Q = 1 - P$. Note, though, that $Q \neq P_E \otimes P_E$.

We now multiply Eq. (6.9) by P and use that $P + Q = 1$, together with the fact that $P\vec{Y} = 0$ [c.f. Eq. (6.3)]. We then get

$$P\vec{\gamma}^{\,n+1} = P(X \otimes X)P\vec{\gamma}^{\,n} + P(X \otimes X)Q\vec{\gamma}^{\,n}. \tag{6.12}$$

Similarly, multiplying Eq. (6.9) by Q we find

$$Q\vec{\gamma}^{\,n+1} = Q(X \otimes X)Q\vec{\gamma}^{\,n} + Q(X \otimes X)P\vec{\gamma}^{\,n} + \vec{Y}. \tag{6.13}$$

Now comes the crucial idea of the Nakajima and Zwanzig method [6, 7]. We interpret Eqs. (6.12) and (6.13) as two coupled equations for the variables $P\vec{\gamma}^{\,n}$ and $Q\vec{\gamma}^{\,n}$. Since our interest is in $P\vec{\gamma}^{\,n}$, we first solve Eq. (6.13), assuming a given $P\vec{\gamma}^{\,n}$, and then substitute the result in Eq. (6.12). Eq. (6.13) is of the form (6.4) with $\alpha = Q(X \otimes X)$ and $g(n) = Q(X \otimes X)P\vec{\gamma}^{\,n} + \vec{Y}$. Eq. (6.5) then gives

$$Q\vec{\gamma}^{\,n} = (Q(X \otimes X))^n Q\vec{\gamma}^{\,0} + \sum_{r=0}^{n-1} (Q(X \otimes X))^{n-r-1} \Big[Q(X \otimes X)P\vec{\gamma}^{\,r} + \vec{Y} \Big].$$

Plugging this in Eq. (6.12) we then arrive at

$$P\vec{\gamma}^{\,n+1} = P(X \otimes X)P\vec{\gamma}^{\,n} + \sum_{r=0}^{n-1} \hat{K}_{n-r-1} P\vec{\gamma}^{\,r} + \vec{\mathcal{G}}_n, \tag{6.14}$$

where

$$\hat{K}_{n-r-1} = P(X \otimes X)[Q(X \otimes X)]^{n-r-1} Q(X \otimes X), \tag{6.15}$$

is the memory kernel in vectorized form (i.e., as a matrix of size $(2N_S+2N_E)^2$). The term $\vec{\mathcal{G}}_n$, on the other hand, is a function that depends only on the initial state of the ancillas and reads

$$\vec{\mathcal{G}}_n = P(X \otimes X)[Q(X \otimes X)]^n Q\vec{\gamma}^{\,0} + \sum_{r=0}^{n-1} P(X \otimes X)[Q(X \otimes X)]^{n-r-1} \vec{Y}.$$

What is left is to rewrite Eq. (6.14) as an equation for the evolution of the system's CM θ^n only. We introduce the $(2N_S)^2 \times (2N_S+2N_E)^2$ rectangular matrix π defined such that $\pi\vec{\gamma}^{\,n} = \vec{\theta}^{\,n}$. For instance, in the case $N_S = N_E = 1$, the matrix π will be 4×16, of

the form (for more intuition on this matrix, see Appendix B)

$$\pi = \begin{pmatrix} 1 & 0 & 0 & 0 & 0 & 0 & 0 & 0 & \dots & 0 \\ 0 & 1 & 0 & 0 & 0 & 0 & 0 & 0 & \dots & 0 \\ 0 & 0 & 0 & 0 & 1 & 0 & 0 & 0 & \dots & 0 \\ 0 & 0 & 0 & 0 & 0 & 1 & 0 & 0 & \dots & 0 \end{pmatrix} \tag{6.16}$$

We also notice that $P = \pi^{\mathrm{T}}\pi$ and $\pi\pi^{\mathrm{T}} = \mathbb{I}_{(2N_S)^2}$. Multiplying Eq. (6.14) on the left by π we then get

$$\vec{\theta}^{\,n+1} = (X_{11} \otimes X_{11})\vec{\theta}^{\,n} + \sum_{r=0}^{n-1} \hat{\mathcal{K}}_{n-r-1}\vec{\theta}^{\,r} + \vec{G}_n, \tag{6.17}$$

where we also used the fact that $\pi(X \otimes X)\pi^{\mathrm{T}} = X_{11} \otimes X_{11}$. Here $\vec{G}_n = \pi\vec{\mathcal{G}}_n$ is again a term that depends only on the initial conditions of the ancillas, whereas

$$\hat{\mathcal{K}}_n = \pi\hat{K}_n\pi^{\mathrm{T}} = \pi(X \otimes X)\big[Q(X \otimes X)\big]^{n+1}\pi^{\mathrm{T}},$$

is the memory kernel, now expressed as a matrix of size $(2N_S)^2 \times (2N_S)^2$ acting on $\vec{\theta}^{\,r}$. This can also be written more symmetrically, by exploiting the fact that $Q^2 = Q$. We can then arrange it as

$$\hat{\mathcal{K}}_n = \pi(X \otimes X)Q\big[Q(X \otimes X)Q\big]^{n}Q(X \otimes X)\pi^{\mathrm{T}}. \tag{6.18}$$

The extra Q's outside the square brackets are placed simply to ensure the result also holds for $n = 0$. This is the final form of the MK. Crucially, notice how it depends *only* on the matrix X of the Markovian embedding (4.20).

To obtain a matrix difference equation for θ^n we must "unvec" Eq. (6.17); that is, apply the inverse map of (6.7). Unvecing the first term is trivial since, by Eq. (6.8),

$$\mathrm{unvec}\big[(X_{11} \otimes X_{11})\vec{\theta}^{\,n}\big] = X_{11}\theta^n X_{11}^{\mathrm{T}}.$$

The memory kernel (6.18), on the other hand, cannot be unvecked as a single product of

$A\theta^n B$. Instead, it is convenient to express it as

$$\hat{\mathcal{K}}_n = \sum_{ij} \kappa_{ij}^n M_j \otimes M_i, \tag{6.19}$$

where κ_{ij}^n are real coefficients and $\{M_i\}$ are a set of operators spanning the vector space of $2N_S$-dimensional real matrices. Decomposed in this form, the unvecked version of the memory kernel will then be, from (6.8),

$$\mathcal{K}_n(\theta) = \sum_{ij} \kappa_{ij}^n M_i \theta M_j^{\mathrm{T}}. \tag{6.20}$$

Finally, the form of the coefficients κ_{ij}^n can be found if we assume that the M_i form an orthogonal basis with respect to the Hilbert-Schmidt norm $(A|B) = \mathrm{tr}(A^{\mathrm{T}}B)$ (which is the case of the Pauli basis, for instance). Multiplying Eq. (6.19) by $M_j \otimes M_i$ and tracing then yields, by orthogonality,

$$\kappa_{ij}^n = \frac{\mathrm{tr}\left[(M_j^{\mathrm{T}} \otimes M_i^{\mathrm{T}})\hat{\mathcal{K}}_n\right]}{\mathrm{tr}(M_i^{\mathrm{T}}M_i)\,\mathrm{tr}\left(M_j^{\mathrm{T}}M_j\right)}. \tag{6.21}$$

This, together with Eq. (6.18), is all that is required to compute the memory kernel. With all these definitions, one may now finally unvec Eq. (6.17), leading to

$$\theta^{n+1} = X_{11}\theta^n X_{11}^{\mathrm{T}} + \sum_{r=0}^{n-1} \mathcal{K}_{n-r-1}(\theta^r) + G_n, \tag{6.22}$$

where $G_n = \mathrm{unvec}(\vec{G}_n) = \mathrm{unvec}(\pi\vec{\mathcal{G}}_n)$ is, again, a term depending only on the initial states of the ancillas.

6.2.2 Memory Kernel for the BS dynamics

We now illustrate the memory kernel for the two maps considered in Sec. 4.3, starting with the BS dynamics. In general, the structure of the memory kernel will be quite complicated. For the BS dynamics [Eq. (4.21)], however, the only non-zero coefficient in Eq. (6.21) is κ_{11}^n, the term proportional to the identity. In this case the memory kernel is therefore rather simple, as it is just a c-number multiplying all entries of θ^r. A more compact formula for

the MK in this case is given in Appendix B.

Results for the BS dynamics are shown in Fig. 6.3. The upper panel corresponds to $\lambda_s = 0.5$, which is similar to Fig. 4.3. As can be seen, for $\lambda_e > 0$ (Fig. 6.3(a)) the memory kernel's decay is oscillatory, with an exponential envelope. For $\lambda_e < 0$, oscillations are also observed, but these are rather different in nature and more asymmetrical with respect to the horizontal axis. When $\lambda_s = 0.05$ the situation changes (Figs. 6.3(c) and (d)). The dynamics of $\langle a^\dagger a \rangle$ is still quite similar to that of $\lambda_s = 0.5$, shown in Fig. 4.3, except that the time-scales become much longer. But in the MK one sees something entirely different. In particular, one finds that while κ_{11}^n continues to oscillate when $\lambda_e > 0$, it now becomes exclusively negative for $\lambda_e < 0$. In this case therefore, all past values of θ^r tend to contribute negatively to the evolution.

Negative values in the memory kernel are rather important, as they are associated with faster convergence. The reason is that the CM is a positive matrix and the first

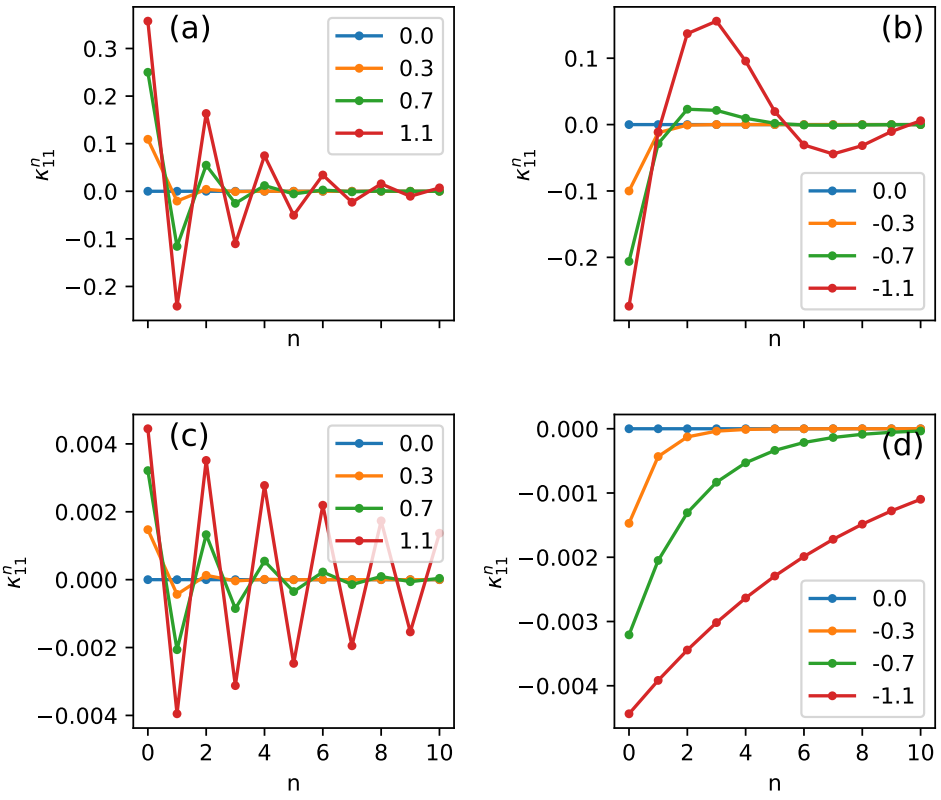

Figure 6.3: The memory Kernel for the BS dynamics, Eq. (4.21). In this case the only non-zero entry in Eq. (6.2) is κ_{11}^n, the term proportional to the identity. The plots are for $\lambda_s = 0.5$ (upper panel) and $\lambda_s = 0.05$ (lower panel), with $\lambda_e > 0$ (left) and $\lambda_e < 0$ (right).

term in (6.2) is always positive. The negativities observed in Fig. 6.3 therefore represent an accelerated draining of excitations from the system. This sheds light on some of the behaviors previously observed for the number operator (Fig. 4.3) and mutual information (Fig. 6.1).

It is possible to condensed a lot of information about the memory kernel by plotting κ_{11}^n in the (λ_s, λ_e) plane, for different values of n. This is shown in Fig. 6.4. Each plot corresponds to a different value of n, from 0 up to 8. The dependence on the relative signs of λ_s and λ_e is clearly visible, as is the overall damping of the memory with increasing n.

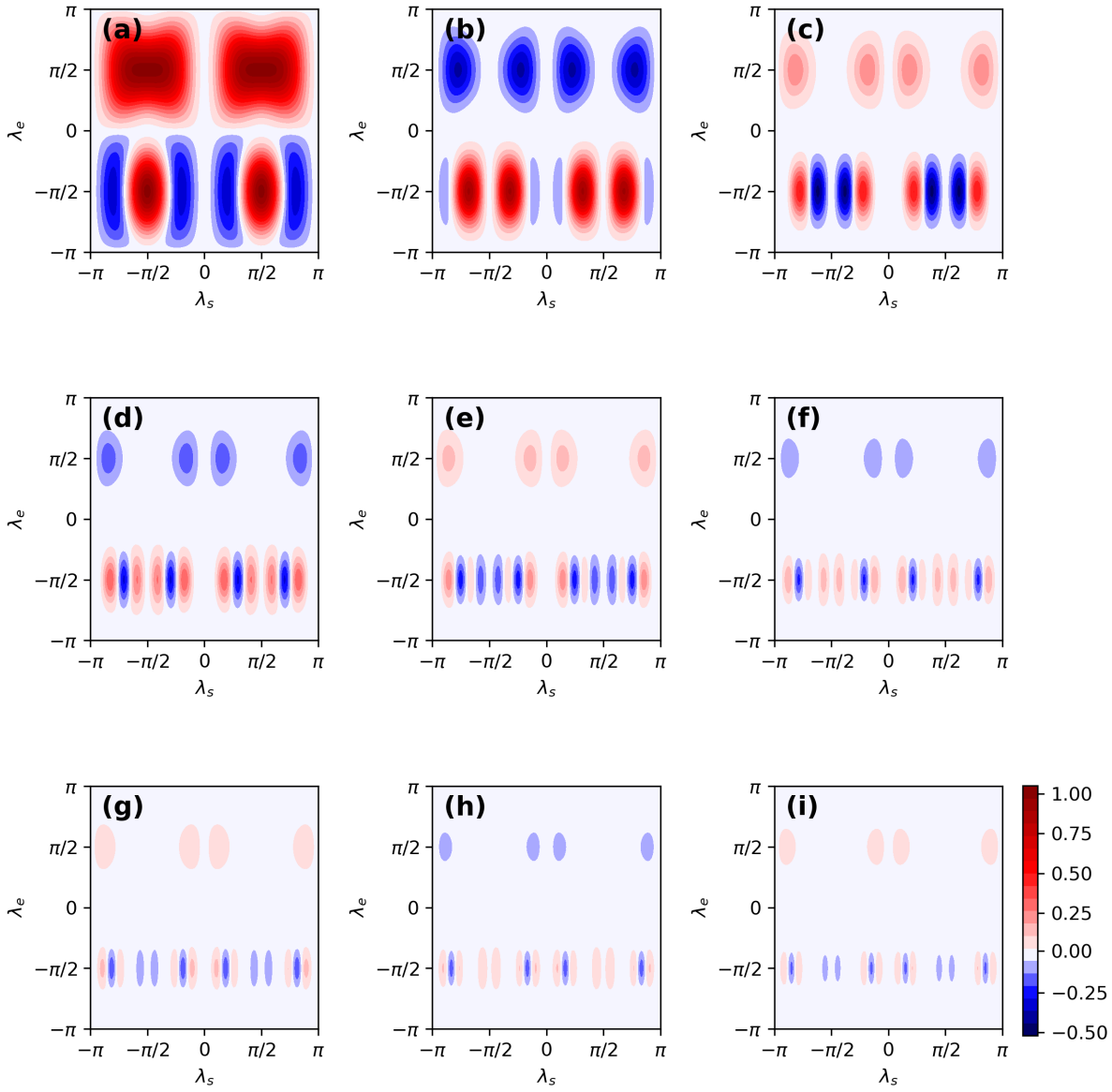

Figure 6.4: Diagrams for the memory kernel of the BS dynamics. Each plot shows κ_{11}^n in the (λ_s, λ_e) plane for a different value of n, from $n = 0$ to $n = 8$.

Particularly interesting, this map is able to very clearly pinpoint the regions have negative memory kernels, something which is found to be highly non-trivial.

6.2.3 Memory Kernel for the TMS dynamics

Next we turn to the TMS case (4.23). In this case it is found that there are, in total,

$$\mathcal{K}_n(\theta) = \kappa^n_{11}\theta + \kappa^n_{1z}\theta\sigma_z + \kappa^n_{z1}\sigma_z\theta + \kappa^n_{zz}\sigma_z\theta\sigma_z. \tag{6.23}$$

These quantities are plotted in Fig. 6.5 for the stable dynamics ($\nu_e < \nu_e^{\text{crit}}$), with $\lambda_s = 0.1$. All four coefficients are found to decay in time in an oscillatory fashion.

The physics of each coefficient, however, is not necessarily transparent. In order to

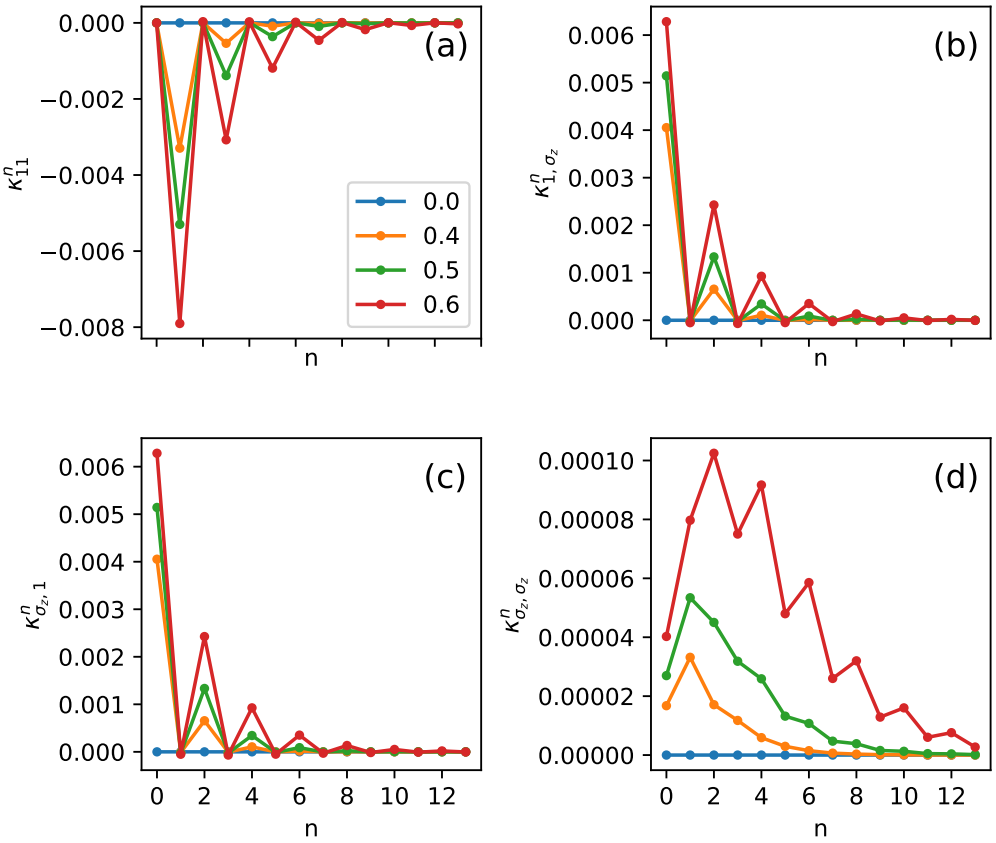

Figure 6.5: The memory Kernel for the (stable) TMS dynamics, Eq. (4.23) with $\lambda_s = 0.1$ and different values of λ_e. Each curve corresponds to a different entry of Eq. (6.2); namely, κ^n_{11}, κ^n_{1,σ_z}, $\kappa^n_{\sigma_z,1}$ and $\kappa^n_{\sigma_z,\sigma_z}$.

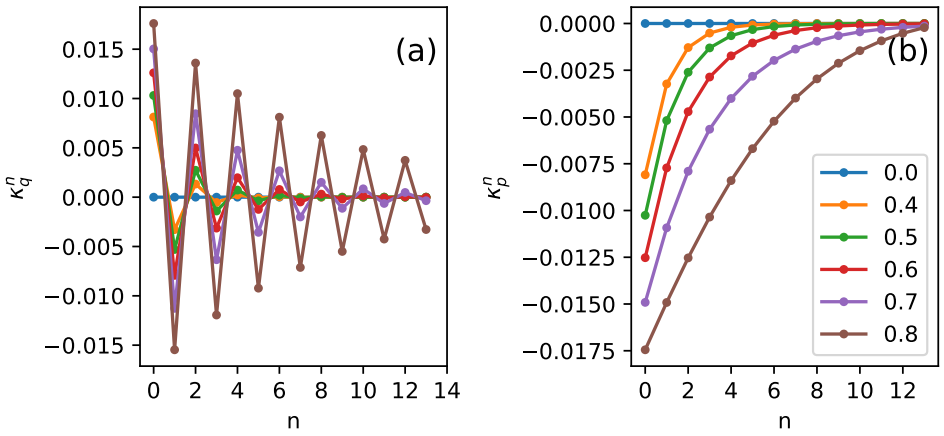

Figure 6.6: The MK for $\langle Q^2 \rangle$ and $\langle P^2 \rangle$, Eq. (6.24), for the TMS dynamics. Other parameters are the same as Fig. 6.5.

gain better intuition, let us focus on the diagonal entries of θ^n. In this case one finds that

$$\Big(\mathcal{K}_n(\theta)\Big)_{11} = \big(\kappa_{11}^n + \kappa_{1z}^n + \kappa_{z1}^n + \kappa_{zz}^n\big)\theta_{11}^n := \kappa_q^n \theta_{11}^n,$$
$$\Big(\mathcal{K}_n(\theta)\Big)_{22} = \big(\kappa_{11}^n - \kappa_{1z}^n - \kappa_{z1}^n + \kappa_{zz}^n\big)\theta_{22}^n := \kappa_p^n \theta_{22}^n. \tag{6.24}$$

The coefficients κ_q^n and κ_p^n therefore describe the individual memory kernels of $\langle Q^2 \rangle$ and $\langle P^2 \rangle$, which are different in the TMS dynamics.

These two contributions are shown in Fig. 6.6, for the same parameters as in Fig. 6.5. We also present diagrams in the (λ_s, ν_e) plane in Figs. 6.7 and 6.8. The plots in Fig. 6.6 reveal an extremely interesting asymmetry between the two quadratures. We see that the memory associated with $\langle Q^2 \rangle$ is oscillatory, whereas that associated with $\langle P^2 \rangle$ is always negative and decays monotonically. This asymmetry is a consequence of our choice of two-mode squeezing in the TMS interaction (4.8). Figs. 6.7 and 6.8, however, show that the situation is more intricate. Indeed, for fixed (λ_s, ν_e), κ_q is found to oscillate with n. But for κ_p this is not necessarily the case.

Finally, in Fig. 6.9 we compare the previous result with the case of ν_e in the vicinity, and larger than, $\nu_e^{\text{crit}} = 0.8813$; i.e., in the situation where the dynamics diverges. As can be seen, in this case both κ_q and κ_p diverge as well (notice the different scale of the horizontal axis). This is therefore contrary to our usual notion of memory: It means that

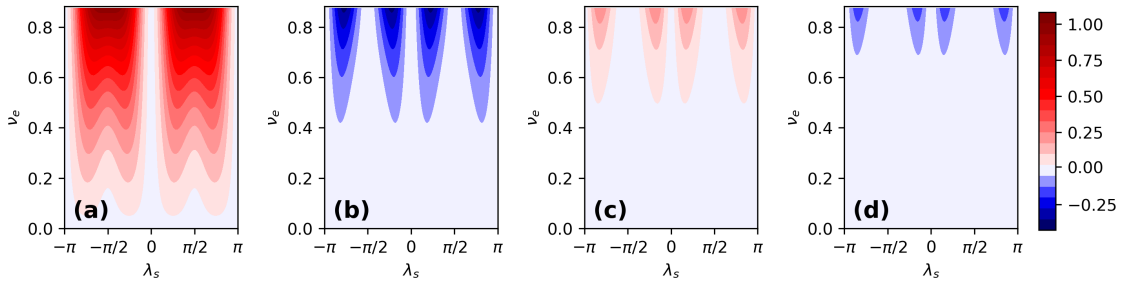

Figure 6.7: Diagrams for the memory kernel coefficient κ_q^n [Eq. (6.24)] of the TMS dynamics, in the (λ_s, ν_e) place, for $n = 0, \ldots, 3$.

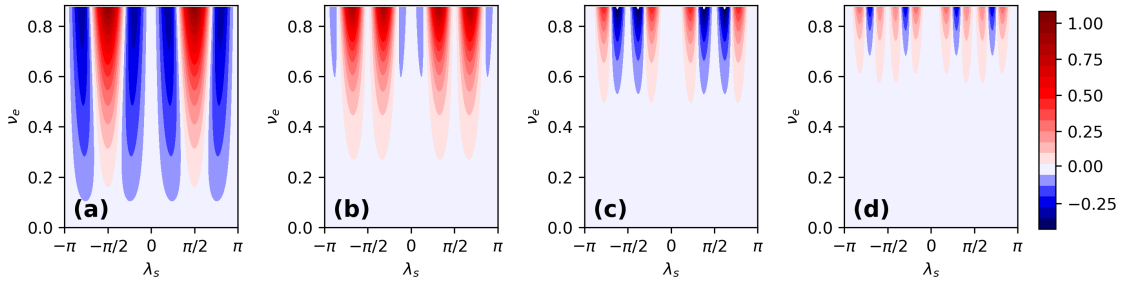

Figure 6.8: Similar to Fig. 6.7, but for κ_p^n.

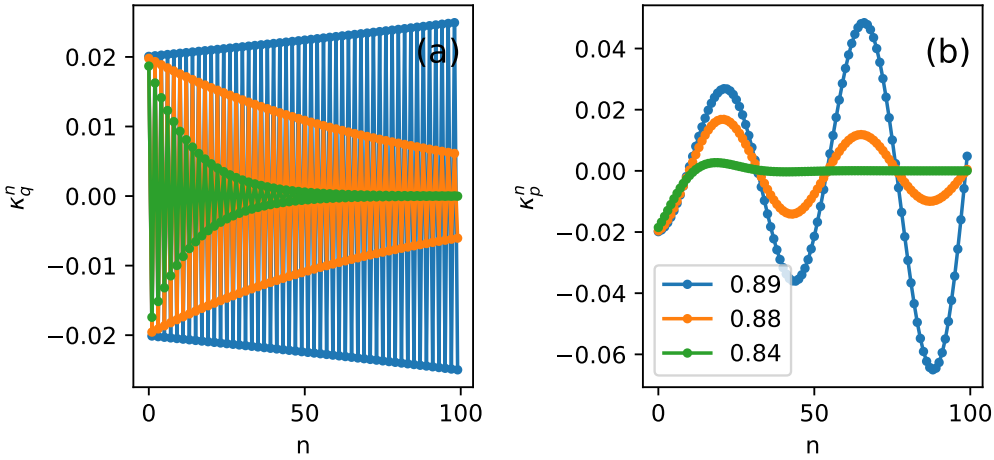

Figure 6.9: Similar to Fig. 6.6, but for values of ν_e close to, and larger than, $\nu_e^{\text{crit}} = 0.8813$.

the system retains a stronger memory from events in the distant past, than those in the recent one. In other words, the relative importance of past events accumulate.

6.3 Gaussian CP-Divisibility

Even though the MK explicitly shows the dependence on previous states, this alone does not necessarily imply a non-Markovian dynamic [11]. It is therefore important to contrast the MK with an actual test of non-Markovianity. Here we focus on CP-divisibility of intermediate maps, introduced in Sec. 5.4. The formulation for Gaussian dynamics, at the level of the covariance matrix, in Refs. [104, 105]. Any Gaussian CPTP map, as seen in Sec. 3.4, must have the form $\theta \to \mathcal{X}\theta\mathcal{X}^{\mathrm{T}} + \mathcal{Y}$, where $\mathcal{X}$ and $\mathcal{Y}$ are matrices satisfying [63, 114]

$$\mathcal{M}[\mathcal{X}, \mathcal{Y}] := 2\mathcal{Y} + i\Omega - i\mathcal{X}\Omega\mathcal{X}^{\mathrm{T}} \geq 0, \tag{6.25}$$

with $\Omega = i\sigma_y$ the symplectic form. Here $\mathcal{M} \geq 0$ means the matrix must be positive semidefinite.

In our case, the evolution of the system's CM, from time 0 to n, must therefore also be of this form:

$$\theta^n = \mathcal{X}_n\theta^0\mathcal{X}_n^{\mathrm{T}} + \mathcal{Y}_n. \tag{6.26}$$

The matrices $\mathcal{X}_n$ and $\mathcal{Y}_n$ can be read from the $(1,1)$ block of the general solution (6.6) and are independent of the initial state θ^0; viz.,

$$\mathcal{X}_n = (X^n)_{11}, \tag{6.27}$$

$$\mathcal{Y}_n = (X^n)_{12}\epsilon(X^{n\mathrm{T}})_{12} + \sum_{r=0}^{n-1}\left[X^{n-r-1}Y(X^{\mathrm{T}})^{n-r-1}\right]_{11}, \tag{6.28}$$

where the subscripts i, j refer here to specific blocks. This easiness in reading of the corresponding map matrices is another significant advantage of the Markovian embedding representation (4.20).

To probe whether the dynamics is divisible, we consider the map taking the system from n to $m > n$. Assuming that $\mathcal{X}_n$ and $\mathcal{Y}_n$ are invertible, which is true in our case, this will have the form [104]

$$\theta^m = \mathcal{X}_{mn}\theta^n\mathcal{X}_{mn}^{\mathrm{T}} + \mathcal{Y}_{mn}, \tag{6.29}$$

where

$$\mathcal{X}_{mn} = \mathcal{X}_m\mathcal{X}_n^{-1}, \qquad \mathcal{Y}_{mn} = \mathcal{Y}_m - \mathcal{X}_{mn}\mathcal{Y}_n\mathcal{X}_{mn}^{\mathrm{T}}. \tag{6.30}$$

The dynamics is then considered divisible when the intermediate maps (6.29) are a proper CPTP Gaussian map. That is, when $\mathcal{M}[\mathcal{X}_{mn}, \mathcal{Y}_{mn}] \geq 0$ [Eq. (6.25)].

The above criteria can be used not only as a dichotomic measure of divisibility, but also as a figure of merit [104]. This is accomplished by defining

$$\mathcal{N}_{mn} = \sum_k \frac{|m_k| - m_k}{2}, \quad \{m_k\} = \text{eigs}\Big(\mathcal{M}[\mathcal{X}_{mn}, \mathcal{Y}_{mn}]\Big). \tag{6.31}$$

This quantity is always non-negative and the map is divisible iff $\mathcal{N}_{mn} \equiv 0$ for all m, n. Otherwise, the magnitude of $\mathcal{N}_{mn}$ quantifies the extent to which divisibility is broken for that choice of m, n.

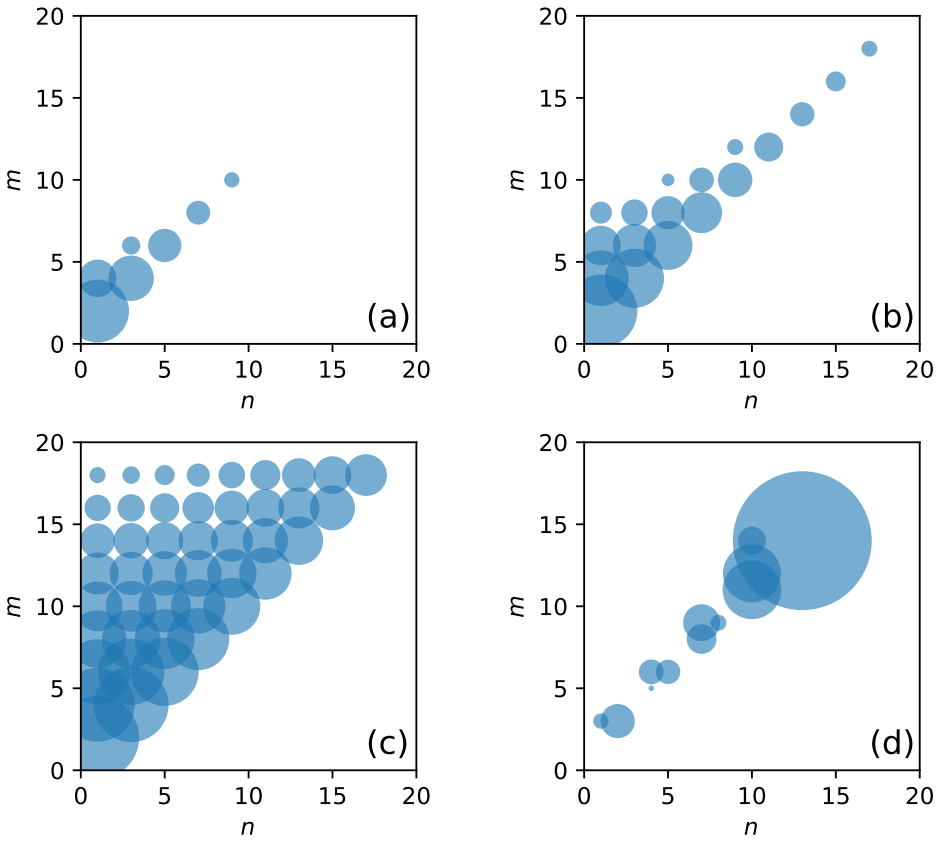

Figure 6.10: Example of the divisibility criteria for the BS dynamics. The plots show $\mathcal{N}_{mn}$ in the (n, m) plane, with the size of each point reflecting the magnitude of $\mathcal{N}_{mn}$. All curves are for $\lambda_s = 1.1$ and (a) $\lambda_e = 0.75$, (b) 0.9, (c) 1.1 and (d) -0.7.

6.3.1 BS dynamics

We begin our investigation of $\mathcal{N}_{mn}$ by focusing on the BS dynamics [Eq. (4.21)]. An example of the behaviour of (6.31) is shown in Fig. 6.10, where we plot $\mathcal{N}_{mn}$ in the (n, m) plane, with fixed $\lambda_s = 1.1$ and different values of λ_e. The magnitude of $\mathcal{N}_{mn}$ is represented by the size of each point. These diagrams are interpreted as follows. We start with Fig. 6.10(a). In this case we see that, for $n = 1$, $\mathcal{N}_{mn}$ is non-zero only for $m = 2$ and $m = 4$, being smaller in the latter. For $n = 3$ the map is always divisible. And for $n = 3$, it is not divisible only for $m = 4$ and 6. These irregularities are a consequence of the oscillatory character of the parameters appearing, e.g., in Eq. (4.21). Still concerning Fig. 6.10(a), we see notwithstanding that as n gets large, the map tends to be Markovian for all m. As we increase λ_e, however, as in Figs. 6.10(b) and (c), we see that overall the regions where $\mathcal{N}_{mn} > 0$ tend to increase. They increase both as a function of n, as well as a function of m for fixed n.

When $\lambda_e < 0$, however, strange things happen [Fig. 6.10(d)]. In this case we find that there can be highly irregular values of (n, m) which yield non-zero $\mathcal{N}_{mn}$ which, in fact, can reach significantly large values. For instance, the largest value plotted in Fig. 6.10(d) is for $n = 13$, $m = 14$ and has the value $\mathcal{N} \sim 69.7$. For $n = 16$, $m = 17$, however, one finds $\mathcal{N} \sim 10309$ (not shown). This is to be contrasted with Fig. 6.10(a), whose largest value is $\mathcal{N} = 3.42$. We present these results simply to emphasize that $\mathcal{N}_{mn}$ can oscillate violently. The reason is due to the term $\mathcal{X}_n^{-1}$ in Eq. (6.30), which can blow up for certain values of λ_s, λ_e and n.

Next we turn to the divisibility of a single collision; that is, with $m = n + 1$. Plots of $\mathcal{N}_{n+1,n}$ in the (λ_s, λ_e) plane are shown in Fig. 6.11. The overall behaviour is found to alternate with even and odd n. For n even, the map is always divisible for $\lambda_e > 0$ and potentially non-divisible within certain regions of $\lambda_e < 0$. Conversely, for n odd, one finds that divisibility breaks down in significant portions of the (λ_s, λ_e) plane. An additional illustration of the complex dependence of $\mathcal{N}_{n+1,n}$ on λ_s, λ_e, n is provided in Fig. 6.12, where we plot $\mathcal{N}_{n+1,n}$ as a function of n for selected values of λ_s and λ_e. From this figure, both the even/odd behavior, as well as the dramatic variations in the (λ_s, λ_e) plane can be more clearly appreciated.

The behavior of $\mathcal{N}_{n+1,n}$ in Fig. 6.11 is exacerbated close to the special points $\lambda_{s(e)} =$

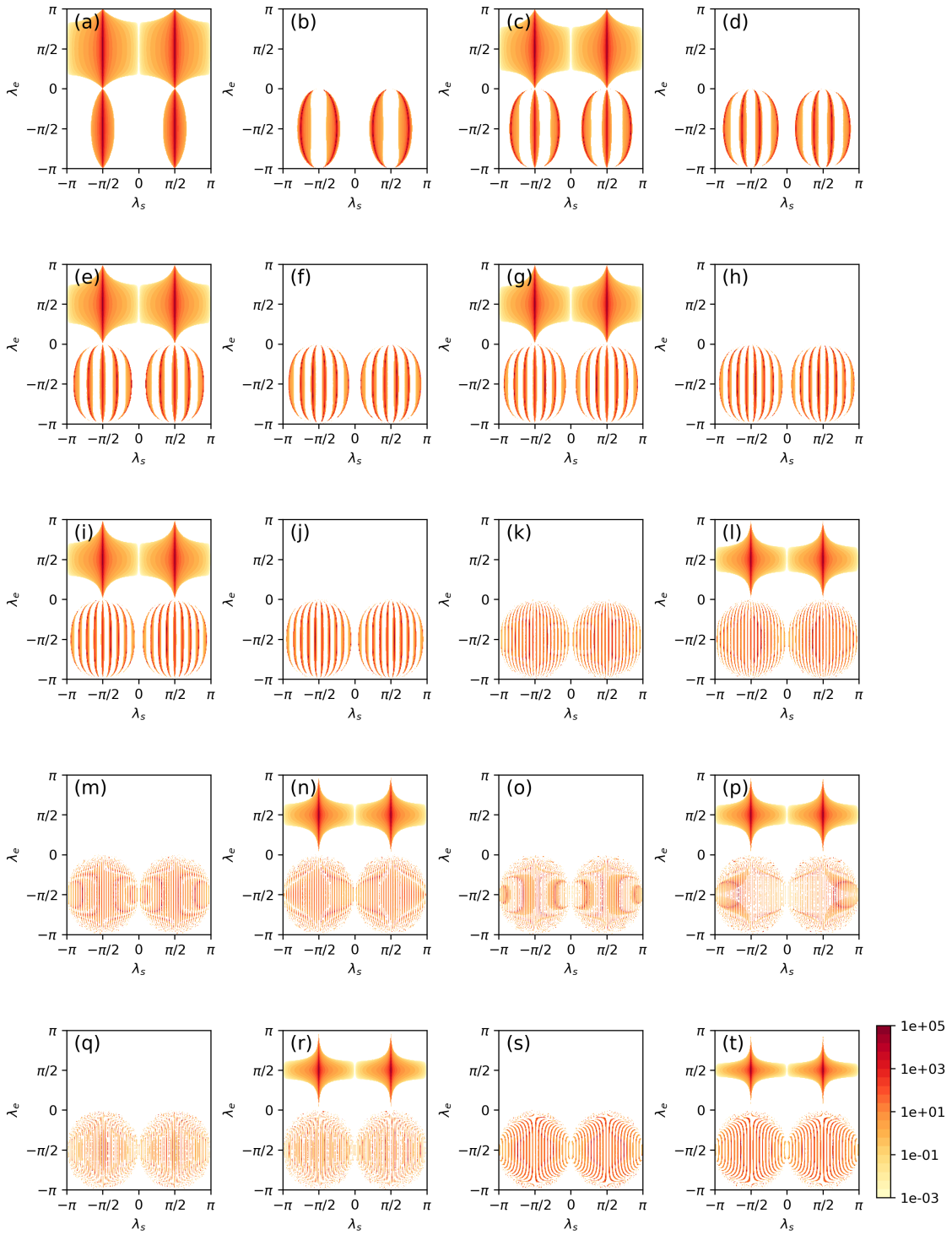

Figure 6.11: CP-divisibility measure $\mathcal{N}_{n+1,n}$ [Eq. (6.31)] in the (λ_s, λ_e) plane, for the BS dynamics. Each plot corresponds to a different values of n: in the first 2 lines, n ranges from 1 to 8 in steps of 1. In the remaining lines, $n = 9, 10, 20, 21, 30, 31, 40, 41, 50, 51$ and $100, 101$.

$\pi/2$. For instance, in the vicinity of $\lambda_s = \pi/2$, the dynamics is non-divisible even for infinitesimally small λ_e. This occurs because $\lambda_s = \pi/2$ corresponds to the full SWAP, where the CM of the system is completely transferred to the ancilla. As a consequence, when then next ancilla arrives to interact with the system, it will always contain a significant amount of information about it. We therefore expect that in the limit $n \to \infty$ the diagrams in Fig. 6.11 should converge to narrow lines going through these special points (although, unfortunately, we cannot actually verify this since the simulation cost becomes prohibitive for extremely large n).

We may also study similar diagrams for collisions that are more broadly spaced in time. In Fig. 6.13 we present results for $\mathcal{N}_{1,1+m}$ for different values of m (we focus on even values, $m = 2, 4, \ldots$). This therefore describes the long-term memory of the map, concerning the first collision. Two features stand out from this figure. First, as one would expect, the overall region in the (λ_s, λ_e) plane where the map is CP-divisible tends to shrink with increasing m. However, the regions around $\lambda_s = \pm\pi/2$ tend to be remarkably

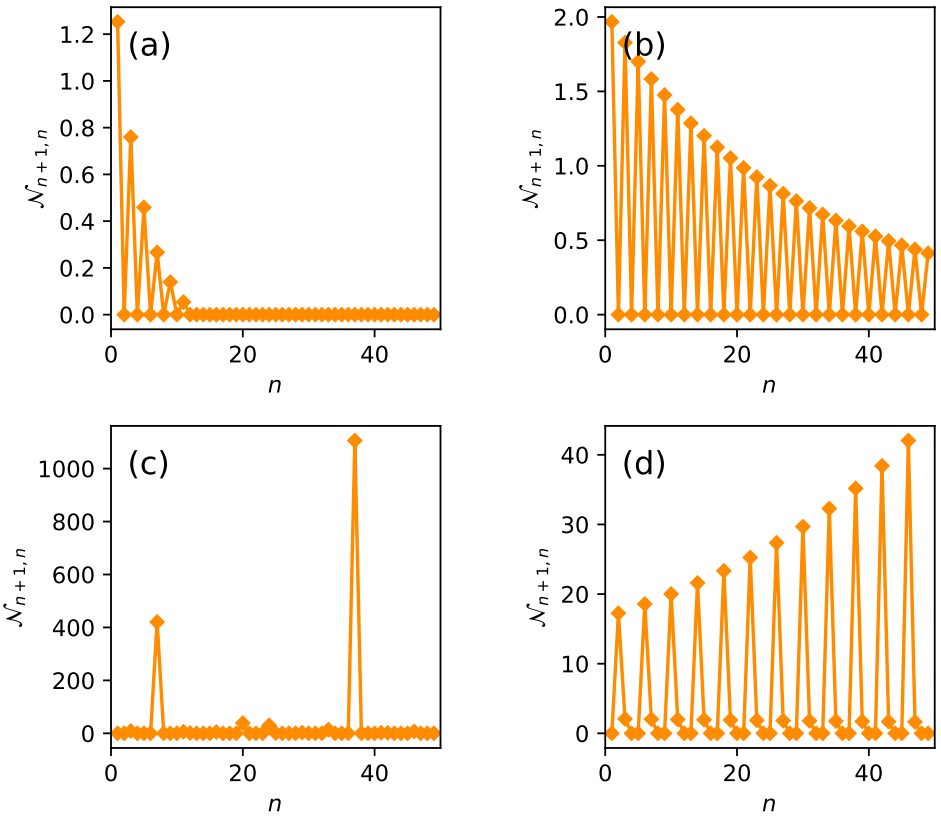

Figure 6.12: CP divisibility measure $\mathcal{N}_{n+1,n}$ as a function of n, for the BS dynamics with $\lambda_s = 0.8$ and $\lambda_e = 0.9, 1.3, -0.5, -0.8$. Complements Fig. (6.11).

persistent, remaining highly non-divisible even for large m.

The results in Figs. 6.11 and 6.13 refer to divisibility for specific times (n, m). We can also combine all data and ask, for which regions in the (λ_s, λ_e) plane, the BS dynamics is divisible for all (n, m). This is shown in Fig. 6.14. As expected, for most choices of parameters, the map will not be CP-divisible for some (n, m). Notwithstanding, there are regions where the map is always divisible. These regions tend to be concentrated close to $\lambda_e = 0$ (or $\lambda_e = \pi$, which is equivalent). And they exist even for large values of λ_s.

A direct comparison with the memory kernel, Sec. 6.2, is not generally possible since

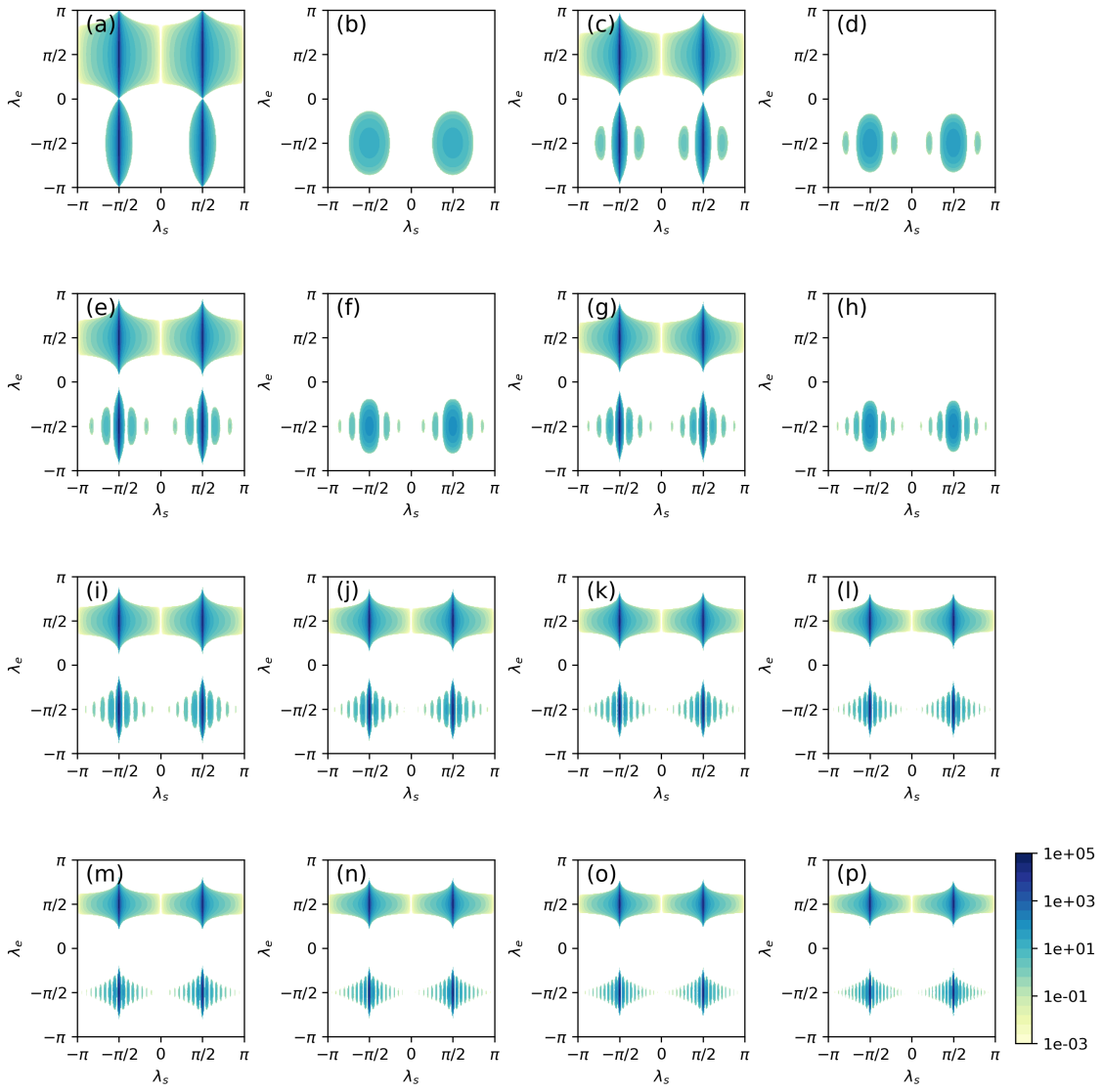

Figure 6.13: CP-divisibility measure, $\mathcal{N}_{m,1}$ [Eq. (6.31)] in the (λ_s, λ_e) plane, for the BS dynamics. Each plot corresponds to a different values of m: in the first 2 lines, m ranges from 2 to 9 in steps of 1. In the 3rd and 4th, from $m = 10$ to 24 in steps of 2. lines,

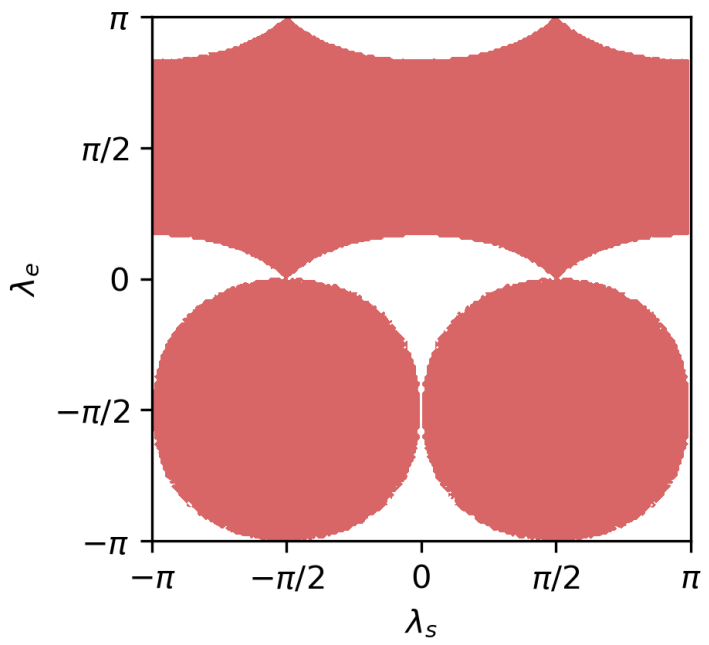

Figure 6.14: Regions in the (λ_s, λ_e) plane where the BS dynamics is *not* CP-divisible for at least one choice of (n, m).

both refer to different physical aspects of the problem. But if we focus on $\mathcal{N}_{n+1,n}$, then some comparison is possible. Recall that the MK describes how the dynamics from $n \to n+1$ is affected by previous times. Thus, regions where the memory kernel is large tend to be accompanied by regions where $\mathcal{N}_{n+1,n} > 0$. This is indeed the case, as can be seen by comparing Fig. 6.11 with 6.4.

6.3.2 TMS dynamics

The situation for the TMS dynamics is dramatically different. Diagrams for $\mathcal{N}_{n+1,n}$ in the (λ_s, ν_e) plane are shown in Fig. 6.15 for different values of n. In contrast to the BS maps, now most of parameter space is non-divisible. Moreover, the region where it is non-divisible increases for longer times. And finally, what is perhaps the least intuitive, the regions where the map is non-divisible are denser for *small*, instead of large, ν_e (although the values of $\mathcal{N}_{n+1,n}$ are smaller correspondingly smaller). This is a consequence of the fact that the TMS dynamics spontaneously creates excitations in the system, which implies that for large ν_e a substantial amount of noise is introduced, making the map more likely to be divisible. If $\nu_e = 0$ the map is, of course, divisible by construction.

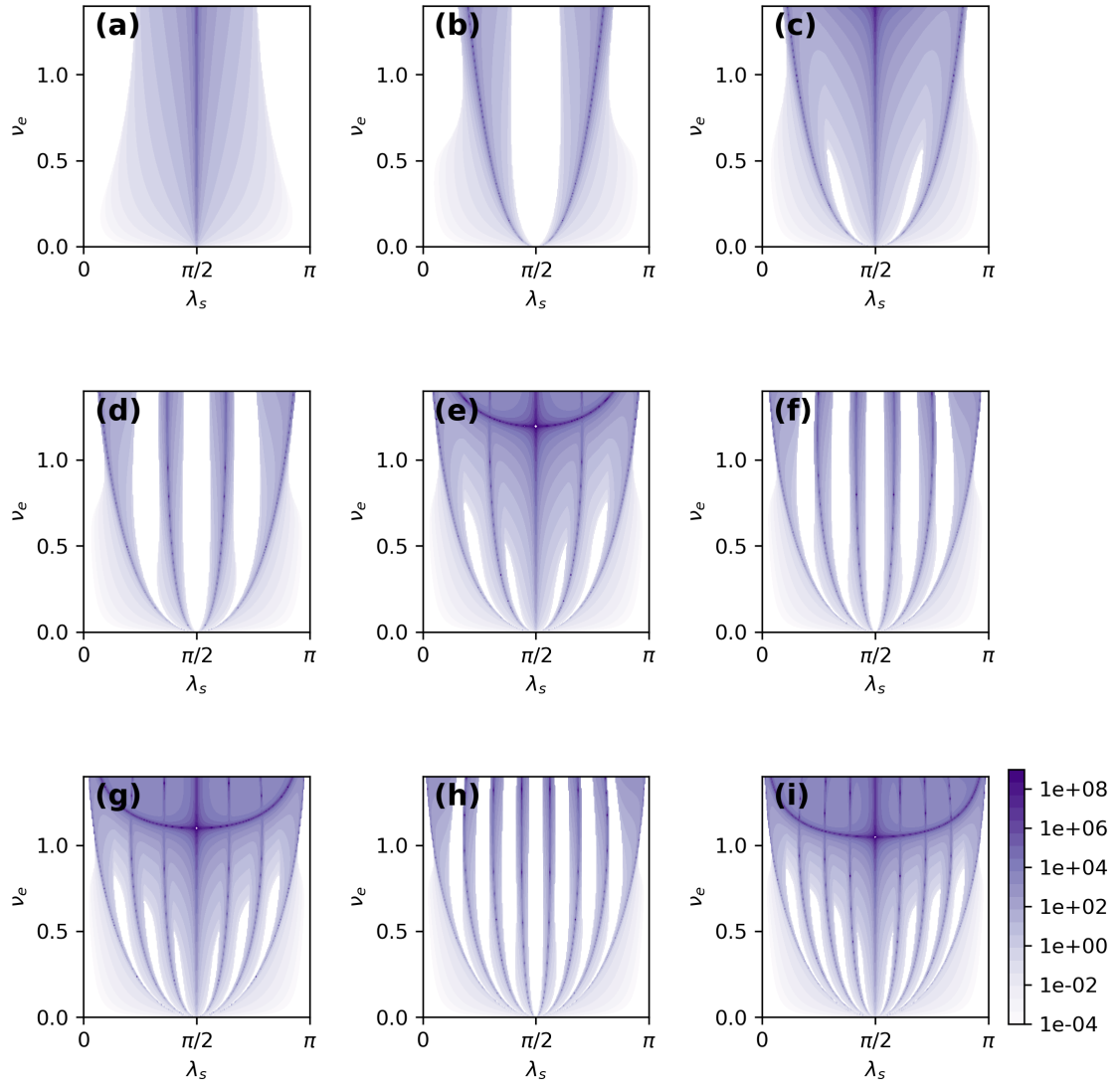

Figure 6.15: CP-divisibility measure, $\mathcal{N}_{n+1,n}$ [Eq. (6.31)] in the (λ_s, ν_e) plane, for the TMS dynamics. Each plot corresponds to a different values of n, from 1 to 9 in steps of 1.

However, the results in Fig. 6.15 show that for arbitrarily small, but non-zero ν_e, the map is already non-divisible, albeit with a small $\mathcal{N}_{n+1,n}$. As with the BS dynamics, one could also combine all these diagrams to ask whether there are regions in the (λ_s, ν_e) where the map is always divisible, for all (n, m).

The answer to this question is, in this case, negative: for the TMS dynamics the dynamics is never divisible, except for the trivial line $\nu_e = 0$. This represents a major difference in comparison with teh BS dynamics and, once again, is ultimately a property of the entangling nature of the two-mode squeezing interaction (4.8).

Chapter 7

Conclusions

In this dissertation we presented a robust framework for studying non-Markovianity in collisional models from multiple perspectives. We showed that the dynamics can be cast in terms of a Markovian embedding of the covariance matrix [Eq. (4.20)], which yields closed expressions for the mutual information [Eq. (5.1)], the memory kernel [Eq. (6.1)] and the divisibility monotone [Eq. (6.31)]. We analyzed in detail two types of interactions, a beam-splitter implementing a partial SWAP, and a two-mode squeezing which entangles the ancillas and, at the same time, feeds excitations into the system. By analizing several memory quantifiers for these two representative scenarios, this helped to shed light on the intricate mechanism behind memory effects in the quantum domain. Results of this work were reported in the preprint [91].

Essential to this work was the use of two main ingredients described in Chapter 4. First, collisional models, which allow us to introduce non-Markovianity in a fully controllable way. By means of the Markovian embedding (Sec. 4.2), the full non-Markovian dynamics is captured in the map $\Phi(.)$ [Eq. (4.3)], and the dynamics it generates [Eq. (4.4)], with ϱ^n containing all the relevant information characterizing the non-Markovianity of the evolution. And second, continuous-variable Gaussian operations, which replace the complicated dynamics of the density matrix into a much simpler map for the covariance matrix (Sec. 4.3). The global evolution at the level of density matrix [Eq. (4.2)] is converted into an equation for the global covariance matrices [Eq. (4.10)], and the unitaries [Eqs. (4.6)-(4.8)] are replaced by symplectic matrices [Eqs. (4.11)-(4.15)].

The Markovian embedding then allowed us to compute the memory effects in the

dynamics of γ^n. To begin with, the mutual information [Eq. (5.1)] is easily computed from the symplectic eigenvalues of γ^n. Next, the time-non-local dynamics defining the memory kernel [Eq. (5.2)] can be rewritten at the level of the system covariance matrix [Eq. (6.2)]. The memory kernel depends only on the matrix X and can be computed using [Eq. (6.18)]. One can also write a Kraus decomposition of the MK with coefficients κ_{ij}^n [Eq. (6.21)]. Finally, the intermediate map taking the system from time n to time m is given by [Eqs. (6.29) and (6.30)]. A monotone of CP-divisibility is obtained [Eq. (6.31)] and depends only on the X and Y. All methods described are implemented in the associated python, which provides an efficient and simple way of simulating a broad range of scenarios [72].

In particular, we have focused on two types of maps. The system-ancilla interaction was always fixed to be of beam-splitter-type (partial SWAP). But the ancilla-ancilla interaction could be either beam-splitter or a two-mode squeezing. The behaviour of the two are dramatically different. For the former, we have found that the combination of the two beam-splitter interactions lead to strong resonance effects that cause most quantities to oscillate in time and also depend sensibly on the relative signs of the interaction strengths (c.f. Figs. 6.4 or 6.11). For the BS dynamics, there is also a non-negligible portion of parameter space in which the dynamics is always Markovian (Fig. 6.14). Conversely, in the TMS dynamics excitations are constantly being generated in the system. As a consequence, the dynamics is only stable for certain values of the interaction strength (Fig. 4.4). If the interaction is too strong, the occupations in the system diverge (never reach a steady-state). Interestingly, this is also reflected in the memory kernel, which acquires infinitely long memory (Fig. 6.9). The TMS dynamics is also always non-Markovian (never CP-divisible; Fig. 6.15), unless the ancilla-ancilla interaction is strictly zero. This reflects the entangling nature of the two-mode squeezing. The magnitude of the non-Markovianity, of course, is small for weak interactions. This is clearly seen, for instance, in the memory kernel, Fig. 6.7.

Our framework can be readily extended to a broad range of scenarios. We begin by mentioning problems which are straightforward extensions of our results. Throughout the dissertation, we have focused on ancillas initially prepared in the vacuum state. Studying different initial preparations would be interesting since the memory kernel does not

depend on this, but CP-divisibility does. It would be particularly interesting to study the introduction of single-mode squeezing in the ancillas.

Another natural extension would be to consider different types of interactions, as in Refs [57, 61]. In particular, one thing that we have not explored are interactions that lead to "non-diagonal" memory kernels. As discussed below [Eq. (6.2)], a MK involving the identity or σ_z is always diagonal, meaning that each entry of θ^n is only affected by the same entry at past times. A memory kernel involving $\sigma_\pm$, however, would imply, for instance, that $\langle Q^2\rangle_n$ could be affected by past values of $\langle P^2\rangle_n$. This could, in principle, generate a plethora of interesting effects. Another possibility would be the inclusion of stochastic SWAPs, as in Refs. [54, 55].

In Ref. [62], the authors asked, within a collisional model context, whether it was possible to pinpoint the backflow of information to either changes in the environmental states, or the buildup of correlations between system and environment. This question is relevant since these are the two main ingredients entering in the 2nd law of thermodynamics in the quantum domain [115, 116]. That is to say, they are the two quantities measuring the degree of irreversibility of a process. We believe that this question could be directly addressed within our framework. Whether the Markovian embedding suffices for this end, however, is not clear at the moment. For instance, the mutual information studied in Sec. 5.2 is only between S and E_{n+1} and thus correspond to only a part of the full system-environment correlations. Notwithstanding, even if the embedding does not suffice, the fact that the approach deals only with covariance matrices still allows one to study numerically dynamics involving large numbers of ancillas.

Concerning less trivial extensions, throughout this work we have assumed that the Markov memory length is 1. That is, each ancilla E_n only propagates information to its nearest neighbor. The extension to arbitrary memory length, as studied in Refs. [57, 61], would be quite interesting. And it is also amenable to our framework, provided one extends the Markovian embedding to have longer memory.

Finally, we mention that the basic ideas set up could also serve as a starting point for exploring the Gaussian formulation of process tensors [108–110], which provide an alternative, and much broader, way of characterizing non-Markovianity. In fact, this could perhaps also be used as a way to bridge process tensors and the memory kernel.

Appendix A

Stability Theory

We are interested in studying the fixed point stability of the Markovian embedding equation (4.20), i.e. solutions that satisfy $\gamma^{n+1} = \gamma^n$. To this end, we use the vectorized form (6.9) and label the vectorized fixed point solution as $\vec{\gamma^*}$:

$$\vec{\gamma^*} = X \otimes X \vec{\gamma^*} + \vec{Y}. \tag{A.1}$$

As long as $\det(\mathbb{I} - X \otimes X) \neq 0$ a fixed point solution can be readily found as

$$\vec{\gamma^*} = (\mathbb{I} - X \otimes X)^{-1} \vec{Y}. \tag{A.2}$$

The stability of $\vec{\gamma^*}$ will be associated to the eigenvalues of the $X \otimes X$ matrix. Or, what is equivalent, the eigenvalues of X. If their modulus are below 1, the fixed point will be a globally asymptotic state (GAS) and all trajectories will converge to γ^* for large enough n. Otherwise, it may diverge.

The eigenvalues of the matrix X for the BS channel, Eq. (4.21), read

$$\frac{1}{2}\Big(- wx + x \pm \sqrt{(w+1)^2 x^2 + 4wy^2}\Big). \tag{A.3}$$

Using the (λ_s, λ_e) parametrization, one finds that the only values not satisfying the GAS conditions are $\lambda_e = \pm\pi/2$ or $\lambda_s = 0, \pi$, which represent, respectively, the case where no particle flow to the ancillas and when the system does not interact at all. Excluding those

points, the fixed point is a GAS given by:

$$\gamma^*_{BS} = \begin{pmatrix} \epsilon & 0 \\ 0 & \epsilon \end{pmatrix}. \tag{A.4}$$

That is, the map tends to homogenize the system to the same initial state of the ancillas. This, of course, is what is expected of a beam-splitter/partial SWAP dynamics. It is notwithstanding interesting that it remains true even in the case of ancilla-ancilla interactions and non-Markovian dynamics.

Similarly, the eigenvalues of X for the TMS case, Eq. (4.23), read

$$\begin{aligned} &\frac{1}{2}\Big((1+\tilde{w})x \pm \sqrt{(\tilde{w}-1)^2x^2 - 4\tilde{w}y^2}\Big), \\ &\frac{1}{2}\Big((1-\tilde{w})x \pm \sqrt{(\tilde{w}+1)^2x^2 + 4\tilde{w}y^2}\Big). \end{aligned} \tag{A.5}$$

These eigenvalues only fulfill the GAS requirements in the interval where $\nu_e \in [0, \sinh^{-1}(1)]$. This therefore defines the critical value $\nu_e^{\text{crit}} = \sinh^{-1}(1)$, after which the dynamics diverges. Inside this interval, the fixed point is a GAS given by

$$\gamma^*_{TMS} = \begin{pmatrix} \left(\frac{2\sinh^2(\nu_e)}{1-\sinh^2(\nu_e)} + 1\right)\epsilon & 0 \\ 0 & \left(\frac{2\sinh^2(\nu_e)}{1-\sinh^2(\nu_e)} + 1\right)\epsilon \end{pmatrix}. \tag{A.6}$$

Thus, we see that system and ancilla once again tend to homogenize. However, the ancilla initial state ϵ is now amplified by a factor which is always larger than unity and diverges when $\nu_e = \nu_e^{\text{crit}}$. We also call attention to the fact that γ^*_{TMS} is a product state, so that no correlations survive in the long-time limit.

Appendix B

Memory Kernel for the BS dynamics

In this appendix we discuss how to obtain a more compact expression for the memory kernel (6.2), in the case of the BS dynamics. This case is simpler because the only non-zero coefficient is κ^n_{11}, which is proportional to the identity map. That is to say, in this case the MK is actually just a c-number, instead of a superoperator.

To accomplish this, we exploit in more detail the tensor structure of the matrices used in Sec. 6.2 (now all specialized to $N_S = N_E = 1$). We being by noting that the matrix X of the BS dynamics, Eq. (4.21), can also be written as

$$X = \chi \otimes \mathbb{I}, \qquad \chi = \begin{pmatrix} x & y \\ yw & -xw \end{pmatrix}, \tag{B.1}$$

where χ is now a simple 2×2 matrix and, in this appendix, $\mathbb{I}$ will always refer to the identity of dimension 2. Similarly, the projection operator P_S in Eq. (6.10) can be written as

$$P_S = p_s \otimes \mathbb{I}, \qquad p_s = \begin{pmatrix} 1 & 0 \\ 0 & 0 \end{pmatrix}. \tag{B.2}$$

Thus, the matrix P in Eq. (6.11) becomes

$$P = p_s \otimes \mathbb{I} \otimes p_s \otimes \mathbb{I}. \tag{B.3}$$

This type of tensor structure, favouring slots 1 and 3, is simply a consequence of the vectorization procedure, Eq. (6.8).

The matrix p_s can be further decomposed as

$$p_s = |0\rangle\langle 0|, \qquad |0\rangle = \begin{pmatrix} 1 \\ 0 \end{pmatrix}. \tag{B.4}$$

Dirac's notation is introduced here just for clarity; the state $|0\rangle$ is completely unrelated to the actual Hilbert space basis of the system. The advantage of this decomposition is that it allows us to write the isometry π, in Eq. (6.16), as

$$\pi = \langle 0| \otimes \mathbb{I} \otimes \langle 0| \otimes \mathbb{I}. \tag{B.5}$$

This now clearly shows that π contracts slots 1 and 3, while acting trivially on 2 and 4.

At this point, it is convenient to simplify the notation and introduce indices $1, 2, 3, 4$, to refer to which slow of the tensor product the operators act. Thus, for instance, we will henceforth write

$$X \otimes X = \chi \otimes \mathbb{I} \otimes \chi \otimes \mathbb{I} := \chi_1 \chi_3, \tag{B.6}$$

meaning χ_1 acts on slot 1 and χ_3 on slot 3. Similarly, $P = p_s^1 p_s^3$ and, therefore, $Q = 1 - p_s^1 p_s^3 := Q_{13}$ is a matrix acting only on slots 1 and 3 (we emphasize that Q_{13} cannot be written as a simple product of an operator acting on 1 and another acting on 3). Notice how the special structure appearing in Eq. (B.6) is unique of the BS dynamics. For other types of dynamics, $X \otimes X$ would in general act non-trivially on all four slots. Due to this simplification, the quantity appearing inside $\pi(\dots)\pi^{\mathrm{T}}$ in Eq. (6.18) will be an operator acting only on slots 1 and 3.

Next we turn to Eq. (6.21), describing the coefficients κ_{ij}^n. The contraction $\pi(\dots)\pi^{\mathrm{T}}$ eliminates slots 1 and 3, so that $(M_j^{\mathrm{T}} \otimes M_i^{\mathrm{T}})$ is effectively multiplying matrices from slots 2 and 4. Thus, one may equivalently write

$$(M_j^{\mathrm{T}} \otimes M_i^{\mathrm{T}})\pi(\dots)\pi^{\mathrm{T}} = \pi\Big[(\mathbb{I} \otimes M_j^{\mathrm{T}} \otimes \mathbb{I} \otimes M_i^{\mathrm{T}})\dots\Big]\pi^{\mathrm{T}},$$

where $(\dots)$ refers to all terms inside $\pi(\dots)\pi^{\mathrm{T}}$ in Eq. (6.18). But from the arguments above, these quantities act only on slots 1 and 3. Combining this with the fact that $\mathrm{tr}(A \otimes B) = \mathrm{tr}(A)\,\mathrm{tr}(B)$ explains why, in the BS case, the only non-trivial coefficient

will be κ^n_{11}, corresponding to $M_i = M_j = \mathbb{I}$. This coefficient may then be written as

$$\kappa^n_{11} = \mathrm{tr}_{13}\left\{\pi_{13}\Big[\chi_1\chi_3(Q_{13}\chi_1\chi_3Q_{13})^n\chi_1\chi_3\Big]\pi^{\mathsf{T}}_{13}\right\},$$

where the remaining trace is now only over slots 1 and 3. Finally, we use Eq. (B.5) to express π in terms of $\langle 0|$. This allows us to write

$$\kappa^n_{11} = \langle 00|\,\bar\chi\left(\bar Q\,\bar\chi\,\bar Q\right)^n\bar\chi\,|00\rangle, \tag{B.7}$$

where $|00\rangle = |0\rangle\otimes|0\rangle$, $\bar\chi = \chi\otimes\chi$ and $\bar Q = \mathbb{I}_4 - p_s\otimes p_s$ are all objects of dimension 4. Eq. (B.7) therefore provides a compact representation of the memory Kernel for the BS dynamics. It is expressed solely in terms of $|0\rangle$, χ and p_s, [Eqs. (B.1) and (B.4)]. And it requires exponentiating only operators of dimension 4, in comparison with (6.18) which would have dimension 16.

Bibliography

[1] H.-P. Breuer, F. Petruccione, *et al.*, *The theory of open quantum systems*. Oxford University Press on Demand, 2002.

[2] M. O. Scully and M. S. Zubairy, *Quantum optics*, 1999.

[3] A. Rivas and S. F. Huelga, *Open quantum systems*. Springer, 2012, vol. 13.

[4] G. Lindblad, "On the generators of quantum dynamical semigroups," *Communications in Mathematical Physics*, vol. 48, no. 2, pp. 119–130, 1976.

[5] J. Doob, "Stochastic processes, 1953," *New York*, 1990.

[6] S. Nakajima, "On quantum theory of transport phenomena: Steady diffusion," *Progress of Theoretical Physics*, vol. 20, no. 6, pp. 948–959, 1958.

[7] R. Zwanzig, "Ensemble method in the theory of irreversibility," *The Journal of Chemical Physics*, vol. 33, no. 5, pp. 1338–1341, 1960.

[8] S. M. Barnett and S. Stenholm, "Hazards of reservoir memory," *Physical Review A*, vol. 64, no. 3, p. 033 808, 2001.

[9] A. Shabani and D. A. Lidar, "Completely positive post-markovian master equation via a measurement approach," *Physical Review A*, vol. 71, no. 2, p. 020 101, 2005.

[10] M. J. Hall, J. D. Cresser, L. Li, and E. Andersson, "Canonical form of master equations and characterization of non-markovianity," *Physical Review A*, vol. 89, no. 4, p. 042 120, 2014.

[11] L. Mazzola, E.-M. Laine, H.-P. Breuer, S. Maniscalco, and J. Piilo, "Phenomenological memory-kernel master equations and time-dependent markovian processes," *Physical Review A*, vol. 81, no. 6, p. 062 120, 2010.

[12] F. Liu, X. Zhou, and Z.-W. Zhou, "Memory effect and non-markovian dynamics in an open quantum system," *Physical Review A*, vol. 99, no. 5, p. 052 119, 2019.

[13] B. Vacchini, "Generalized master equations leading to completely positive dynamics," *Physical Review Letters*, vol. 117, no. 23, p. 230 401, 2016.

[14] F. C. Binder, J. Thompson, and M. Gu, "Practical unitary simulator for non-markovian complex processes," *Physical review letters*, vol. 120, no. 24, p. 240 502, 2018.

[15] Á. Rivas, S. F. Huelga, and M. B. Plenio, "Quantum non-markovianity: Characterization, quantification and detection," *Reports on Progress in Physics*, vol. 77, no. 9, p. 094 001, 2014.

[16] H.-P. Breuer, E.-M. Laine, J. Piilo, and B. Vacchini, "Colloquium: Non-markovian dynamics in open quantum systems," *Reviews of Modern Physics*, vol. 88, no. 2, p. 021 002, 2016.

[17] H.-P. Breuer, E.-M. Laine, and J. Piilo, "Measure for the degree of non-markovian behavior of quantum processes in open systems," *Physical review letters*, vol. 103, no. 21, p. 210 401, 2009.

[18] D. Chruściński, Á. Rivas, and E. Størmer, "Divisibility and information flow notions of quantum markovianity for noninvertible dynamical maps," *Physical review letters*, vol. 121, no. 8, p. 080 407, 2018.

[19] R. Vasile, S. Maniscalco, M. G. Paris, H.-P. Breuer, and J. Piilo, "Quantifying non-markovianity of continuous-variable gaussian dynamical maps," *Physical Review A*, vol. 84, no. 5, p. 052 118, 2011.

[20] E.-M. Laine, J. Piilo, and H.-P. Breuer, "Measure for the non-markovianity of quantum processes," *Physical Review A*, vol. 81, no. 6, p. 062 115, 2010.

[21] Á. Rivas, S. F. Huelga, and M. B. Plenio, "Entanglement and non-markovianity of quantum evolutions," *Physical review letters*, vol. 105, no. 5, p. 050 403, 2010.

[22] S. Hou, X. Yi, S. Yu, and C. Oh, "Alternative non-markovianity measure by divisibility of dynamical maps," *Physical Review A*, vol. 83, no. 6, p. 062 115, 2011.

[23] S. Luo, S. Fu, and H. Song, "Quantifying non-markovianity via correlations," *Physical Review A*, vol. 86, no. 4, p. 044 101, 2012.

[24] D. Chruściński and A. Kossakowski, "Markovianity criteria for quantum evolution," *Journal of Physics B: Atomic, Molecular and Optical Physics*, vol. 45, no. 15, p. 154 002, 2012.

[25] D. Chruscinski and A. Kossakowski, "Witnessing non-markovianity of quantum evolution," *The European Physical Journal D*, vol. 68, no. 1, p. 7, 2014.

[26] A. Costa, R. Angelo, and M. Beims, "Monogamy and backflow of mutual information in non-markovian thermal baths," *Physical Review A*, vol. 90, no. 1, p. 012 322, 2014.

[27] P. Strasberg and M. Esposito, "Response functions as quantifiers of non-markovianity," *Physical review letters*, vol. 121, no. 4, p. 040 601, 2018.

[28] L. A. Souza, H. S. Dhar, M. N. Bera, P. Liuzzo-Scorpo, and G. Adesso, "Gaussian interferometric power as a measure of continuous-variable non-markovianity," *Physical Review A*, vol. 92, no. 5, p. 052 122, 2015.

[29] F. F. Fanchini, G. Karpat, B. Cakmak, L. Castelano, G. Aguilar, O. J. Farias, S. Walborn, P. S. Ribeiro, and M. De Oliveira, "Non-markovianity through accessible information," *Physical Review Letters*, vol. 112, no. 21, p. 210 402, 2014.

[30] X.-M. Lu, X. Wang, and C. Sun, "Quantum fisher information flow and non-markovian processes of open systems," *Physical Review A*, vol. 82, no. 4, p. 042 103, 2010.

[31] J. Rau, "Relaxation phenomena in spin and harmonic oscillator systems," *Physical Review*, vol. 129, no. 4, pp. 1880–1888, 1963, ISSN: 0031899X.

[32] V. Scarani, M. Ziman, P. Štelmachovič, N. Gisin, V. Bužek, and V. Bužek, "Thermalizing quantum machines: Dissipation and entanglement," *Physical Review Letters*, vol. 88, no. 9, p. 097 905, 2002, ISSN: 00319007.

[33] M. Ziman, P. Štelmachovič, V. Buzžek, M. Hillery, V. Scarani, and N. Gisin, "Diluting quantum information: An analysis of information transfer in system-reservoir interactions," *Physical Review A. Atomic, Molecular, and Optical Physics*, vol. 65, no. 4, p. 042 105, 2002, ISSN: 10502947.

[34] B.-G. Englert and G. Morigi, "Five Lectures On Dissipative Master Equations," in *Coherent Evolution in Noisy Environments - Lecture Notes in Physics*, A. Buchleitner and K. Hornberger, Eds., Berlin, Heidelberg: Springer, 2002, p. 611.

[35] S. Attal and Y. Pautrat, "From Repeated to Continuous Quantum Interactions," *Annales Henri Poincaré*, vol. 7, no. 1, pp. 59–104, 2006, ISSN: 1424-0637.

[36] C. Pellegrini and F. Petruccione, "Non-Markovian quantum repeated interactions and measurements," *Journal of Physics A: Mathematical and Theoretical*, vol. 42, no. 42, p. 425 304, 2009, ISSN: 1751-8113.

[37] D. Karevski and T. Platini, "Quantum nonequilibrium steady states induced by repeated interactions," *Physical review letters*, vol. 102, no. 20, p. 207 207, 2009.

[38] G. T. Landi, E. Novais, M. J. de Oliveira, and D. Karevski, "Flux rectification in the quantum x x z chain," *Physical Review E*, vol. 90, no. 4, p. 042 142, 2014.

[39] V. Giovannetti and G. M. Palma, "Master equations for correlated quantum channels," *Physical Review Letters*, vol. 108, no. 4, p. 040 401, 2012, ISSN: 00319007.

[40] P. Strasberg, G. Schaller, T. Brandes, and M. Esposito, "Quantum and information thermodynamics: A unifying framework based on repeated interactions," *Physical Review X*, vol. 7, no. 2, p. 021 003, 2017.

[41] F. Barra, "The thermodynamic cost of driving quantum systems by their boundaries," *Scientific reports*, vol. 5, p. 14 873, 2015.

[42] G. De Chiara, G. Landi, A. Hewgill, B. Reid, A. Ferraro, A. J. Roncaglia, and M. Antezza, "Reconciliation of quantum local master equations with thermodynamics," *New Journal of Physics*, vol. 20, no. 11, p. 113 024, 2018.

[43] A. O. Caldeira and A. J. Leggett, "Influence of dissipation on quantum tunneling in macroscopic systems," *Physical Review Letters*, vol. 46, no. 4, p. 211, 1981.

[44] J. A. Gross, C. M. Caves, G. J. Milburn, and J. Combes, "Qubit models of weak continuous measurements: markovian conditional and open-system dynamics," *Quantum Science and Technology*, vol. 3, no. 2, p. 024 005, 2018.

[45] F. Ciccarello, "Collision models in quantum optics," *Quantum Measurements and Quantum Metrology*, vol. 4, pp. 53–63, 2017, ISSN: 2299-114X.

[46] K. A. Fischer, R. Trivedi, V. Ramasesh, I. Siddiqi, and J. Vučković, "Scattering into one-dimensional waveguides from a coherently-driven quantum-optical system," *Quantum*, vol. 2, p. 69, 2018.

[47] H. Pichler and P. Zoller, "Photonic Quantum Circuits with Time Delays," *Physical Review Letters*, vol. 116, p. 093 601, 2016.

[48] D. Cilluffo, A. Carollo, S. Lorenzo, J. A. Gross, G. M. Palma, and F. Ciccarello, "Collisional picture of quantum optics with giant emitters," pp. 37–39, 2020.

[49] T. Rybár, S. N. Filippov, M. Ziman, and V. Bužek, "Simulation of indivisible qubit channels in collision models," *Journal of Physics B: Atomic, Molecular and Optical Physics*, vol. 45, no. 15, p. 154 006, 2012.

[50] N. Bernardes, A. Carvalho, C. Monken, and M. F. Santos, "Environmental correlations and markovian to non-markovian transitions in collisional models," *Physical Review A*, vol. 90, no. 3, p. 032 111, 2014.

[51] N. K. Bernardes, A. R. Carvalho, C. Monken, and M. F. Santos, "Coarse graining a non-markovian collisional model," *Physical Review A*, vol. 95, no. 3, p. 032 117, 2017.

[52] E. Mascarenhas and I. De Vega, "Quantum critical probing and simulation of colored quantum noise," *Physical Review A*, vol. 96, no. 6, p. 062 117, 2017.

[53] Z.-X. Man, Y.-J. Xia, and R. L. Franco, "Temperature effects on quantum non-markovianity via collision models," *Physical Review A*, vol. 97, no. 6, p. 062 104, 2018.

[54] F. Ciccarello, G. Palma, and V. Giovannetti, "Collision-model-based approach to non-markovian quantum dynamics," *Physical Review A*, vol. 87, no. 4, p. 040 103, 2013.

[55] F. Ciccarello and V. Giovannetti, "A quantum non-markovian collision model: Incoherent swap case," *Physica Scripta*, vol. 2013, no. T153, p. 014 010, 2013.

[56] R. McCloskey and M. Paternostro, "Non-markovianity and system-environment correlations in a microscopic collision model," *Physical Review A*, vol. 89, no. 5, p. 052 120, 2014.

[57] B. Çakmak, M. Pezzutto, M. Paternostro, and Ö. Müstecaplıoğlu, "Non-markovianity, coherence, and system-environment correlations in a long-range collision model," *Physical Review A*, vol. 96, no. 2, p. 022 109, 2017.

[58] S. Kretschmer, K. Luoma, and W. T. Strunz, "Collision model for non-markovian quantum dynamics," *Physical Review A*, vol. 94, no. 1, p. 012 106, 2016.

[59] S. Campbell, F. Ciccarello, G. M. Palma, and B. Vacchini, "System-environment correlations and markovian embedding of quantum non-markovian dynamics," *Physical Review A*, vol. 98, no. 1, p. 012 142, 2018.

[60] S. Lorenzo, F. Ciccarello, and G. M. Palma, "Composite quantum collision models," *Physical Review A*, vol. 96, no. 3, p. 032 107, 2017.

[61] J. Jin and C.-s. Yu, "Non-markovianity in the collision model with environmental block," *New Journal of Physics*, vol. 20, no. 5, p. 053 026, 2018.

[62] S. Campbell, M. Popovic, D. Tamascelli, and B. Vacchini, "Precursors of non-markovianity," *New Journal of Physics*, vol. 21, no. 5, p. 053 036, 2019.

[63] A. Serafini, *Quantum continuous variables: a primer of theoretical methods*. CRC press, 2017.

[64] A. Ferraro, S. Olivares, and M. G. Paris, "Gaussian states in continuous variable quantum information," *arXiv preprint quant-ph/0503237*, 2005.

[65] G. Adesso and F. Illuminati, "Entanglement in continuous-variable systems: Recent advances and current perspectives," *Journal of Physics A: Mathematical and Theoretical*, vol. 40, no. 28, p. 7821, 2007.

[66] G. Adesso, S. Ragy, and A. R. Lee, "Continuous variable quantum information: Gaussian states and beyond," *Open Systems & Information Dynamics*, vol. 21, no. 01n02, p. 1 440 001, 2014.

[67] A. S. Holevo, "One-mode quantum gaussian channels: Structure and quantum capacity," *Problems of Information Transmission*, vol. 43, no. 1, pp. 1–11, 2007.

[68] F. Caruso, V. Giovannetti, and A. S. Holevo, "One-mode bosonic gaussian channels: A full weak-degradability classification," *New Journal of Physics*, vol. 8, no. 12, p. 310, 2006.

[69] R. Simon, E. Sudarshan, and N. Mukunda, "Gaussian-wigner distributions in quantum mechanics and optics," *Physical Review A*, vol. 36, no. 8, p. 3868, 1987.

[70] R. Simon, Sudarshan, and N. Mukunda, "Gaussian pure states in quantum mechanics and the symplectic group," *Physical Review A*, vol. 37, no. 8, p. 3028, 1988.

[71] R. Simon, N. Mukunda, and B. Dutta, "Quantum-noise matrix for multimode systems: U (n) invariance, squeezing, and normal forms," *Physical Review A*, vol. 49, no. 3, p. 1567, 1994.

[72] *"The code repository can be found in https://github.com/gtlandi/gaussianonmark"*.

[73] R. Shankar, *Principles of quantum mechanics*. Springer Science & Business Media, 2012.

[74] K. Gottfried and T.-M. Yan, *Quantum mechanics: fundamentals*. Springer Science & Business Media, 2013.

[75] J. J. Sakurai and E. D. Commins, *Modern quantum mechanics, revised edition*, 1995.

[76] M. Le Bellac, *Quantum physics*. Cambridge University Press, 2011.

[77] R. P. Feynman, A. R. Hibbs, and D. F. Styer, *Quantum mechanics and path integrals*. Courier Corporation, 2010.

[78] S. Weinberg, *Lectures on quantum mechanics*. Cambridge University Press, 2015.

[79] J. Watrous, *The theory of quantum information*. Cambridge University Press, 2018.

[80] K. Kraus, "General state changes in quantum theory," *Annals of Physics*, vol. 64, no. 2, pp. 311–335, 1971.

[81] R. Loudon, *The quantum theory of light*. OUP Oxford, 2000.

[82] A. Altland and B. D. Simons, *Condensed matter field theory*. Cambridge university press, 2010.

[83] P. M. Chaikin, T. C. Lubensky, and T. A. Witten, *Principles of condensed matter physics*. Cambridge university press Cambridge, 1995, vol. 10.

[84] S. M. Girvin and K. Yang, *Modern condensed matter physics*. Cambridge University Press, 2019.

[85] R. Shankar, *Quantum Field Theory and Condensed Matter: An Introduction*. Cambridge University Press, 2017.

[86] P. Coleman, *Introduction to many-body physics*. Cambridge University Press, 2015.

[87] P. Kaye, R. Laflamme, M. Mosca, *et al.*, *An introduction to quantum computing*. Oxford university press, 2007.

[88] M. A. Nielsen and I. Chuang, *Quantum computation and quantum information*, 2002.

[89] K. Husimi, "Some formal properties of the density matrix," *Proceedings of the Physico-Mathematical Society of Japan. 3rd Series*, vol. 22, no. 4, pp. 264–314, 1940.

[90] R. Simon, N. Mukunda, and E. Sudarshan, "Partially coherent beams and a generalized abcd-law," *Optics communications*, vol. 65, no. 5, pp. 322–328, 1988.

[91] R. R. Camasca and G. T. Landi, "Memory kernel and divisibility of gaussian collisional models," *arXiv preprint arXiv:2008.00765*, 2020.

[92] W. F. Stinespring, "Positive functions on c*-algebras," *Proceedings of the American Mathematical Society*, vol. 6, no. 2, pp. 211–216, 1955.

[93] A. Chiuri, C. Greganti, L. Mazzola, M. Paternostro, and P. Mataloni, "Linear optics simulation of quantum non-markovian dynamics," *Scientific reports*, vol. 2, p. 968, 2012.

[94] B.-H. Liu, L. Li, Y.-F. Huang, C.-F. Li, G.-C. Guo, E.-M. Laine, H.-P. Breuer, and J. Piilo, "Experimental control of the transition from markovian to non-markovian dynamics of open quantum systems," *Nature Physics*, vol. 7, no. 12, pp. 931–934, 2011.

[95] N. K. Bernardes, J. P. Peterson, R. S. Sarthour, A. M. Souza, C. Monken, I. Roditi, I. S. Oliveira, and M. F. Santos, "High resolution non-markovianity in nmr," *Scientific reports*, vol. 6, p. 33 945, 2016.

[96] N. K. Bernardes, A. Cuevas, A. Orieux, C. Monken, P. Mataloni, F. Sciarrino, and M. F. Santos, "Experimental observation of weak non-markovianity," *Scientific reports*, vol. 5, no. 1, pp. 1–7, 2015.

[97] A. Orieux, A. d'Arrigo, G. Ferranti, R. L. Franco, G. Benenti, E. Paladino, G. Falci, F. Sciarrino, and P. Mataloni, "Experimental on-demand recovery of entanglement by local operations within non-markovian dynamics," *Scientific reports*, vol. 5, no. 1, pp. 1–8, 2015.

[98] N. G. Van Kampen, *Stochastic processes in physics and chemistry*. Elsevier, 1992, vol. 1.

[99] S. M. Ross, J. J. Kelly, R. J. Sullivan, W. J. Perry, D. Mercer, R. M. Davis, T. D. Washburn, E. V. Sager, J. B. Boyce, and V. L. Bristow, *Stochastic processes*. Wiley New York, 1996, vol. 2.

[100] E. Parzen, *Stochastic processes*. SIAM, 1999.

[101] J. R. Norris, *Markov chains*, 2. Cambridge university press, 1998.

[102] S. P. Gudder, *Stochastic methods in quantum mechanics*. Courier Corporation, 2014.

[103] S. Hou, S. Liang, and X. Yi, "Non-markovianity and memory effects in quantum open systems," *Physical Review A*, vol. 91, no. 1, p. 012 109, 2015.

[104] G. Torre, W. Roga, and F. Illuminati, "Non-markovianity of gaussian channels," *Physical Review Letters*, vol. 115, no. 7, p. 070 401, 2015.

[105] P. Liuzzo-Scorpo, W. Roga, L. A. Souza, N. K. Bernardes, and G. Adesso, "Non-markovianity hierarchy of gaussian processes and quantum amplification," *Physical Review Letters*, vol. 118, no. 5, p. 050 401, 2017.

[106] J. Cerrillo and J. Cao, "Non-markovian dynamical maps: Numerical processing of open quantum trajectories," *Physical Review Letters*, vol. 112, no. 11, p. 110 401, 2014.

[107] F. A. Pollock and K. Modi, "Tomographically reconstructed master equations for any open quantum dynamics," *Quantum*, vol. 2, p. 76, 2018.

[108] F. A. Pollock, C. Rodriguez-Rosario, T. Frauenheim, M. Paternostro, and K. Modi, "Operational markov condition for quantum processes," *Physical review letters*, vol. 120, no. 4, p. 040 405, 2018.

[109] F. A. Pollock, C. Rodriguez-Rosario, T. Frauenheim, M. Paternostro, and K. Modi, "Non-markovian quantum processes: Complete framework and efficient characterization," *Physical Review A*, vol. 97, no. 1, p. 012 127, 2018.

[110] P. Taranto, S. Milz, F. A. Pollock, and K. Modi, "Structure of quantum stochastic processes with finite markov order," *Physical Review A*, vol. 99, no. 4, p. 042 108, 2019.

[111] K. Kraus, *States, Effects, and Operations: Fundamental Notions of Quantum Theory*, A. Böhm, J. D. Dollard, and W. H. Wooters, Eds. Heidelberg: Springer, 1983, p. 154.

[112] S. Elaydi, *An introduction to difference equations*. Springer Science & Business Media, 2005.

[113] D. A. Turkington, *Generalized Vectorization, Cross-Products, and Matrix Calculus*. Cambridge: Cambridge University Press, 2013, p. 275, ISBN: 978-1107032002.

[114] G. Lindblad, "Cloning the quantum oscillator," *Journal of Physics A: Mathematical and General*, vol. 33, no. 28, p. 5059, 2000.

[115] M. Esposito, K. Lindenberg, and C. Van den Broeck, "Entropy production as correlation between system and reservoir," *New Journal of Physics*, vol. 12, no. 1, p. 013 013, 2010, ISSN: 1367-2630.

[116] A. M. Timpanaro, J. P. Santos, and G. T. Landi, "Landauer's Principle at Zero Temperature," *Physical Review Letters*, vol. 124, no. 24, p. 240 601, 2020, ISSN: 0031-9007.